

# **Final Report**

**on the Project**

## **Plasma Cathodes for High Pressure Glow Discharges**

**Grant No: F49620-97-1-0228**

**May 1, 1997 to July 31, 2000**

**submitted to**

**Dr. Robert J. Barker**

**Air Force Office of Scientific Research**

801 N. Randolph St., Rm 732  
Arlington, VA 22203-1977  
Phone: (703) 696-8574  
FAX: (703) 696-8481  
e-mail: robert.barker@afosr.af.mil

**by**

**Karl H. Schoenbach**

Old Dominion University, Norfolk VA 23529  
Phone: (757) 683-4625  
FAX: (757) 683-3220  
e-mail: schoenbach@ece.odu.edu

20000925 037

# REPORT DOCUMENTATION PAGE

AFRL-SR-BL-TR-00-

Public reporting burden for this collection of information is estimated to average 1 hour per response, including gathering and maintaining the data needed, and completing and reviewing the collection of information. Send collection of information, including suggestions for reducing this burden, to Washington Headquarters Services, Directorate for Information Operations and Reports, 1215 Jefferson Davis Highway, Suite 1204, Arlington, VA 22202-4302, and to the Office of Management and Budget, Paperwork Project, Washington, DC 20503.

MS.  
his  
on

0409

1. AGENCY USE ONLY (Leave blank)		2. REPORT DATE		3. REPORT TYPE AND DATES COVERED 01 May 1997 to 31 Jul 2000 Final	
4. TITLE AND SUBTITLE (New World Vistas) Plasma Cathodes for high pressure glow discharges				5. FUNDING NUMBERS 61102F 2301/EV	
6. AUTHOR(S) Professor Schoenbach					
7. PERFORMING ORGANIZATION NAME(S) AND ADDRESS(ES) Old Dominion Univ Rsch Foundation Inc 800 West 46th Street PO Box 6369 Norfolk, VA 23508-0369				8. PERFORMING ORGANIZATION REPORT NUMBER	
9. SPONSORING/MONITORING AGENCY NAME(S) AND ADDRESS(ES) AFOSR/NE 801 North Randolph Street Rm 732 Arlington, VA 22203-1977				10. SPONSORING/MONITORING AGENCY REPORT NUMBER  F49620-97-1-0228	
11. SUPPLEMENTARY NOTES					
12a. DISTRIBUTION AVAILABILITY STATEMENT APPROVAL FOR PUBLIC RELEASE; DISTRIBUTION UNLIMITED				12b. DISTRIBUTION CODE	
13. ABSTRACT (Maximum 200 words)  The extension of the atmospheric pressure air glows to centimeter and larger volumes has been demonstrated: in transverse direction through parallel operation of two single microhollow cathode sustained glow discharges, - in longitudinal direction through increased voltage operation. Limits in discharge stability dependent on the discharge current have been explored. It was found that dc operation is limited to approximately 20 mA per microhollow cathode discharge. Pulsed operation allowed us to increase the current up to approximately 100 mA in the microsecond time regime before glow-to-arc transition occurs.					
14. SUBJECT TERMS				15. NUMBER OF PAGES	
				16. PRICE CODE	
17. SECURITY CLASSIFICATION OF REPORT  UNCLASSIFIED		18. SECURITY CLASSIFICATION OF THIS PAGE  UNCLASSIFIED		19. SECURITY CLASSIFICATION OF ABSTRACT  UNCLASSIFIED	
				20. LIMITATION OF ABSTRACT  UL	

## **TABLE OF CONTENTS**

<b>Summary</b>	<b>2</b>
<b>Achievements</b>	<b>3</b>
<b>Stability</b>	<b>4</b>
<b>Temporal Control</b>	<b>5</b>
<b>Gas Temperature</b>	<b>6</b>
<b>Electron Density</b>	<b>7</b>
<b>Plasma Volume</b>	<b>9</b>
<b>Power Consumption</b>	<b>13</b>
<b>Cooperative Efforts</b>	<b>15</b>
<b>Publications and Presentations</b>	<b>16</b>

## SUMMARY

The cathode fall of a self-sustained glow discharge is the a region of highest electric field, and consequently the region where glow-to-arc transitions are most likely to be initiated. Reducing the cathode fall voltage of a glow discharge in atmospheric pressure air from more than hundred volts air to tens of volts has allowed us to generate stable, direct current glow discharges in atmospheric air. This was obtained by using a microhollow cathode discharge as electron emitter for the glow discharge cathode. First experiments with single discharges of millimeter dimensions have proven the concept of high pressure glow discharge stabilization. The extension of the atmospheric pressure air glows to centimeter and larger volumes has been demonstrated: in transverse direction through parallel operation of two single microhollow cathode sustained glow discharges, - in longitudinal direction through increased voltage operation. Limits in discharge stability dependent on the discharge current have been explored. It was found that dc operation is limited to approximately 20 mA per microhollow cathode discharge. Pulsed operation allowed us to increase the current up to approximately 100 mA in the microsecond time regime before glow-to-arc transition occurs. The current in the air glow discharge can be controlled independent of the electric field in the air plasma by varying the plasma cathode current. This has been demonstrated by turning the discharge on and off, through plasma cathode control, on a submillisecond time scale. Electron densities of more than  $10^{13} \text{ cm}^{-3}$  and gas temperatures of less than 2000 K, sustained for times exceeding 10 ms are goal values of the plasma rampart program. Anyone of the three conditions has been reached with this discharge concept. Electron densities in the atmospheric pressure air discharges on the order of  $10^{13} \text{ cm}^{-3}$  have been measured by using laser interferometry. The gas temperature was measured by means of emission spectroscopy of the rotational spectrum of nitrogen. The temperature could be kept at and below 2000 K for low discharge currents ( $<4 \text{ mA}$ ), or, at higher currents, when helium was added to air. The electrical power required to sustain a  $10^{13} \text{ cm}^{-3}$  electron density in 1 atm air was found to be  $5 \text{ kW/cm}^3$ , consistent with theoretical estimates. Experimental studies to lower this power consumption have been initiated. They are based on a pulsed electric field induced shift of the electron energy distribution to higher energies. This shift causes a nonlinear increase in ionization rates and consequently a nonlinear increase in plasma decay time. The maximum duration of the electric field pulses is limited to times shorter than the time constant for the development of glow-to-arc transitions, typically much less than 50 ns. Pulsed electric fields of 10 ns duration have been applied to the dc plasma, and an increase in plasma decay time from tens of nanoseconds at electric fields of 10 kV/cm to several microseconds at electric fields at 40 kV/cm. The pulsed electric field method was also applied to an atmospheric pressure air plasma at Stanford University (Prof. C. Kruger). According to the results obtained at Stanford University the pulsed electric field method results in power saving by more than two orders of magnitude when the discharge is operated in a repetitive mode.

## Achievements

The goal statement for the Air Plasma Rampart Program (APRP) is: "to discover physical mechanisms for significantly reducing the power consumption for creating and maintaining a stable plasma volume of five centimeter minimum dimension with free electron densities of at least  $10^{13} \text{ cm}^{-3}$  for durations greater than 10 ms in sea level air at gas temperatures below 2,000 K. Instabilities, particularly the Glow-to-Arc Transition (GAT) which evolves from the cathode fall of glow discharges, have been a major obstacle for the operation of stable, atmospheric pressure glow discharges. The use of microhollow cathode discharges [K.H. Schoenbach et al, Appl. Phys. Lett. 68, 13 (1996), and Plasma Sources Science and Techn. 6, 469 (1997)] as stabilizing elements in the cathode fall region and as voltage controlled electron sources for high-pressure glow discharges in air was the main topic of this research work. Another important topic, reduction of the power consumption of atmospheric pressure glow discharges, was addressed in the final year of this grant.

Scientific achievements over the funding period of this grant are listed below:

1. We are able to generate weakly ionized, direct current air plasmas without additives at atmospheric pressure and above, by using microhollow cathode discharges as plasma cathodes.
2. The current in these discharges discharges, and consequently the electron density and gas temperature can be varied by modulating the microhollow cathode current.
3. The gas temperature of the air plasmas was measured and found to be approximately 2000 K and above depending on discharge current.
4. Electron densities have been measured and found to be on the order of  $10^{13} \text{ cm}^{-3}$  in 10 mA atmospheric pressure air discharges.
5. Parallel operation of atmospheric pressure air plasma discharges has been demonstrated.
6. The distance between the discharge electrodes has been extended from millimeters to more than one centimeter.
7. The power density required to sustain these dc plasmas was found to be on the order of  $\text{kW/cm}^3$ , in accordance with theoretical values [R.J. Vidmar, IEEE Trans. Plasma Science 18, 733 (1990)].
8. Experiments with pulsed electric fields superimposed to the dc plasma (performed both at Old Dominion University and Stanford University) indicate power savings by more than two orders of magnitude, bringing the required power density into the tens of  $\text{W/cm}^3$  [Robert H. Stark and Karl H. Schoenbach, "Electron Heating in Pulsed Atmospheric Pressure Glow Discharges," submitted to J. Appl. Phys.].

A summary of the achievement with respect to the goal space is shown in Fig. 1.

In addition to the work on plasma cathodes we have concentrated our efforts (DURIP grant: Test Facility for Atmospheric Pressure Plasmas, Grant No: F49620-98-1-0347) to the development of relevant diagnostic techniques for atmospheric pressure plasmas, particularly, power consumption, gas temperature and electron density.

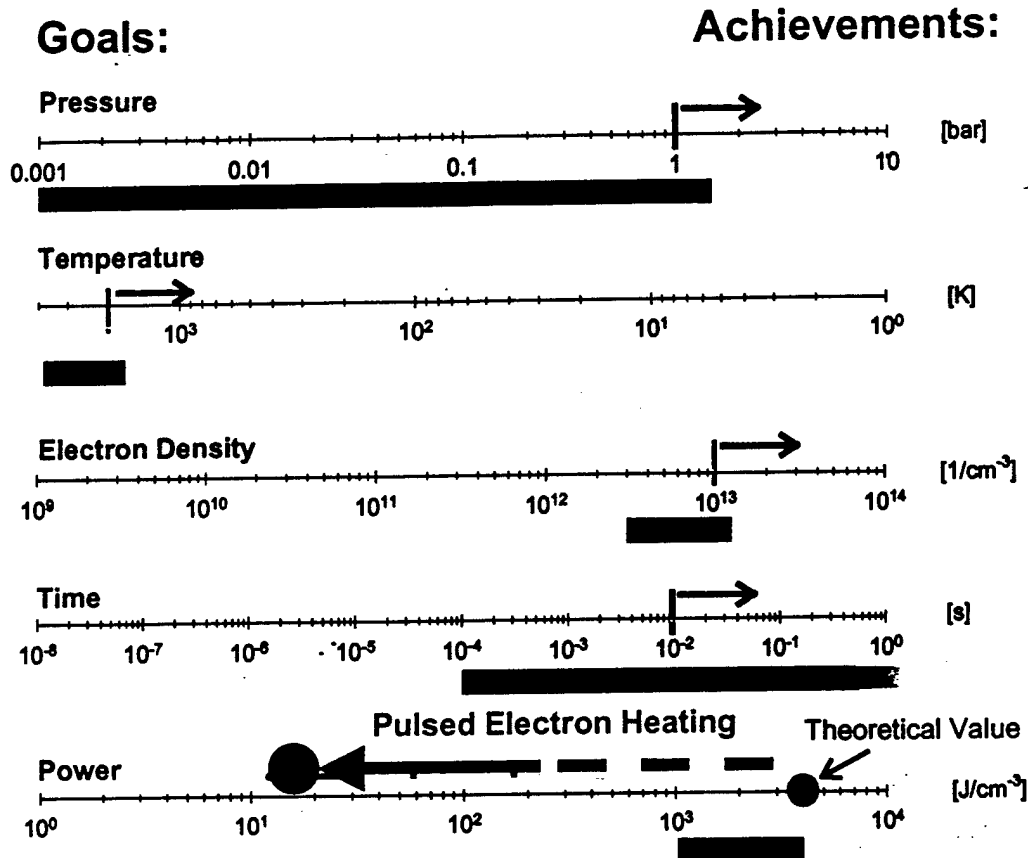
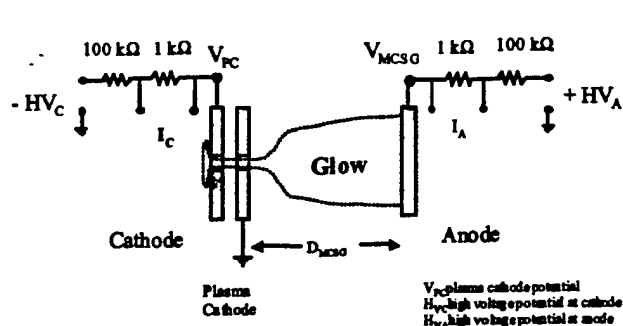


Fig. 1 Goals and Achievements

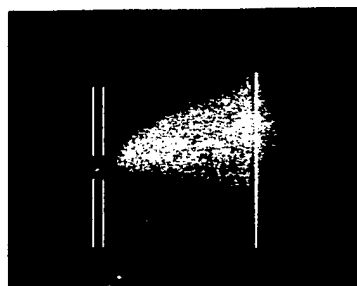
## 1. Stability

We were able to demonstrate experimentally the concept of using microhollow cathode discharges (MHCD) as plasma cathodes for high pressure glow discharges in general, first in argon, later in air. The typical electrode geometry and a photograph of an atmospheric pressure argon discharge is shown in Fig. 2. A paper has been published on our initial results (Robert H. Stark and Karl H. Schoenbach, *J. Appl. Phys.* **85**, 2075 (1999)) and a patent application on this novel concept has been submitted. The concept has been successfully applied to atmospheric pressure air, and the results of this study have been published (Robert H. Stark and Karl H. Schoenbach, *Appl. Phys. Lett.* **74**, 3770 (1999)).

The range of stable operation for both dc, and pulsed plasma cathodes based on microhollow cathode discharges was explored. The current density limit is determined by the onset of glow-to-arc transitions. It was found that discharges in one atmosphere air can be run in a stable mode up to approximately 20 mA. This corresponds to a current density in the hollow cathode of more than 250 A/cm<sup>2</sup>. In the pulsed mode discharge currents of almost 100 mA could be obtained for microsecond duration.



## Experimental Setup



- MCS glow discharge in argon at atmospheric pressure.
- $I_{MHCD} = 470 \mu A$ ,  $I_{MCS} = 500 \mu A$ ,  $V_{MHCD} = 169 V$ ,
- $V_{MCS} = 213 V$ ,  $d = 0.2 cm$

J. Appl. Phys., Vol. 85, No. 4, 15 Feb. 1999

Fig. 2 Experimental setup, and photograph of an argon atmospheric pressure glow.

## 2. Temporal Control

Voltage-current measurements of the hollow cathode discharge and the microhollow sustained glow discharge in atmospheric air, show that above a certain threshold current, required to ignite the microhollow cathode sustained glow, the current of the MHCD and that of the sustained glow are almost identical (Fig. 3). Variations in the microhollow discharge current, which can be obtained by small variations in microhollow discharge voltage cause identical changes in the sustained glow, independent of the voltage across

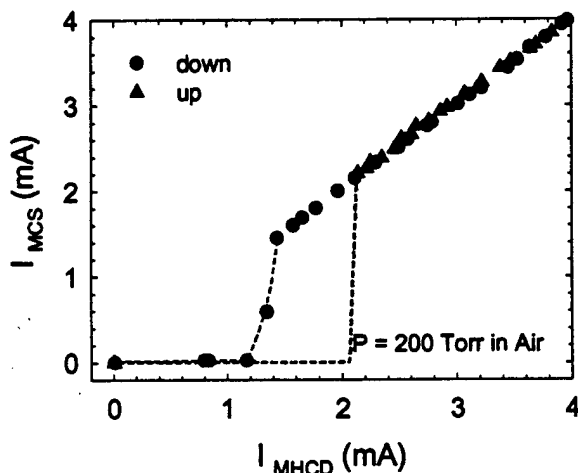


Fig. 3 Current of glow discharge ( $I_{MCS}$ ) versus plasma cathode current ( $I_{MHCD}$ ).

the glow. This controllability has been demonstrated in a switching experiment. With a voltage, greater than the sustaining voltage, applied to the main discharge gap, the microhollow cathode discharge was turned on and turned off. It could be shown that the current in the main discharge followed exactly the current of the micro discharge (plasma cathode). Experimental results are shown in Fig. 4.

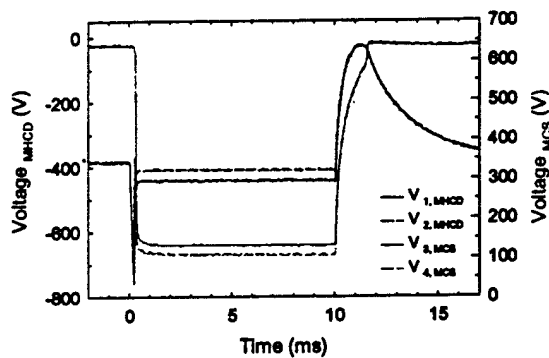


Fig. 4a Temporal development of the currents and voltages in a pulsed microhollow controlled glow discharge.

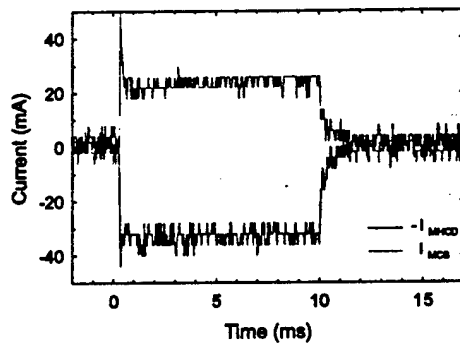


Fig. 4b Temporal development of the control current in the microhollow cathode discharge and the controlled current in the glow discharge

### 3. Gas Temperature

In order to obtain information on the gas temperature emission spectroscopy has been used. The rotational structure of the C to B transition in molecular nitrogen is being measured and used to extract information on the rotational temperature which is assumed to be identical with the gas temperature. The method is described in a paper presented at the 1999 AIAA (Rolf Block, Olaf Toedter, and Karl H. Schoenbach, Proc. 30<sup>th</sup> AIAA Plasmadynamics and Lasers Conf., Norfolk, VA, July 1999, paper AIAA-99-3434). The model which is used can be easily implemented and provides good estimates of the temperature. A more sophisticated model for the N<sub>2</sub> emission, with higher accuracy, has been developed by Christophe Laux et al (Christophe O. Laux, Richard J. Gessman, and Charles H. Kruger, "Measurements and Modeling of the Absolute Radiative Emission of Air Plasma between 190 and 800 nm," to be submitted to JQSRT, Summer 1999). In a joint project with the team at Stanford University, C. Laux has applied his model to our



plasma. The results are described in a second paper presented at the 1999 AIAA (Robert H. Stark, Uwe Ernst, Mohamed El-Bandrawy, Christophe Laux, and Karl H. Schoenbach, 30<sup>th</sup> AIAA Plasmadynamics and Lasers Conf., Norfolk, VA, July 1999). The gas temperature was found to depend linearly on the discharge current at currents up to 8 mA and seems to saturate at higher currents (Fig. 5).

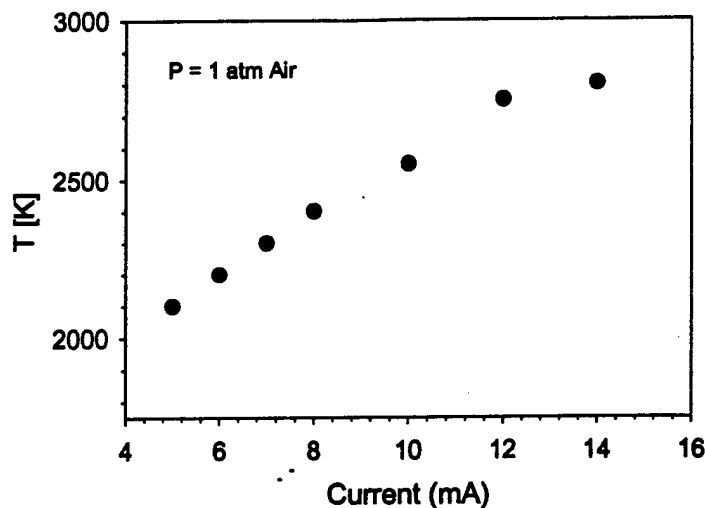


Fig. 5. Gas temperature in atmospheric pressure glow discharges with electron densities of approximately  $10^{13} \text{ cm}^{-3}$ .

In addition to emission spectroscopy we have applied CO<sub>2</sub> laser interferometry to obtain information on the gas temperature [Frank Leipold, Robert H. Stark, Ahmed El-Habachi, and Karl H. Schoenbach, "Electron Density Measurements in an Atmospheric Pressure Air Plasma by Means of IR Heterodyne Interferometry" to appear in Journal of Physics D: Applied Physics]. Laser interferometry was used in order to obtain the required spatial resolution of less than 100  $\mu\text{m}$ , a characteristic length of the Microhollow cathode discharge sustained plasmas.

The phase shift is determined by electrons and by heavy particles. In the range of interest, at electron densities of  $10^{13} \text{ cm}^{-3}$  and for the wavelength of the laser (10.6  $\mu\text{m}$ ) the heavy particle contribution to the index of refraction are dominant. However, using the fact that the time scale for the electron generation is much faster than heating of the gas, the contributions of electrons and heavy particles could be separated. Fast variations of the phase were assumed to be due to changes in the electron density, slower variations due to changes in the heavy particle density. The density of the heavy particles, atoms and molecules, is related to the gas temperature,  $T$ , through the ideal gas law,  $p = NkT$ . The results of these measurements on a one atmosphere air discharge (Fig. 6a) are shown in Fig. 6b.

#### 4. Electron Density

Laser interferometry has also allowed us to determine the electron density. The results of the measurements are shown in Fig. 6b. In order to obtain the value of the electron

density, independently from the laser interferometric method, we have used electrical diagnostics (current and voltage) and optical diagnostics (appearance of the plasma).

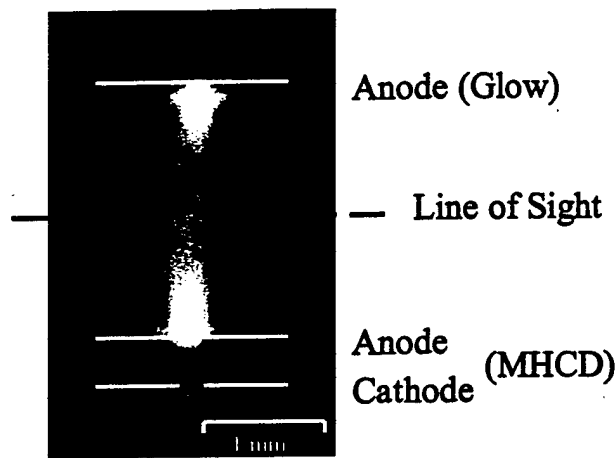


Fig. 6a. Side-on photograph of a microhollow cathode sustained atmospheric pressure air discharge. The gap is 2 mm, the current 10 mA, the sustaining voltage 360 V

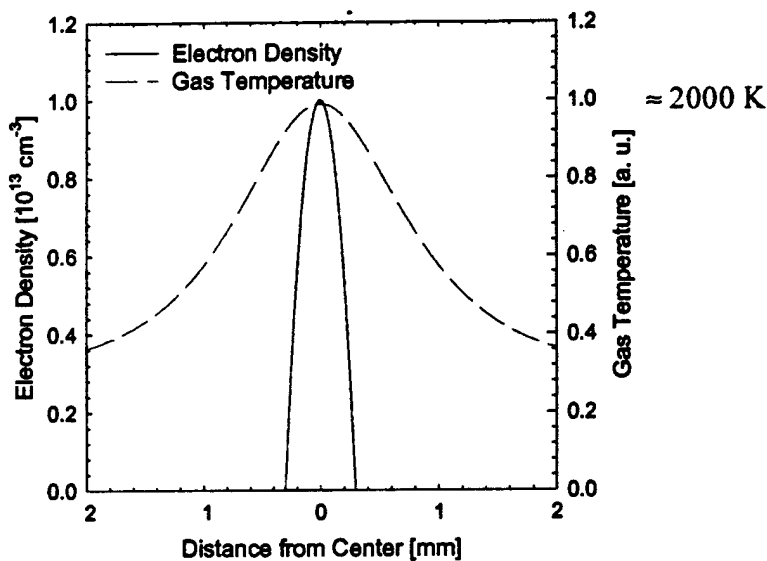


Fig. 6b. Radial electron density and temperature profile for the discharge plasma.

These fundamental diagnostic methods allow us to obtain information on stability, power consumption, average electric field,  $E$ , and current density,  $J$ , and through electron mobility data, information on the electron density,  $n_e$ . The electron mobility in air at room temperature,  $\mu_e$ , is related to the gas pressure,  $p$ , in the following way:

$$\mu_e p = 0.45 \cdot 10^6 \text{ cm torr/Vs} \quad [\text{Y.P. Raizer, } \underline{\text{Gas Discharge Physics}}, \text{ Springer, 1997, p. 11}].$$

Correcting the equation for the measured temperature of 2,000 K provides us with a value of the electron mobility at atmospheric pressure of  $3.9 \cdot 10^3 \text{ cm}^2/\text{Vs}$ . The electron density in the positive column of the atmospheric pressure air glow discharge can then be obtained from Ohm's law,  $J = en_e\mu_e E$ . It is  $5 \cdot 10^{12} \text{ cm}^{-3}$  for  $E = 1.2 \text{ kV/cm}$  and  $J = 3.8 \text{ A/cm}^2$ .

## 5. Plasma Volume

Large volume atmospheric pressure air plasmas, based on the microhollow cathode discharge sustained glow can be obtained by

1. increasing the electrode gap of the MHCD sustained glow discharge, and by
2. extending the plasma in lateral direction by superimposing the individual MHCD sustained glow discharges (formation of arrays).

Experiments with extended gap length have been performed. Fig. 7 shows photographs of discharges between electrodes of 4 mm and 20 mm distance between the electrodes. The maximum distance over which a glow discharge in atmospheric pressure air can be sustained is dependent on the discharge current. The distance increases from approximately 8 mm for 4 mA discharges to about 20 mm for 13 mA discharges [Fig. 8, insert].

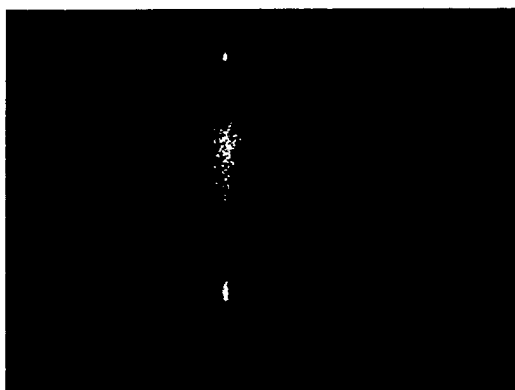
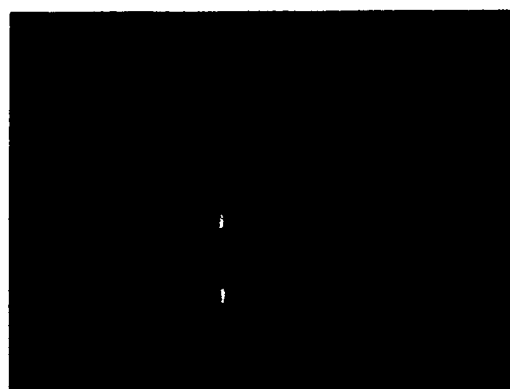
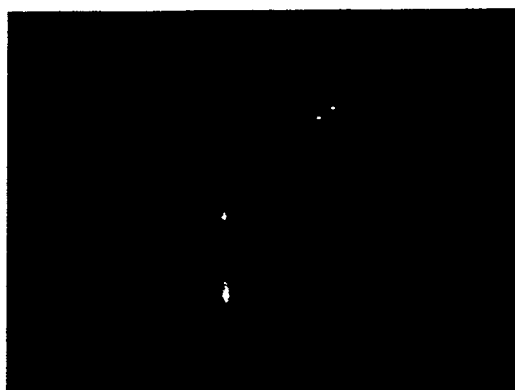


Fig. 7a. Upper left: Discharge in atmospheric pressure air with a current of 5 mA. The electrode gap is 7 mm.

Fig. 7 b. Upper right: Same as in Fig. 7 a, but at a current of 5 mA.

Fig. 7c. Same as 7a, but with an electrode gap of 20 mm.

The information on the maximum distance for which a stable discharge could be operated was obtained by increasing the gap in small steps and recording the discharge voltage at each step [Fig. 8]. This method allows us to determine the cathode fall voltage, which is the voltage value at which the voltage versus distance curves intersect the abscissa. The cathode fall in this discharge which is sustained by a microhollow cathode discharge is

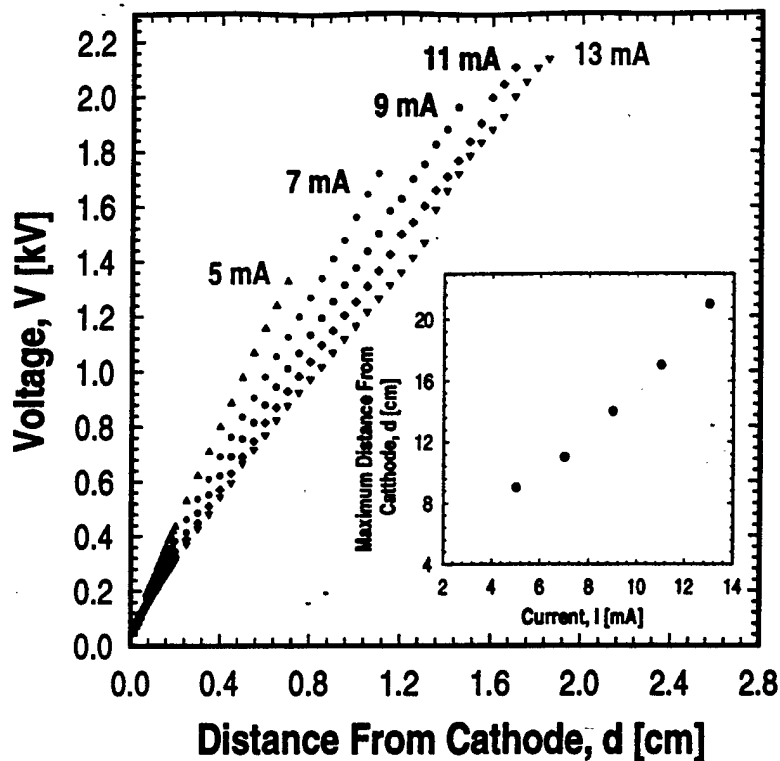


Fig. 8. Discharge voltage versus gap length with current as variable parameter. The gap length over which the discharges is stable depends on the discharge current [insert].

not zero, but has a finite value, dependent on the discharge current [Fig. 9]. It ranges between 40 and 20 V, with the highest value for the lowest current. This is still small

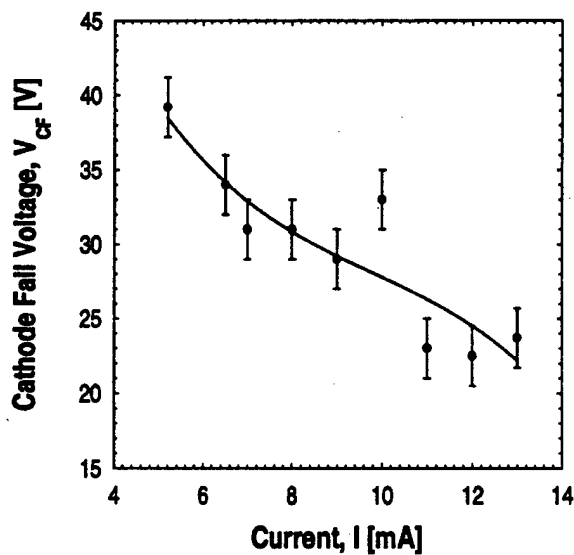


Fig. 9 Cathode fall voltage versus discharge current

compared to the normal cathode fall voltage of air, which is in the range from 180 V to 420 V for air [A. v. Engel and M. Steenbeck, Elektrische Gasentladungen, ihre Physik und Technik, vol 2, p. 103].

Differentiating the voltage versus distance curve allows us to obtain the electric field distribution. The result for the 13 mA discharge is shown in Fig. 10. The electric field decreases from a value of 1.6 kV/cm close to the cathode to a constant value of 1.1 kV/cm at distances greater than 1 cm. As the electric field, the current density decreases with increasing distance from the cathode (due to the increasing plasma cross-section as shown in Fig. 7c). The electron density in such a discharge decreases from  $2 \cdot 10^{12} \text{ cm}^{-3}$  at the cathode to approximately  $10^{11} \text{ cm}^{-3}$  in the range of constant J and E.

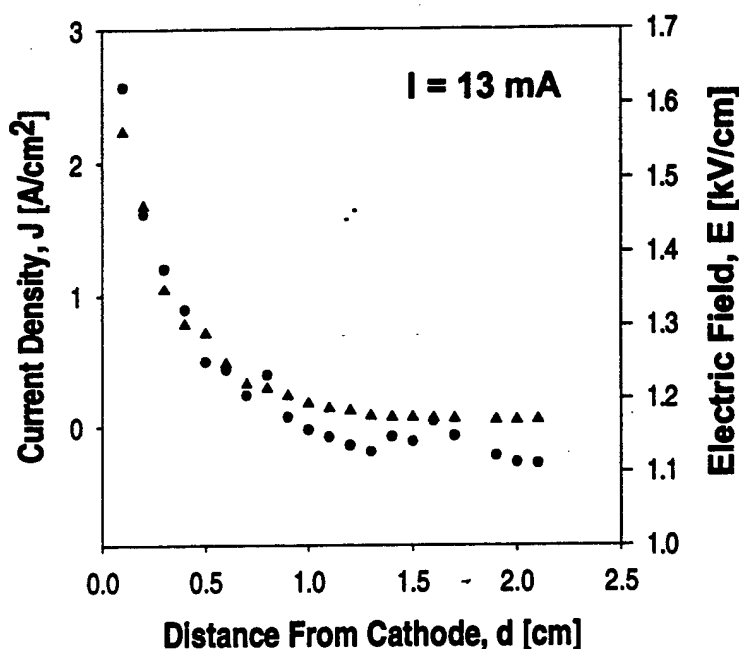


Fig. 10 Electric field intensity (red circles) and current density (green triangles) versus distance from cathode

Parallel operation of MHCD sustained glow discharges in air without ballast was demonstrated in the pressure range below hundred Torr, where the current-voltage characteristic of the MHCD has a positive slope. For higher pressures, and particularly for atmospheric pressure air the slope was found to be negative [Fig. 11], which indicates that ballasting of the individual discharges is necessary.

Atmospheric pressure air experiments have therefore be performed with parallel discharges. A photograph of such "discharge arrays" is shown in Fig. 12. It shows to parallel, ballasted discharges in atmospheric pressure air, 4 mm apart between electrodes 1.2 cm apart. The discharges merge and generate a homogeneous plasma in the gap between the electrodes. Instead of individually ballasting the discharges it is possible to use distributed ballast. The results of experiments in argon where a semi-insulating semiconductor was used as anode and distributed ballast indicated that this relatively simple method will allow us to operate arrays of discharges at atmospheric pressure air.

Results of parallel operation studies were published in IEEE Trans. Plasma Science (W. Shi, R.H. Stark, and K.H. Schoenbach, IEEE Trans. Plasma Science 27, 16 (1999)).

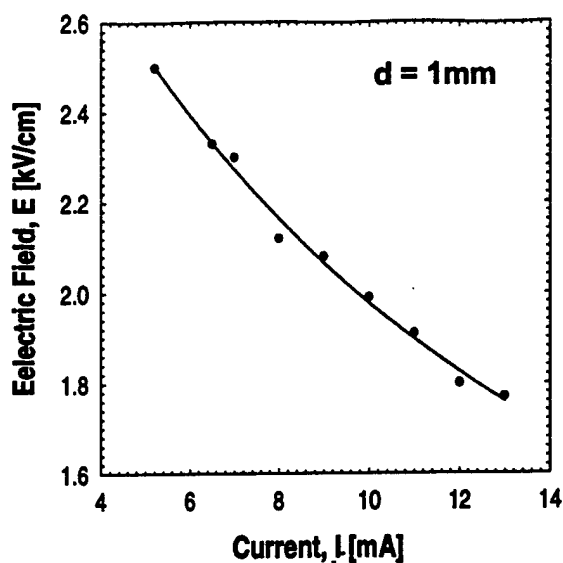


Fig. 11. Electric field measured at a distance of 1 mm from the cathode versus discharge current.

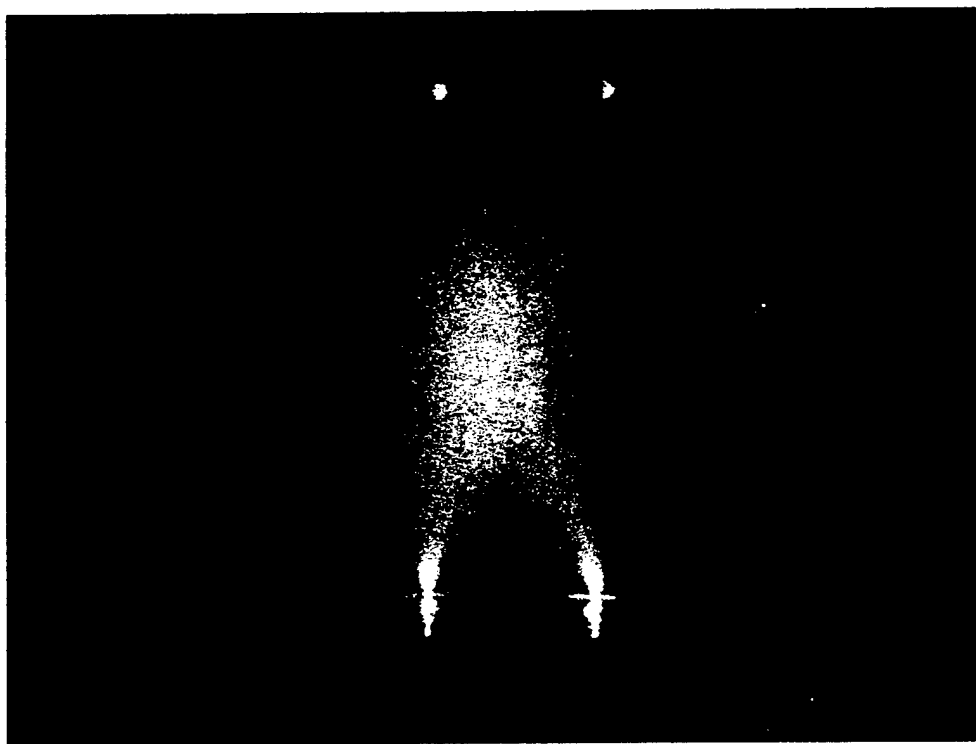


Fig. 12 Atmospheric pressure glow discharges in air sustained by two microhollow cathode glow discharges (bottom). The distance between the discharges is 4 mm, the gap is 1.2 cm.

## 6. Power Consumption

The theoretical value for the power per unit volume,  $P$ , required to sustain a plasma with a given electron density,  $n_e$ , is:

$$P = n_e W_{\text{ion}}/\tau$$

where  $W_{\text{ion}}$  is the average energy to generate an electron-ion pair, and  $\tau$  is the plasma lifetime. With  $W_{\text{ion}}$  for dry air being 33.7 eV, and  $\tau$  for an air plasma with an electron density of  $10^{13} \text{ cm}^{-3}$  being 10 ns [R.J. Vidmar, IEEE Trans. Plasma Science 18, 733 (1990)] the calculated value of  $P$  is  $5.4 \text{ kW/cm}^3$ . This value is almost identical with our experimental result of  $5.3 \text{ kW/cm}^3$ . The microhollow cathode sustained air plasma can therefore be considered as baseline plasma for nonthermal atmospheric pressure air discharges.

The parameters, which describe the plasma at its present state are listed in Fig. 1 and are compared with the goals of the plasma rampart program. Whereas the goals to reach a stable atmospheric pressure air plasma, scalable in size, at gas temperatures of less than 2,000 K and electron densities of  $10^{13} \text{ cm}^{-3}$  and greater have been achieved, the power consumption for the dc discharge operation is so far too high to be useful in Air Plasma Ramparts.

In order to reduce the power consumption several approaches have been considered:

- use of gas additives (such as He, or organic gases with low ionization potential),
- combustion
- heating of the electrons.

Experiments using helium (He) as additive have been performed. It was found that it has a positive effect on the gas temperature [Fig. 13], however, the reduction in power density was far less than required for use in Plasma Ramparts.

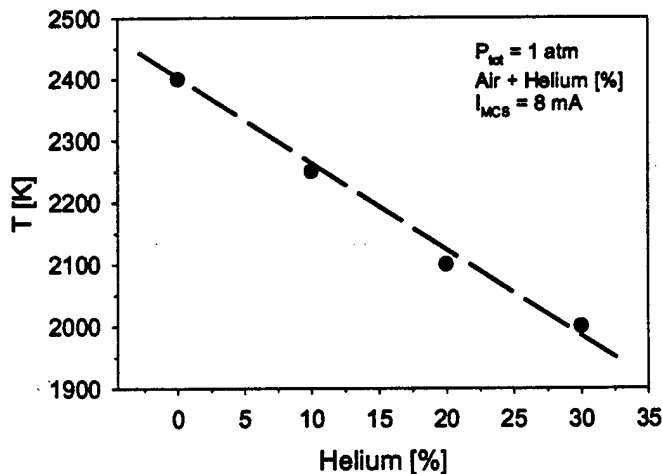


Fig. 13 Reduction in gas temperature with increasing concentration of helium in air.

The second approach seemed to be more promising. Combustion plasmas have been studied at Stevens Institute of Technology by E. Kunhardt. A stable discharge was generated in a hydrocarbon-air mixture at atmospheric pressure between parallel plate electrodes with a 7 cm separation. The initiating potential for the glow was 15 kV, while the sustaining voltage was found to be 1.6 kV. Assuming a cathode fall voltage of 250 V, the average electric field in the bulk of the discharge is 190 V/cm, more than an order of magnitude lower than the electric field in the raw air discharge. Power densities of far less than one kW/cm<sup>3</sup> can be expected by using this method. The reason for this reduction was assumed to be increased detachment of electrons from negative ions. However initial experiments in our lab have not yet confirmed the expected savings in power when the discharge was operated in the combustion mode. The experimental setup, and some results of the combustion experiment are described in the third progress report for this project.

The third approach, heating of the electrons (or, in other words, shifting of the electron energy distribution to larger values of energy,  $\epsilon$ ) seems to offer the highest rate of success. The concept can be understood by considering the effect of the electron energy distribution,  $f(\epsilon)$ , on the rate coefficients for gain and loss processes in the plasma and transport coefficients. Rate coefficients are defined as:

$$k = (2/m)^{1/2} \int \sigma(\epsilon) \epsilon^{1/2} f(\epsilon) d\epsilon$$

where  $\sigma(\epsilon)$  is the cross-section for the respective gain or loss process, and  $m$  is the electron mass. Another loss process, with respect to electron energy rather than electron density, is vibrational excitation, which for nitrogen has a peak at approximately 2 eV. Heating of the electron by using unmodulated or modulated pulses with duration of less than the electron relaxation time will not only reduce the losses in electron density but, more important, increase the gain. An strong increase in ionization can be expected, since the cross-section for ionization increases over the entire relevant range of electron energies in a self-sustained gas discharge. The transport coefficients are also affected by the electron heating. The electron mobility for dc plasmas, e.g. is defined as:

$$\mu = -(4\pi/3) (e/m) \int v^3 \partial f_0 / \partial v / \nu_m dv$$

where  $v$  is the electron velocity,  $\nu_m$  is the collision frequency, and  $f_0$  is the isotropic part of the distribution function,  $f$ . Again, the shape of the distribution function affects through the mobility, the electron density.

In order to study the effect of pulsed electric fields on the electron density, we have built a 10 ns pulse generator and applied the pulse to our dc plasma. The results of this study, which are described in the attached manuscript on 'Electron Heating in Pulsed Atmospheric Pressure Glow Discharges (submitted for publication in J. Appl. Phys.) are very encouraging with respect to power savings.



## 7. Cooperative Efforts

A set of diagnostic techniques, appropriate for the evaluation of APRP plasmas has been discussed and documented. Contributors to the "Recipe Booklet" were, besides the P.I. of this project, Charles Krueger and Christophe Laux of Stanford, Erich Kunhardt of Stevens Institute of Technology, Richard Miles of Princeton, and Rolf Block and Olaf Toedter of Old Dominion University. The topics of the booklet are a) electron density measurement techniques, and b) gas temperature measurement techniques. Editors are Dan Kelley (Boeing) and Karl H. Schoenbach (Old Dominion University).

Besides the collaborative work with the Stanford, Princeton and Stevens group on the development of diagnostic techniques for the APRP plasma, the ODU team has established research ties to the research group at Stevens, University of Wisconsin, and Stanford. K. Becker at Stevens is performing spectral measurements in the VUV on microhollow cathode discharges, with the goal to obtain information on the electron energy distribution. He has observed neon excimer emission at 86 nm, indicating electron energies greater than 15 eV. The discharge chamber for these studies was provided by ODU. Prof. Scharer at the University of Wisconsin, Madison, is working with us on microwave diagnostics of plasmas. He is using temporarily a microwave interferometer which was obtained by ODU [K.L. Kelly, J.E. Scharer, M. Laroussi, R. Block, and K.H. Schoenbach, "Measuring Electron Densities in Highly Collisional Plasmas Using a 110 GHz Interferometer," Conf. Record, IEEE Intern. Conf. Plasma Science, New Orleans, 2000, paper 2P26, p. 147], and will provide guidance in setting up a similar experiment at ODU. The cooperation with the group at Stanford on modeling of nitrogen spectra has resulted in a joint publication (Robert H. Stark, Uwe Ernst, Mohamed El-Bandrawy, Christophe Laux, and Karl H. Schoenbach, 30<sup>th</sup> AIAA Plasmadynamics and Lasers Conf., Norfolk, VA, July 1999).

Most recently (spring 2000) we have intensified our collaboration with the Stanford University group under the guidance of Prof. C. Kruger. A similar pulse generator as used at Old Dominion University has been provided to this group to support their studies on pulsed electric field effect on atmospheric pressure plasmas. Dr. R. Stark, a senior scientist in our laboratory has helped to set the system up, and has assisted in the measurements at Stanford. The results of this collaborative effort have strongly supported the pulsed electric field concept, and have been published as a conference paper [Manoj Nagulapally, Graham V. Candler, Christophe O. Laux, Lan Yu, Denis Packan, Charles H. Kruger, Robert H. Stark, Karl H. Schoenbach, "Experiments and Simulations of DC and Pulsed Discharges in Air Plasmas," 31<sup>st</sup> AIAA Plasmadynamics and Lasers Conf., Denver, CO, July 2000, paper AIAA 2000-2417].

## **Publications and Presentations**

### **Journal Publications**

Robert H. Stark and Karl H. Schoenbach, "Electron Heating in Pulsed Atmospheric Pressure Glow Discharges," submitted to J. Appl. Phys.

Frank Leipold, Robert H. Stark, Ahmed El-Habachi, and Karl H. Schoenbach, "Electron Density Measurements in an Atmospheric Pressure Air Plasma by Means of IR Heterodyne Interferometry" to appear in Journal of Physics D: Applied Physics

Karl H. Schoenbach, Ahmed El-Habachi, Mohamed M. Moselhy, Wenhui Shi, and Robert H. Stark, "Microhollow Cathode Discharge Excimer Lamps," Invited Paper, Physics of Plasmas 7, 2186 (2000).

Robert H. Stark and Karl H. Schoenbach, "Direct Current Glow Discharges in Atmospheric Air," Appl. Phys. Lett. 74, 3770 (1999).

W. Shi, R.H. Stark, and K.H. Schoenbach, "Parallel Operation of Microhollow Cathode Discharges," IEEE Trans. Plasma Science 27, 16 (1999).

Robert H. Stark and Karl H. Schoenbach, "Direct current high-pressure glow discharges," J. Appl. Phys. 85, 2075 (1999).

### **Publications in Conference Proceedings**

Manoj Nagulapally, Graham V. Candler, Christophe O. Laux, Lan Yu, Denis Packan, Charles H. Kruger, Robert H. Stark, Karl H. Schoenbach, "Experiments and Simulations of DC and Pulsed Discharges in Air Plasmas," 31<sup>st</sup> AIAA Plasmadynamics and Lasers Conf., Denver, CO, July 2000, paper AIAA 2000-2417.

Rolf Block, Mounir Laroussi, Frank Leipold, and Karl H. Schoenbach, "Optical Diagnostics for Non-Thermal High Pressure Discharges," Proc. 14<sup>th</sup> Intern. Symp. Plasma Chemistry, Prague, Czech Republic, August 1999, Volume II, p. 945.

Robert H. Stark, Uwe Ernst, Mohamed El-Bandrawy, Christophe Laux, and Karl H. Schoenbach, "Direct Current Glow Discharges in Atmospheric Air," Proc. 30<sup>th</sup> AIAA Plasmadynamics and Lasers Conf., Norfolk, VA, July 1999, paper AIAA-99-3666.

Rolf Block, Olaf Toedter, and Karl H. Schoenbach, "Gas Temperature Measurements in High Pressure Glow Discharges in Air," Proc. 30<sup>th</sup> AIAA Plasmadynamics and Lasers Conf., Norfolk, VA, July 1999, paper AIAA-99-3434.

## Abstracts of Conference Presentations

Robert H. Stark and Karl H. Schoenbach, "Electron Heating in Atmospheric pressure Air Discharges," Conf. Record, IEEE Intern. Conf. Plasma Science, New Orleans, 2000, paper 1A05, p. 83.

Rolf Block, Abdel-Aleam H. Mohamed, and Karl H. Schoenbach, "Plasma Cathode Sustained Filamentary Glow Discharges in Atmospheric Air," Conf. Record, IEEE Intern. Conf. Plasma Science, New Orleans, 2000, paper 1P23, p. 110.

Robert H. Stark, Ahmed El-Habachi, and Karl H. Schoenbach, "Parallel Operation of Microhollow Cathode Discharges," Conf. Record, IEEE Intern. Conf. Plasma Science, New Orleans, 2000, paper 1P24, p. 111.

K.L. Kelly, J.E. Scharer, M. Laroussi, R. Block, and K.H. Schoenbach, "Measuring Electron Densities in Highly Collisional Plasmas Using a 110 GHz Interferometer," Conf. Record, IEEE Intern. Conf. Plasma Science, New Orleans, 2000, paper 2P26, p. 147.

Frank Leipold, Robert H. Stark, Ahmed El-Habachi, and Karl H. Schoenbach, "Electron Density Measurements in Pulsed Atmospheric Pressure Plasmas by IR Heterodyne Interferometry," Conf. Record, IEEE Intern. Conf. Plasma Science, New Orleans, 2000, paper 3P24, p. 178.

Invited: K.H. Schoenbach "Microhollow Cathode Discharge Excimer Lamps," Bull APS (DPP), Vol. 44, No. 7, November 1999, S12 5, p. 285.

Frank Leipold, Robert H. Stark, Ahmed El-Habachi, Karl H. Schoenbach, "Electron Density and Temperature Measurements in an Atmospheric Pressure Air Plasma by Heterodyne Interferometry," Bull APS (GEC), Vol. 44, No. 4, October 1999, ETP3 31, p. 24.

Invited: Karl H. Schoenbach, "Microhollow Cathode Discharge Excimer Lamps," Bull APS (GEC) Vol. 44, No. 4, October 1999, LR2 1, p. 66.

Robert H. Stark, Karl H. Schoenbach, "Atmospheric Pressure Glow Discharges in Air," Bull APS (GEC), Vol. 44, No. 4, October 1999, QF2 3, p. 78.

Invited: Rolf Block, Mounir Laroussi, and Karl H. Schoenbach, "Test Facility for High Pressure Plasmas," Proc. IEEE Intern. Conf. Plasma Science, Monterey, CA, June 1999, p. 116.

Robert H. Stark, Uwe Ernst, Rolf Block, Mohamed El-Bandrawy, and Karl H. Schoenbach, "Microhollow Cathode Discharges in Atmospheric Pressure Air," Proc. IEEE Intern. Conf. Plasma Science, Monterey, CA, June 1999, p. 117.

Robert H. Stark and Karl H. Schoenbach, "Microhollow Cathode Discharges as Plasma Cathodes for Atmospheric Pressure Glow Discharges in Air," Proc. IEEE Intern. Conf. Plasma Science, Monterey, CA, June 1999, p. 198.

Uwe Ernst, Robert H. Stark, Karl H. Schoenbach, Klaus Frank, and Werner Hartmann, "Pulsed Operation of Microhollow Cathode Discharges in Atmospheric Air," Proc. IEEE Intern. Conf. Plasma Science, Monterey, CA, June 1999, p. 198.

Invited: Robert H. Stark and Karl H. Schoenbach, "Direct Current Atmospheric Pressure Glow Discharges," Verhandlungen der Deutschen Physikalischen Gesellschaft (DPG), 63. Physikertagung, Heidelberg, Germany, March 1999, p. 349.

Uwe Ernst, Robert H. Stark, Karl H. Schoenbach, Klaus Frank, and Werner Hartmann, "Pulsed Operation of Microhollow Cathode Discharges in Atmospheric Air," Verhandlungen der Deutschen Physikalischen Gesellschaft (DPG), 63. Physikertagung Heidelberg, Germany, March 1999, p. 349.

Robert H. Stark, Wenhui Shi, and Karl H. Schoenbach, "Parallel Operation of Microhollow Cathode Discharges," Verhandlungen der Deutschen Physikalischen Gesellschaft (DPG), 63. Physikertagung Heidelberg, Germany, March 1999, p. 370.

Robert H. Stark, Wenhui Shi, and Karl H. Schoenbach, "Parallel Operation of Microhollow Cathode Discharges," Bull. APS, Vol. 43, No. 6, October 1998, JTP6 8, p. 1466.

Robert H. Stark and Karl H. Schoenbach, "Plasma Cathodes as Electron Sources for Large Volume, High-Pressure Glow Discharges," Bull. APS, Vol. 43, No. 5, October 1998, NW1 1, p. 1478.

Rolf Block, Olaf Toedter, and Karl H. Schoenbach, "Temperature Measurement in Microhollow Cathode Discharges in Atmospheric Air," Bull. APS, Vol. 43, No. 5, October 1998, NW1 2, p. 1478.

Robert H. Stark and Karl H. Schoenbach, "Plasma Cathodes for Large Volume, High-Pressure Glow Discharges," Conf. Record 1998 IEEE Intern. Conf. Plasma Science, Raleigh, NC, Abstract 5C06, p. 241.

Robert H. Stark and Karl H. Schoenbach, "Microhollow Cathode Discharges as Electron Sources," Conf. Record 1998 IEEE Intern. Conf. Plasma Science, Raleigh, NC, Abstract 6P34, p. 276.

Karl H. Schoenbach, Erich E. Kunhardt, Christophe O. Laux, and Charles H. Kruger, "Measurement of Electron Densities in Weakly Ionized Atmospheric Pressure Air," Conf. Record 1998 IEEE Intern. Conf. Plasma Science, Raleigh, NC, Abstract 6P50, p. 283.

Wenhui Shi and Karl H. Schoenbach, "Parallel Operation of Microhollow Cathode Discharges," Conf. Record 1998 IEEE Intern. Conf. Plasma Science, Rayleigh, NC, Abstract 6P51, p. 283.

Robert H. Stark, Ahmed El-Habachi, and Karl H. Schoenbach, "High Pressure, Direct Current Microhollow Electrode Discharges," Verhandlungen der Deutschen Physikalischen Gesellschaft (DPG), 62. Physikertagung Bamberg, Germany, March 1998, P10.1.

Robert H. Stark and Karl H. Schoenbach, "Plasma Cathodes for High Pressure Glow Discharges," Verhandlungen der Deutschen Physikalischen Gesellschaft (DPG), 62. Physikertagung Bamberg, Germany, March 1998, P24.19.

### **Invited Talks**

Karl H. Schoenbach, "Microhollow Cathode Discharges," Applied Research Center Colloquium, Newport News, VA, April 20, 2000.

Karl H. Schoenbach, "Microhollow Cathode Discharges," Erik Jonsson School of Engineering and Computer Science, The University of Texas at Dallas, TX, April 17, 2000.

Karl H. Schoenbach, "Microhollow Cathode Discharges," Department of Mechanical Engineering, University of Minnesota, (Broadcast on UNITE Channel A), February 9, 2000.

Karl H. Schoenbach, "Microhollow Cathode Discharge Excimer Lamps," American Physical Society, 41<sup>st</sup> Annual Meeting of the Division of Plasma Physics, Seattle, WA, November 18, 1999.

Karl H. Schoenbach, "Microhollow Cathode Discharge Excimer Lamps," Gaseous Electronics Conference, Norfolk, VA, October 7, 1999.

K.H. Schoenbach, "High Pressure Hollow Cathode Discharges," Center for Plasma Aided Manufacturing Annual Meeting/Workshop, July 7-8, 1999, Madison, WI.

Rolf Block, Mounir Laroussi, and Karl H. Schoenbach, "Test Facility for High Pressure Plasmas," IEEE Intern. Conf. Plasma Science, Monterey, CA, June 1999.

Robert H. Stark and Karl H. Schoenbach, "Direct Current Atmospheric Pressure Glow Discharges," 63. Physikertagung, Heidelberg, Germany, March 1999.

K.H. Schoenbach, "High Pressure Hollow Cathode Discharges," Department of Electrical Engineering - Electrophysics, University of Southern California, Los Angeles, CA, April 9, 1998.

K.H. Schoenbach, "High Pressure Hollow Cathode Discharges," Seminar, Department of Electrical Engineering, University of Maryland , College Park, MD, April 3, 1998.

### **Patent Application**

"A Novel Plasma Cathode for High-Pressure Glow Discharges", Inventors: Karl H. Schoenbach and Robert H. Stark, submitted: May 1999, as provisional patent application, ODURF 98013, May 2000 as regular patent application.

# **Publications and Presentations**

# **Journal Publications**



# Electron Heating in Pulsed Atmospheric Pressure Glow Discharges

Robert H. Stark and Karl H. Schoenbach  
Physical Electronics Research Institute, Old Dominion University,  
Norfolk, Virginia 23529

## Abstract

The application of nanosecond voltage pulses to weakly ionized atmospheric pressure plasmas allows heating the electrons without considerably increasing the gas temperature, provided that the duration of the pulses is less than the critical time for the development of glow-to-arc transitions. The shift in the electron energy distribution towards higher energies causes a temporary increase in the ionization rate, and consequently a strong rise in electron density. This increase in electron density is reflected in an increased decay time of the plasma after the pulse application. Measurements of the temporal development of the voltage across an atmospheric pressure glow discharge in air and the optical emission in the visible after applying a 10 ns high voltage pulse showed an increase in plasma decay time from tens of nanoseconds to microseconds when the pulsed electric field amplitude was raised from 10 kV/cm to 40 kV/cm. Temporally resolved photographs of the discharge showed that the plasma column expands during this process. The nonlinear electron heating effect can be used to reduce the power consumption in a repetitively operated air plasma considerably compared to a dc plasma operation. Besides allowing power reduction, pulsed electron heating has also the potential to enhance plasma processes, which require elevated electron energies, such as excimer generation for ultra violet lamps.

## Introduction

High pressure glow discharges are used in plasma processing, gas lasers, chemical and bacterial decontamination of gases, and as mirrors and absorbers of microwave radiation. The latter applications require the use of air plasmas at atmospheric pressure. Transient high pressure glow discharges in air, such as barrier discharges [1] and ac discharges are already well established, but recently high pressure dc discharges with dimensions of centimeters have been generated by using novel plasma cathodes [2,3]. One of them is a microhollow cathode discharge sustained plasma, where the microhollow cathode discharge provides the electrons for the main discharge. The elimination of the cathode fall, the cradle for glow-to-arc transition has allowed us to generate dc glow discharges in atmospheric pressure air with electron densities of  $10^{13} \text{ cm}^{-3}$  and gas temperature below 2000 K [4,5]. The electrical power density required to sustain these plasmas is approximately  $5 \text{ kW/cm}^3$ , a power which limits the size of the plasma to values on the order of cubic-centimeter, due to economic and thermal management reasons.

The electric field strength required to sustain the  $10^{13} \text{ cm}^{-3}$  electron density plasma was measured as 1.2 kV/cm. At a gas temperature of 2000 K, the gas density,  $N$ , is  $3.7 \cdot 10^{18} \text{ cm}^{-3}$ , the reduced electric field strength,  $E/N$ , consequently 32 Td. The electron energy distribution function,  $f(\epsilon)$ , where  $\epsilon$  is the electron energy, in these dc high pressure plasmas is fully determined by the reduced electric field,  $E/N$ . For air at atmospheric pressure, and an  $E/N$  of 32 Td it is shown in Fig. 1. The electron energy distribution was calculated by means of "ELENDF" [6]. The cross-section for ionization,  $\sigma_{\text{ion}}$ , of nitrogen and oxygen, the major gas components in air, are shown in the same figure [7]. Multiplying the cross-section with the electron energy distribution and the

square root of the electron energy integrated over the energy provides us with the ionization rate coefficient,  $k$ .

$$k = \frac{1}{2\pi} \cdot \int_0^{\infty} \epsilon^{1/2} \cdot f(\epsilon) \cdot \sigma_{ion}(\epsilon) d\epsilon \quad [1]$$

The ionization rate coefficient increases strongly with  $E/N$  for electric fields which are greater than the electrical field required to sustain the discharge in a steady-state mode (in our case 32 Td). This is shown in fig. 1, where the non-equilibrium electron energy distribution (for the case of a 1 ns rise time pulse of 120 Td amplitude after a time of 50 ns) is clearly shifted into the range of increasing ionization cross-sections. This increase in ionization rate leads to a strong increase in electron density. The electrons transfer their energy to the heavy particles, heating the gas. Gas heating leads to glow-to-arc transitions [2]. For atmospheric pressure glow discharges in air the time constant for the development of an arc is on the order of nanoseconds, the same order of magnitude as the electron relaxation time. The electron relaxation time,  $\tau_e$ , the time the electrons need to transfer their energy to heavy particles by means of electron collisions, is:

$$\tau_e = \frac{M}{2m} \cdot \frac{1}{\nu_c} \quad [2]$$

where  $\nu_c$  is the electron collision frequency which for atmospheric pressure air is about  $10^{12} \text{ s}^{-1}$  [8];  $m$  and  $M$  are the masses of the electrons and the heavy collision partner, gas atoms and molecules, respectively.

In order to shift the electron energy distribution to higher energies, by means of a pulsed electric field, the duration of the pulse needs to be less than the time for the development of glow-to-arc transitions. The higher the electric field, the shorter the pulse needs to be. The increased rate of ionization causes a strong increase in electron density, as noted before. The electron density obtained by applying a 10 ns, trapezoidal pulse, with a rise and fall time of 1 ns, right at the end of the pulse is shown in Fig. 2 with the reduced electric field,  $E/N$ , as variable parameter.

The electron density increases super-linearly from  $1 \cdot 10^{13} \text{ cm}^{-3}$  at 60 Td to  $3.8 \cdot 10^{16} \text{ cm}^{-3}$  at 250 Td. Consequently, assuming that the electron losses after the E-field application are due to recombination only, the decay time of the electron density,  $t_d$ , increases from tens of nanoseconds to microseconds. The decay time is defined as the time it takes to reduce the electron density from its peak value,  $n_{e,p}$ , to an equilibrium value,  $n_{e,0}$ :

$$t_d = (n_{e,p} - n_{e,0}) / (\beta n_{e,0} n_{e,p}) \quad [3]$$

with  $\beta$  being the electron-ion recombination coefficient. This time approaches the constant value:

$$t_d = 1 / (\beta n_{e,0}) \quad [4]$$

for  $n_{e,p} \gg n_{e,0}$ .

For air with an assumed  $\beta \approx 10^{-7} \text{ cm}^3 \text{ s}^{-1}$  [8] and an equilibrium electron density of  $10^{13} \text{ cm}^{-3}$  it is on the order of one microsecond.

In order to explore the electron heating effect of short electric pulses in a high pressure gas we have studied the temporal decay of the electron density in a MHCD sustained plasma in atmospheric pressure air. The temporal development of electron density after applying a short electric pulse is reflected in the temporal development of the electrical parameters of the discharge and the emission of recombination radiation. Both quantities were measured dependent on the amplitude of the applied 10 ns pulse. In addition the temporal development of the discharge plasma was recorded by means of a high speed camera.

### Experimental Setup

A schematic sketch of the experimental setup is shown in Fig. 3. The microhollow cathode discharge (MHCD) serves as plasma cathode, which sustains a stable atmospheric pressure glow discharge [3]. The MHCD plasma is generated between two plane-parallel molybdenum electrodes, which are separated by an alumina spacer, 100  $\mu\text{m}$  in thickness. Electrode distance and diameter of the circular opening in the center of the electrodes are 100  $\mu\text{m}$ , respectively. The glow discharge, sustained by the MHCD plasma cathode, fills the gap between the plasma cathode and a positively biased, third electrode, at a distance of 1 mm. Both, plasma cathode and the supported glow discharge were operated dc in atmospheric humid air at 10 mA discharge current. Inserted into the electrode schematics in Fig. 3 is a side-on photograph of the air glow. The diameter of the plasma column is typically 800  $\mu\text{m}$ . In order to shift the electron energy distribution function to higher energies, a 10 ns, high voltage pulse was superimposed to the dc glow. Also shown in Fig. 3 is a measured pulse form of the high voltage pulse. Rise time and fall time of the trapezoidal pulse is approximately 1 ns.

The trapezoidal high voltage pulse is generated by a pulse forming network (PFN) in strip-line geometry. Fig. 4 shows the schematics of the 10 ns pulse generator. The PFN consists of two metal strips separated by a dielectric. The strip-line has an impedance of 10 Ohm. The electrical energy is switched into the load by means of pressurized spark gaps with nanosecond pulse rise time. The pulse generator is operated in self-breakdown mode at "single shot" conditions.

The discharge current and the voltage across the pulsed glow discharge have been monitored by means of fast rise time, high voltage probes (Tektronix, 350 MHz) and a 400 MHz digitizing oscilloscope (Tektronix TDS 380). In addition, measurements of transient emission of plasma radiation in the visible have been performed. The optical emission from the center of the glow discharge gap was observed side-on by means of a photo multiplier tube (PMT - Hamamatsu 1350) with a sensitivity range between 200 nm and 700 nm. The temporal resolution is determined by the photomultiplier to 2.4 ns. The PMT measurements were complemented by high-speed photography. A high-speed camera (ICCD Max, Stanford Research Institute) was used to study the development of the glow discharge plasma column temporally and spatially resolved. The camera was triggered by the signal of the voltage monitor of the 10 ns pulse generator. The internal delay of the camera, which was approximately 80 ns, limited the study of the plasma to the afterglow phase of the discharge. The camera is equipped with an image intensifier (micro-channel plate, MCP) and allows measurements with a temporal resolution up to 2 ns. However, due to the relatively low level of light emitted by the plasma, the exposure time was set to 200 ns.

### Results

Fig. 5 shows the temporal development of the voltage across the glow discharge plasma in response to high voltage pulses of various amplitudes (superimposed to the dc voltages). The voltage across the dc plasma decreases within a few nanoseconds after application of the pulsed

voltage by one order of magnitude. The sustaining electric field drops to values as low as 300 V/cm for an applied pulse with 20 kV/cm amplitude. Depending on pulse amplitude the discharge electric field remains at this low level for several hundred nanoseconds for 10 kV/cm pulses, up to several microseconds for 30 kV/cm pulses. During recovery of the discharge voltage, at electric fields of approximately 3 kV/cm, a dip in voltage is observed. This dip may be caused by interaction of the glow discharge with the sustaining plasma cathode, which turns on again at this voltage, after seemingly not being active from the time of applied pulse to this point in time. After this dip, the rise of the voltage slows by more than a factor of two.

Fig. 6 shows the temporal development of the optical emission of the plasma in the visible and near ultraviolet in response to the 10 ns voltage pulse for various pulse voltages. When the voltage pulse is applied, the intensity rises within nanoseconds by almost two orders of magnitude over the dc-value. The peak intensity varies only slightly with pulse voltage. After pulsing the intensity decays to the dc-level on a time scale which is several orders in magnitude larger than the duration of the applied pulse.

Fig. 7 shows the increase in decay time with increasing pulsed electric field amplitudes, evaluated from electrical and optical measurements [Fig. 5 and Fig. 6]. The decay time increases nearly linearly with pulsed electric field from 20 ns at 17.5 kV/cm to 3.8  $\mu$ s at 40 kV/cm. For the intensity measurements the decay time has been defined as the time the intensity decays to a constant value - 6.5 in arbitrary units, in Fig. 6 - which corresponds to approximately 10% of the initial intensity values. For the electrical measurements the decay time has been defined as the time for the voltage to increase from its lowest sustaining voltage level to 300 volts, a value which corresponds to approximately 70% of the dc value. The reason for the choice of these definitions for the decay time (which will be discussed in more detail in the following section), rather than using that introduced earlier [equ. 3] is the relatively large noise-to-signal ratio in the measured signals which makes it difficult to determine the time when the voltage and intensity reach the dc level after pulse application.

High-speed photography in the afterglow of the plasma shows the formation of a luminous plasma close to anode. The optical emission of the pulsed plasma was such that even for an exposure time of 200 ns, the remaining parts of the plasma between anode and cathode could not be observed. The diameter of the plasma at the anode is up to 5 to 10 times the diameter of the dc plasma column, which is shown in Fig. 3. It decays on a time scale of microseconds, in accordance with electrical and PMT measurements [Fig. 6 and Fig. 7].

## Discussion

Although the results of the measurements are not comprehensive (e.g. in order to obtain the electron density from electrical measurements, we would need to know the values of the local electric fields and the current density in addition to the electron mobility), certain conclusions on the effect of electrical pulses on the physics of the discharge and on the temporal development of the electron density can be drawn. When the high voltage pulse is applied, the current changes rapidly, and the microhollow cathode discharge is not able anymore to provide the required electrons to sustain the discharge. The current in this phase consists of conduction current plus displacement current. The displacement current is estimated to be on the order of one ampere. Higher currents can only be conduction currents, most likely generated by extending the cathode surface, this means by generating a discharge, which at least for a short time is sustained by gamma processes at the cathode, rather than by the MHCD. This hypothesis is supported by the high-speed photographs, which show an expanded plasma channel after pulse application. With reduced conductivity (increasing voltage across the gap) the plasma cathode eventually takes over

again. This might explain the dip in the recovering voltage seen in Fig. 5, and the subsequent change in slope.

The electron decay time increases linearly with the amplitude of the applied electric field pulse. This is shown in Fig. 7, where the time for voltage recovery, defined as the time where the electrical reaches 3 kV/cm, which is approximately 70% of its dc value, is plotted versus the applied electric field. Since the conductivity is proportional to the electron density, this curve provides us with information on the electron decay time, assuming that the current density stays constant. Also shown in this graph is the decay time of the optical emission, defined as the time where the intensity has decayed to a constant value, which corresponds to approximately 10% of the initial value. Assuming that the decay of the electron density is mainly due to recombination, the optical emission varies with the square of the electron density. For the electron density, a decay of the intensity to 10% would consequently correspond to a decay of the conductivity to 30%. The experimental results, obtained from electrical and optical measurements agree well, and also agree reasonably well with theoretical results [Fig. 2], considering the uncertainty in the value of the recombination coefficient  $\beta$ .

One of the incentives for this study was to explore the pulsed electron heating effect as a means to reduce the power consumption of atmospheric pressure glow discharges in air. For this application a pulsed electric field would be applied repetitively to a base plasma with low degree of ionization. This electrical pulse, if shorter than the time for the development of glow-to-arc transitions, would raise the electron density to values,  $n_{e,p}$ , exceeding the desired electron density,  $n_{e,0}$ , for a particular application. The electron density would then decay. When it reaches the value of  $n_{e,0}$  a second pulse would be applied, to bring the density up to  $n_{e,p}$  again. This process could be repeated ad infinitum.

Experimental studies with the same pulse generator but applied to a differently sustained dc plasma than the one described in this paper, and modeling studies have shown that for the 10 ns pulse, this mode of operation would allow us to create a plasma with an electron density which always exceeds  $n_{e,0}$ , at a fraction of the energy cost that is required to run the discharge only dc [9]. In these experiments the background gas temperature was kept constant over an area of about 1 cm in diameter, large compared to the diameter of the discharge plasma column, using a plasma torch. A two pin electrode configuration has been used to generate an atmospheric pressure dc plasma which than was superimposed by the 10 ns high voltage pulse. It could be shown that it is possible to reduce the power consumption in an atmospheric pressure air plasma by a factor of 150 compared to the dc case using this pulsed electric field method [9].

Is it possible to reduce the power even more by reducing the pulse duration further? Results of ELENDF calculations are shown in Fig. 8 for pulses with duration ranging from 2.5 ns to 20 ns. The lower limit in pulse duration is determined by the present status of the pulsed power technology. Although there are now pulse generators available which generate high voltage pulses with duration down to 300 ps [10], the system costs rise for pulse generators with pulse widths below nanoseconds, possibly offsetting the power savings effect. The upper limit was chosen, because over-voltage pulses with duration much longer than 10 ns generally cause glow-to-arc transitions. The voltage pulses were assumed to have a 1 ns rise and fall time and a flat top.

Shown is the electric field intensity required to reach electron densities of  $5 \cdot 10^{13} \text{ cm}^{-3}$ , starting out with  $10^{13} \text{ cm}^{-3}$  versus pulse duration. This electric field increases with reduced pulse duration. The average power, however, which is defined as the energy provided by the pulse to the plasma, divided by the time it takes for the electron density to relax to its base value, decreases with decreasing pulse duration. Reducing the pulse duration by a factor of 3 from 10 ns to 3.5 ns,

promises to provide additional power savings over the 10 ns pulse by a factor 2. This would reduce the average power density for a  $>10^{13} \text{ cm}^{-3}$  electron density atmospheric pressure air plasma by a factor of 300 from about 5 kW/cm<sup>3</sup> to 16 W/cm<sup>3</sup>.

Besides the use in power reduction, promising applications of the pulsed electric field method are in plasma chemistry. By applying short pulses of high electric fields the electron energy distribution function can be shifted temporarily to high electron energies. Choosing the right electric field strength and consequently the right pulse duration, this technology has the potential to selectively activate and control certain plasma chemical processes [11] which in other types of glow discharges have a low efficiency. Such applications are: plasma processing, e.g., the generation of radicals in plasmas for destruction of volatile organic compounds (VOC's), and the generation of excimers in excimer lamps and excimer lasers.

### **Acknowledgements**

This work was funded by the Air Force Office for Scientific Research (AFOSR) in cooperation with the DDR&E air plasma ramparts MURI program.

## References

- [1] Baldur Eliasson, Hilmar Esrom, Ulrich Kogelschatz, "New Excimer UV Sources for Industrial Applications," ABB Review 3/91, Pub. CH-E3.30833.0E
- [2] E.E. Kunhardt, "Generation of Large-Volume, Atmospheric Pressure, Nonequilibrium Plasmas," IEEE Trans Plasma Sci. **28**, 189 (2000).
- [3] Robert H. Stark and Karl H. Schoenbach, "Direct Current Glow Discharges in Atmospheric Air," Appl. Phys. Lett. **74**, 3770 (1999).
- [4] Robert H. Stark, Uwe Ernst, Mohamed El-Bandrawy, Christophe Laux, and Karl H. Schoenbach, "Direct Current Glow Discharges in Atmospheric Air," 30<sup>th</sup> AIAA Plasmadynamics and Lasers Conf., Norfolk, VA, July 1999, paper AIAA-99-3666.
- [5] Frank Leipold, Robert H. Stark, Ahmed El-Habachi and Karl H. Schoenbach, "Electron Density and Temperature Measurements in an Atmospheric Pressure Air Plasma by IR-Heterodyne Interferometry," to appear in J. Phys. D: Appl. Phys.
- [6] W.L. Morgan and B.M. Penetrante, "ELENDF: A Time-Dependent Boltzmann Solver for Partially Ionized Plasmas," Computer Physics Communications **58**, 127 (1990).
- [7] A.V. Phelps "Excitation and Ionization Coefficients," in Gaseous Dielectrics V, L.G. Christophorou and D.W. Bouldin, eds., Pergamon Press, New York, p. 1, (1987).
- [8] Y.P. Raizer, Gas Discharge Physics, Springer Verlag, Berlin, p. 60 (1991).
- [9] Manoj Nagulapally, Graham V. Candler, Christophe O. Laux, Lan Yu, Denis Packan, Charles H. Kruger, Robert H. Stark, Karl H. Schoenbach, "Experiments and Simulations of DC and Pulsed Discharges in Air Plasmas," 31<sup>st</sup> AIAA Plasmadynamics and Lasers Conf., Denver, CO, July 2000, paper AIAA 2000-2417.
- [10] V.M. Elanov, A.V. Kriklenko, P.M. Yarin, N.I. Daviduk, "100 kV Picosecond all Solid State Pulsers," Abstracts, 24<sup>th</sup> Intern. Power Mod. Symp., Norfolk, June 2000, session VIII, paper 7.
- [11] Hirotake Sugawara, Takuro Shimoda and Yosuke Sakai, "Control of Selectivity in Electron-Molecule Reactions by Impulse Field Electron Acceleration," Int. Symp. on Electron-Molecule Collisions and Swarms, 18-20 July 1999, Tokyo, Japan.

## Figure Caption

Fig. 1 Ionization cross-sections of nitrogen and oxygen, and the steady-state and transient electron energy distribution function (dashed and solid lines, respectively) for electrons in an atmospheric pressure air discharge. The steady state electron energy distribution function holds for a reduced electric field of  $E/N = 32 \text{ Td}$ . The solid line represents the non-equilibrium electron energy distribution obtained by applying a trapezoidal pulse with a rise time of 1 ns and an amplitude of 120 Td, at a time of 50 ns.

Fig. 2 Electron density and decay time due to recombination versus amplitude of the 10 ns applied electric field pulse. The decay time is defined as the time it takes for the plasma to reach the initial electron density, in this case  $10^{13} \text{ cm}^{-3}$ , after pulse application.

Fig. 3 Experimental setup and temporal development of the 10 ns high voltage pulse. The microhollow cathode discharge and the MHCD sustained glow are operated in a direct current mode ( $I = 10 \text{ mA}$ ). A 10 ns high voltage pulse of variable amplitude is applied at the anode, superimposed to the dc voltage.

Fig. 4 Schematics of the 10-Ohm strip-line pulse generator. The load is this case the pulsed plasma. The second switch in the double switch arrangement serves to reduce the rise time.

Fig. 5 Response of the plasma to the high voltage pulse: voltage across the glow discharge versus time for various pulse voltages (gap distance = 1 mm).

Fig. 6 Temporal development of the optical emission in the visible and near UV after pulse application. Parameter is the electrical pulse amplitude (gap distance = 1 mm).

Fig. 7 Plasma decay time versus voltage amplitude of the 10 ns pulse, obtained from the electrical and optical measurements.

Fig. 8 Pulse duration and reduced electric field amplitude, required to increase the electron density from the dc-value ( $n_{e,0} = 10^{13} \text{ cm}^{-3}$ ) to a peak value ( $n_{e,p} = 5 \cdot 10^{13} \text{ cm}^{-3}$ ), and the corresponding electrical power density,  $(E/N)^2(t/t_d)$ , where  $t$  is the pulse duration and  $t_d$  is the decay time.



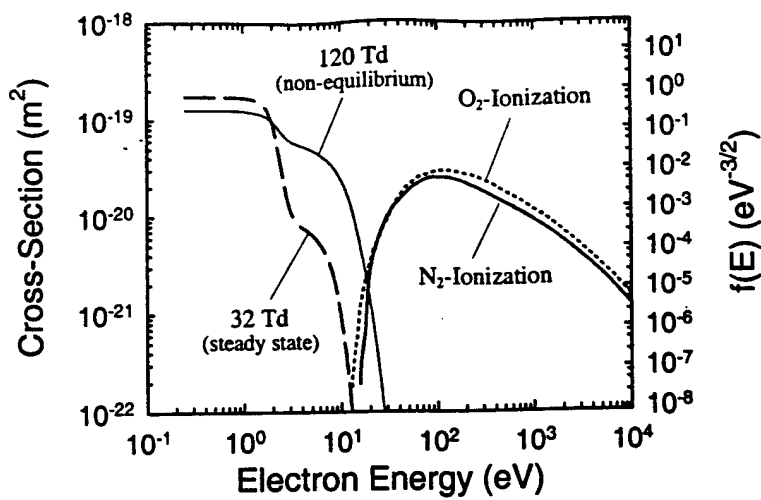


Fig 1

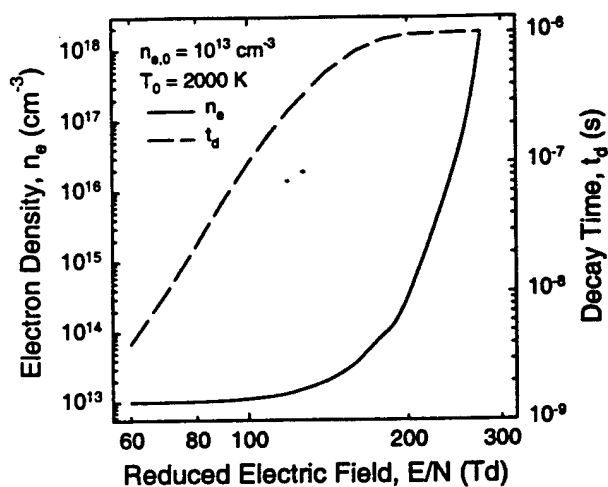


Fig 2

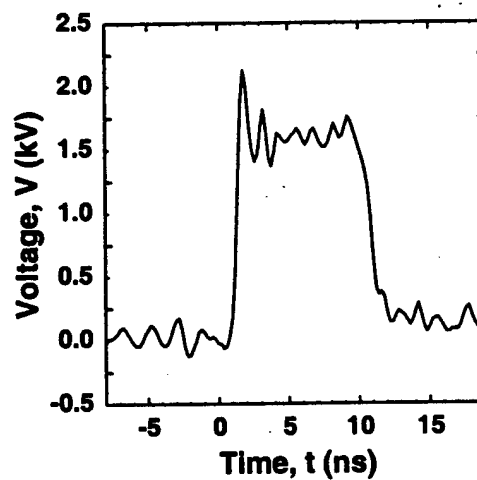
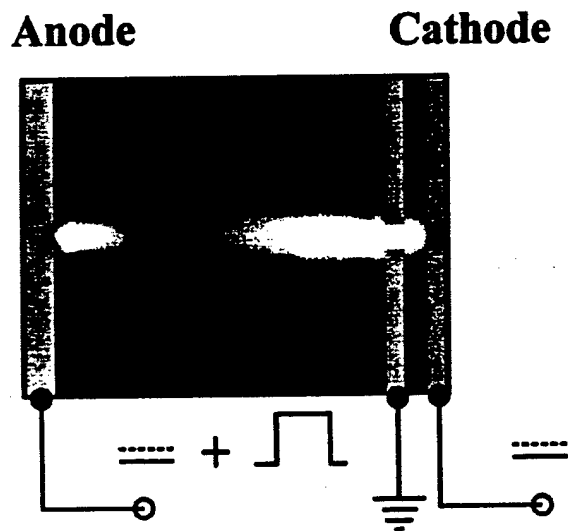


Fig 3

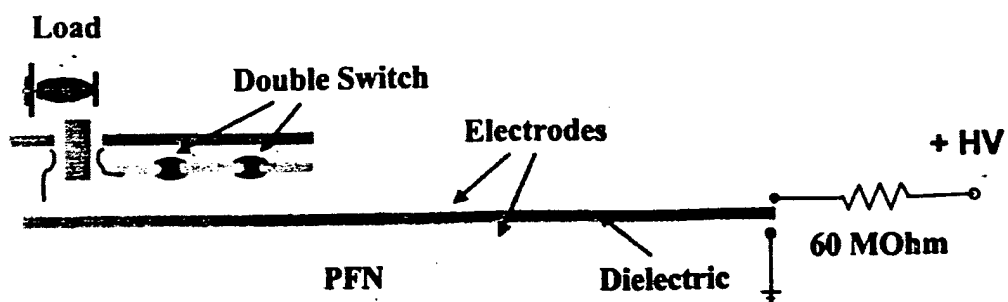


Fig 4

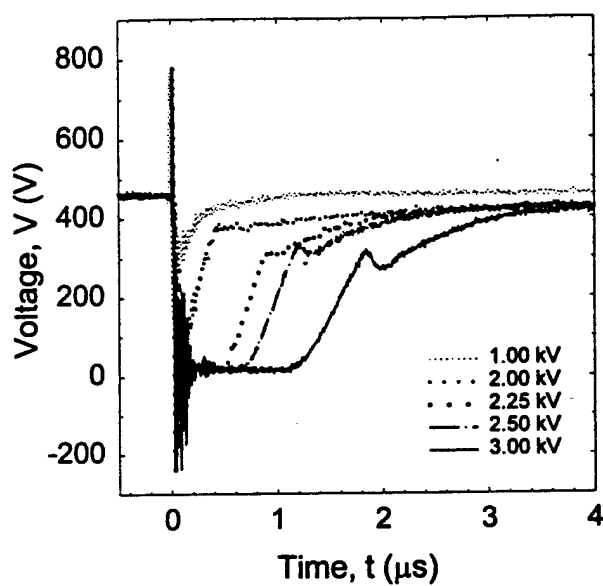


Fig 5

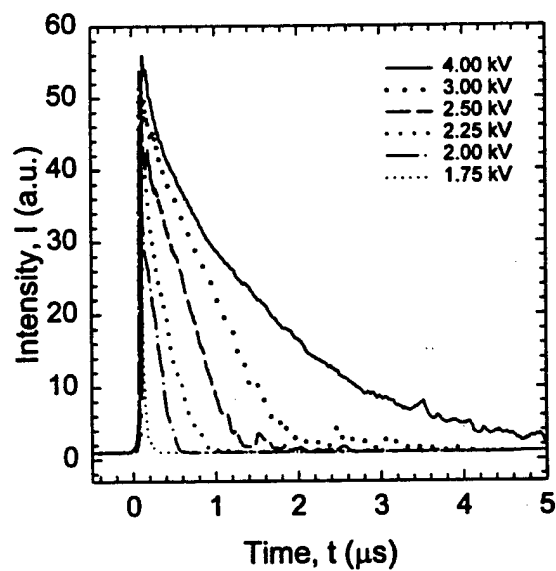


Fig 6

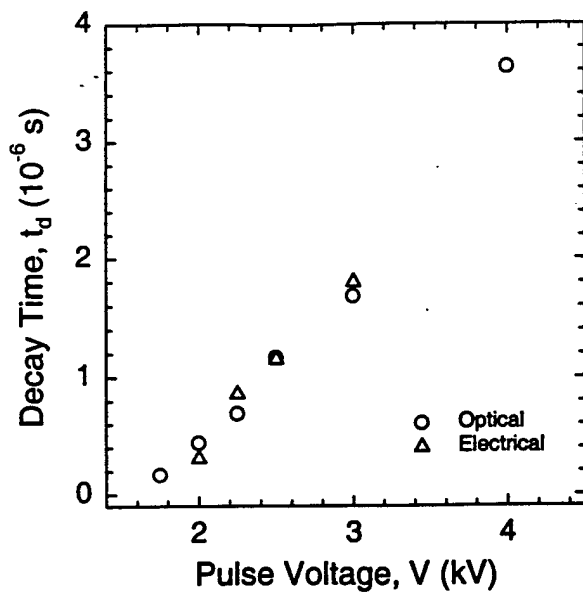


Fig 7

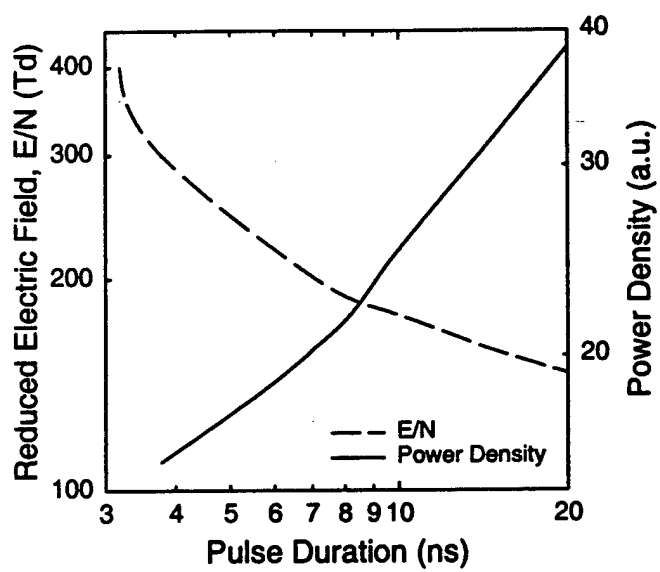


Fig 8

# Electron density measurements in an atmospheric pressure air plasma by means of infrared heterodyne interferometry

Frank Leipold, Robert H Stark, Ahmed El-Habachi and Karl H Schoenbach

Physical Electronics Research Institute, Old Dominion University, Norfolk, VA 23529, USA

Received 6 March 2000

Sunrise Setting  
Marked Proof  
D/112329/PAP

20557oe

Printed on 28/07/00  
at 16.54

**Abstract.** An infrared heterodyne interferometer has been used to measure the spatial distribution of the electron density in direct current, atmospheric pressure discharges in air. Spatial resolution of the electron density in the high-pressure glow discharge with characteristic dimensions on the order of  $100\ \mu\text{m}$  required the use of a  $\text{CO}_2$  laser at a wavelength of  $10.6\ \mu\text{m}$ . For this wavelength and electron densities greater than  $10^{11}\ \text{cm}^{-3}$  the index of refraction of the atmospheric air plasma is mainly determined by heavy particles rather than electrons. The electron contribution to the refractive index was separated from that of the heavy particles by taking the different relaxation times of the two particle species into account. With the discharge operated in a repetitive pulsed mode, the initial rapid change of the refractive index was assumed to be due to the increase in electron density, whereas the following slower rise is due to the decrease in gas density caused by gas heating. By reducing the time between pulses, direct current conditions were approached, and the electron density as well as the gas density, and gas temperature, respectively, were obtained through extrapolation. A computation inversion method was used to determine the radial distribution of the plasma parameters in the cylindrical discharge. For a direct-current filamentary discharge in air, at a current of 10 mA, the electron density was found to be  $10^{13}\ \text{cm}^{-3}$  in the centre, decreasing to half of this value at a radial distance of 0.21 mm. Gaussian temperature profiles with  $\sigma = 1.1\ \text{mm}$  and maximum values of 1000–2000 K in the centre were also obtained with, however, larger error margins than for electron densities.

## 1. Introduction

Microhollow cathode discharges (MHCDs) are high-pressure direct current glow discharges between closely spaced electrodes with an electrode opening of approximately  $100\ \mu\text{m}$  and an electrode distance of about  $200\ \mu\text{m}$ . The MHCDs were shown to serve as plasma cathodes for atmospheric pressure air discharges between the hollow cathode anode and a third, positively biased electrode [1, 2]. They were operated at currents of up to 30 mA, corresponding to current densities of  $4\ \text{A cm}^{-2}$  and at average electric fields of  $1.25\ \text{kV cm}^{-1}$  without reaching the threshold for glow-to-arc transition. Stable discharges over a distance of up to 1 cm have been generated, limited in length only by the available power supply [2]. In order to generate large volumes of high pressure, direct current glow discharges, the filamentary glow discharges need to be operated in parallel. Experiments with resistive electrodes have shown that the parallel operation of MHCDs is possible [3], and the first results with two parallel filamentary, MHCD-sustained air discharges have confirmed this assumption.

Gas temperatures, measured by using the emission spectroscopy of rotational states are of the order of 2000 K [4]. The electron densities in the MHCD-sustained air glow were estimated to be  $10^{13}\ \text{cm}^{-3}$  at power densities of  $5\ \text{kW cm}^{-3}$  [2]. This value was obtained by using the generalized Ohm's law

$$J = \sigma E = en_e \mu E.$$

The value of current density,  $J$ , which was derived from the discharge current and the diameter of the filament, and the electric field value,  $E$ , obtained from the measured discharge voltage and the gap distance, together with the known dependence of the electron mobility,  $\mu$ , allowed us to determine the electron density,  $n_e$ . However, this method is limited in accuracy by assumptions made on the cross section of the current carrying plasma, its homogeneity, and the electric field along the discharge axis.

A more accurate determination of the electron density requires the use of diagnostic techniques with high spatial resolution, of the order of one tenth of the filament diameter,

which is approximately 500  $\mu\text{m}$ . This condition, and that fact that the theory of Langmuir probes for atmospheric pressure plasma is not well developed, excludes the use of Langmuir probes. Thomson scattering, although having a high spatial resolution, is not applicable, since for these high-pressure plasmas Rayleigh scattering dominates over Thomson scattering. Measurement of the Stark broadening of the Balmer  $\beta$  line of hydrogen allowed us to determine the electron density only for values above  $5 \times 10^{13} \text{ cm}^{-3}$  [5]. A common technique for the measurement of electron densities in plasmas is interferometry. For electron densities in the  $10^{13} \text{ cm}^{-3}$  range microwave interferometry is considered the standard technique. However, in order to satisfy the condition for spatial resolution, which requires the use of radiation with less than the typical dimensions of the plasma, for MHCD-sustained plasma diagnostics the use of lasers is required. In the following, this method and the results obtained with it on MHCD-sustained atmospheric pressure air plasmas are discussed.

## 2. Diagnostic technique

The index of refraction,  $n$ , for plasmas with a low degree of ionization (as is the one we are interested in), contains contributions from both electrons and heavy particles and is given by the following equation which holds for optically thin plasma [6]

$$n - 1 = -\frac{e^2}{2(c^2 m_e \epsilon_0 4\pi^2)} \lambda^2 n_e + \left(A + \frac{B}{\lambda^2}\right) \frac{n_{\text{heavy}}}{n_{\text{heavy}_0}}$$

where  $n$  is the refractive index,  $\lambda$  the wavelength of the electromagnetic radiation,  $n_e$  the electron density, and  $n_{\text{heavy}}$  and  $n_{\text{heavy}_0}$  the heavy particle density at a given pressure and temperature and under normal conditions ( $T = 273 \text{ K}$ ,  $p = 1 \text{ bar}$ ), respectively.  $A$  and  $B$  are constants. For air at 1 bar and 273.15 K,  $A$  is  $2.871 \times 10^{-4}$ , and  $B$  is  $1.63 \times 10^{-18} \text{ m}^2$ .

The first term describes the contribution of the electrons, the second term that of neutrals and ions. Unfortunately, for wavelengths of micrometres, required for the spatial resolution of our microplasmas, the electron term was small (about 0.5%) compared with the term which contains the contributions from heavy particles.

In spite of this difficulty infrared (IR) interferometry can be used to determine the electron density in partially ionized atmospheric pressure plasma. Since the time constants for responses to changes in electric field differ strongly for electrons and heavy particles, it becomes possible to separate the effect of these particles on the index of refraction. Further, since the heavy particle density at a given pressure is related to the heavy particle (gas and ion) temperature through the ideal gas law, it is then also possible to obtain information on gas temperature.

The diagnostic method is explained in more detail in the following: consider the temporal variation of electron density and gas temperature in a gas between two electrodes which is subject to a fast rising electric field. After applying a voltage pulse, the gas will break down. This gas break-down process is related to a large increase in electron density, due

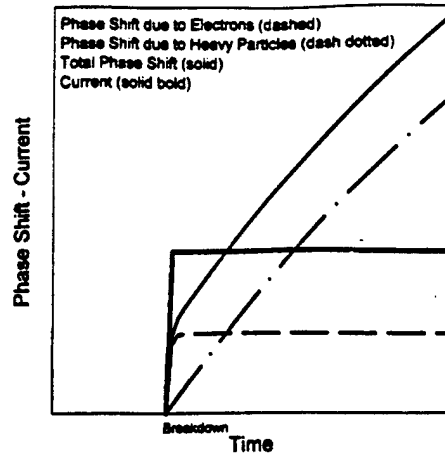


Figure 1. Temporal development of the phase shift  $\Phi$ , in a partially ionized gas, in response to a step function in voltage. The contribution of electrons and that of heavy particles is plotted schematically.

to the Townsend or Streamer mechanism, respectively. In this first phase the energy supplied by the electric field will be transferred into the electron gas. The electrons, in turn, through collisions, transfer energy to the heavy particles. The time constant for a temperature equilibrium is dependent on the gain process, electron energy relaxation, and on energy loss processes, such as conduction and diffusion. It is very large compared with that for the generation of the electrons. The temporal development of the phase shift,  $\Phi$ , due to the increase in electron density, and due to the increase in temperature, in response to a step function in voltage, is schematically depicted in figure 1. Similarly, when the voltage is turned off, the effect of the electrons on the index of refraction will vanish on a much faster time scale than that of heavy particles.

If, after a certain time,  $t_0$ , the voltage pulse is applied again, the plasma will still be affected by the previous pulse. This memory effect will be the stronger, the shorter is the time interval between two pulses. By reducing the time between successive pulses we therefore approach a plasma state which is less and less perturbed by the changes in voltage, and eventually we will reach a state which corresponds to direct current (dc) operation. The information on the steady state electron density can then be obtained by extrapolation. Furthermore, since we are now able to distinguish between electron and temperature effects, we will be able to obtain information on both plasma parameters in one set of measurements where the interval between pulses in a pulse train is the variable parameter.

## 3. Experimental set-up

### 3.1. Atmospheric pressure glow discharge

The electrode system consists of a microhollow electrode system and an additional (third) electrode with variable distance from the microhollow electrodes. The electrode configuration and the plasma is shown in figure 2(a). The MHCD geometry consists of two plane-parallel electrodes with a centred hole in each electrode. The electrodes are

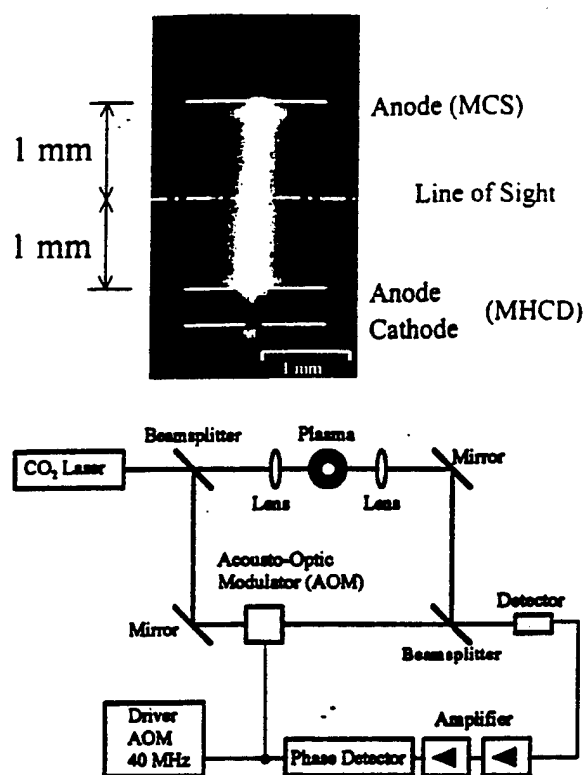


Figure 2. (a) Microhollow cathode sustained atmospheric pressure air discharge. The current is 10 mA, the sustaining voltage is 360 V. (b) Schematics of the IR heterodyne interferometer.

made of 100  $\mu\text{m}$  thin molybdenum foils, and the cathode and anode hole size of the plasma cathode is also 100  $\mu\text{m}$ . The dielectric between the electrodes is alumina ( $\text{Al}_2\text{O}_3$ , 96% purity) of 250  $\mu\text{m}$  thickness. The anode of the microhollow cathode geometry is on ground potential. The third electrode, placed at a distance of 2 mm in front of the plasma cathode is also made of molybdenum and biased positively. It serves as the anode for the microhollow cathode sustained (MCS) glow discharge.

The MCS glow discharge is operated in a pulsed mode. The voltage pulse applied to the anode has an amplitude of 2500 V, and rise and fall times of about 30  $\mu\text{s}$ . The pulse duration was kept at 250 ms. The time between pulses was varied from 100  $\mu\text{s}$  to 50 ms. The discharge current was limited by means of ballast resistor of 200  $\text{k}\Omega$  to 12.5 mA. It was monitored by means of a current viewing resistor. All measurements were performed in atmospheric air, with an average humidity of 30%.

### 3.2. Diagnostic system

In order to measure the phase shift and consequently the refractive index, a Mach-Zehnder heterodyne interferometer operating at a wavelength of  $\lambda = 10.6 \mu\text{m}$  ( $\text{CO}_2$  laser) was used (figure 2(b)). The  $\text{CO}_2$  laser was a continuous wave (cw) laser from Edinburgh Instruments, type PL3, with a maximum power of 30 W. The laser beam was separated in two equal intensity beams by means of a beam splitter.

One beam passes through the atmospheric pressure plasma. In order to provide for the required spatial resolution it was focused into the plasma, with a waist length of about 400  $\mu\text{m}$ . The power density of the focused laser beam does not affect the plasma parameters, as was shown in a separate experiment where the phase shift for a given condition was found to be independent of the laser power density [4]. The plasma could be shifted transverse to the beam direction, (figure 2(a)) allowing us to scan the plasma column. The second beam bypassed the plasma and was frequency shifted by means of a 40 MHz acousto-optic modulator. The beat frequency of 40 MHz, obtained by superimposing both beams, was recorded by an IR detector (Dorotec, PD10.6-3) which operated at room temperature, and the signal was compared with the driver signal of the acousto-optic modulator. The phase shift of the laser beam was transferred to the high-frequency signal and was recorded by a phase detector, which converts the phase shift into a voltage signal. The resolution of the interferometer was about 0.01°.

### 4. Experimental results

The temporal development of the phase shift was recorded simultaneously with the voltage across the discharge, which was measured by means of an electric probe (HP 1137 A). Typical voltage and phase shift traces are shown in figure 3(a). The off-time in this particular experiment was 4 ms. After this time the voltage across the gap between the electrodes rises to almost the full applied voltage of 2500 V, causing breakdown of the gas. The sustaining voltage reaches a steady state value of approximately 350 V after a transient phase of about 200  $\mu\text{s}$ . The phase shifts vary on a time scale of microseconds, except for the period of gas breakdown.

During gas breakdown, the phase shift changes on the same time scale as the voltage. This is shown in figure 3(b), where the time scale used in figure 3(a) was expanded. The observed rise time of 50  $\mu\text{s}$  was mainly determined by the temporal resolution of the electric diagnostic (a low pass filter was used to separate the measurement signal from a superimposed high-frequency signal caused by the acousto-optic modulator) and does not reflect the real time of gas breakdown. The breakdown occurs on a much faster time scale than 50  $\mu\text{s}$ , however, the maximum value of the refractive index was not affected by the slower diagnostic. After this rapid change, the index of refraction rises, first linearly and then exponentially with a time constant of 0.8 ms.

Measurements of the spatial distribution of the phase shift were performed by shifting the discharge in steps of 0.05 mm through the laser beam. The phase shift profiles due to breakdown ( $d\phi_d$  in figure 3(a)) and for the steady state phase ( $d\phi_{\text{heavy}}$  in figure 3(a)) are shown in figures 4 and 5, respectively, for an off-time of 0.5 ms. Both spatial distribution functions can be approximated numerically by assuming basic radial distribution functions: in the case of the phase shift caused by gas breakdown an assumed parabolic radial profile describes the spatial distribution well, in the case of the steady state value, it is a Gaussian profile.

When the time between applied voltage pulses was shortened, the width of the phase shift profile was reduced. Also, the amplitude of the phase shift signal after breakdown

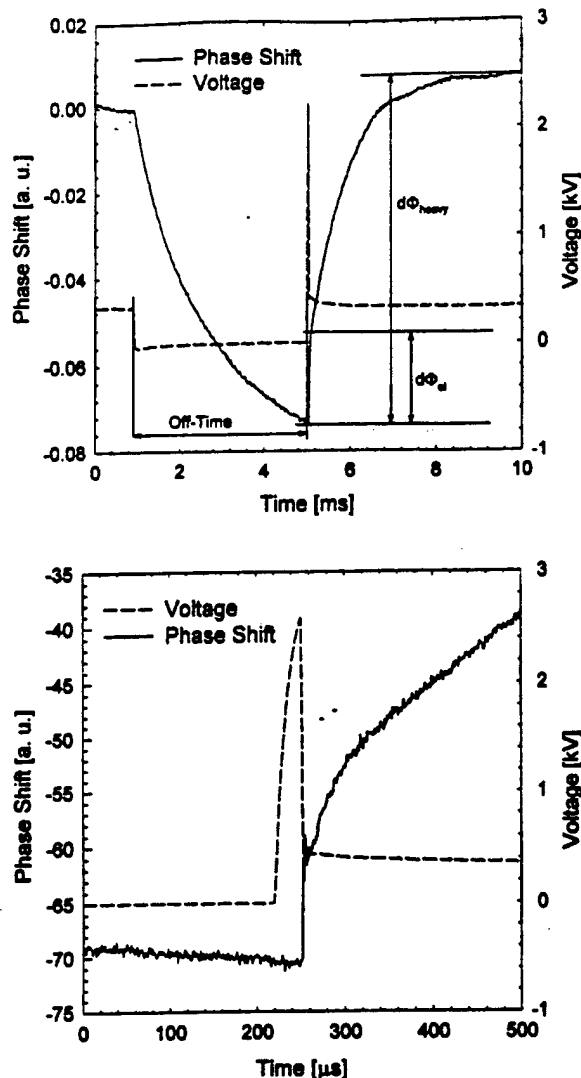


Figure 3. Temporal development of discharge voltage and the corresponding change in phase of the interferometric signal. (a) During on- and off-time; (b) at the time of re-ignition.

decreased. The breakdown voltage, however, changed only slightly. The increases in phase shift ( $d\phi_d$  in figure 3(a)) versus off-time is shown in figure 6.

## 5. Discussion

The rapidly rising phase shift signal caused by gas breakdown is due to the increase in electron density, but also due to the radial expansion of the plasma. The second effect may generally be neglected as will be discussed in the following. The generation of electrons when a voltage pulse is applied in a repetitive mode occurs in a pre-ionized filamentary channel, the size of it being determined by the previous pulse. This assumption is not unreasonable, since experiments with repetitive pulses have shown that positive and negative ions in the afterglow of an atmospheric gas discharge have lifetimes of the order of ms [7], exceeding the longest duration between pulses in our experiment. The channel diameter increases

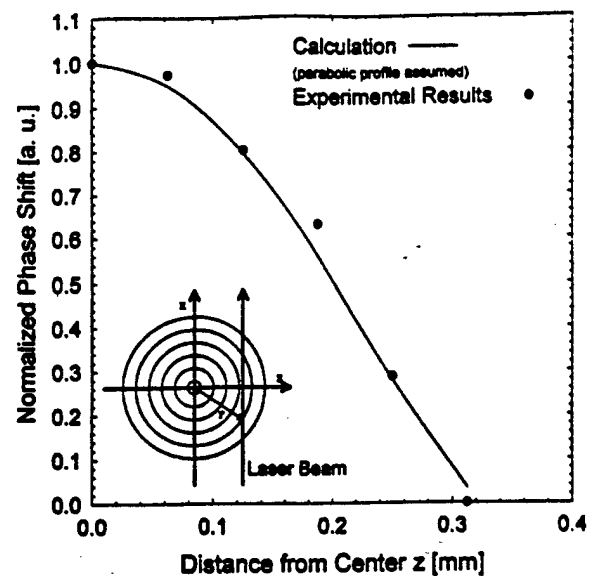


Figure 4. Spatial distribution of the phase shift caused by gas breakdown ( $d\phi_d$  in (a)) for an off-time of 0.5 ms.

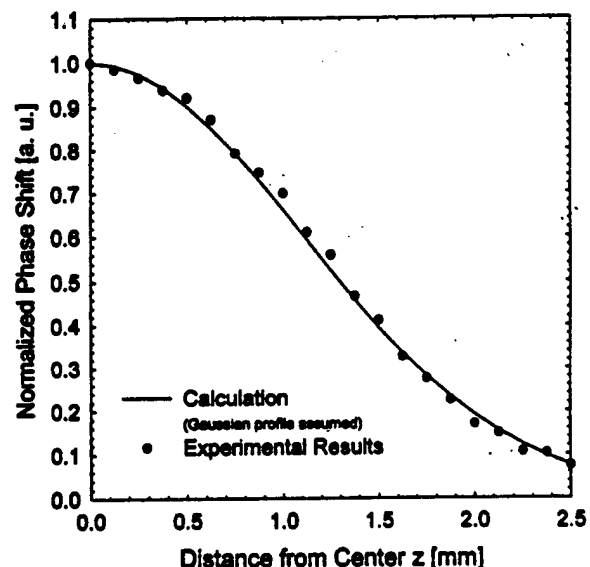


Figure 5. Spatial distribution of the phase shift in steady state ( $d\phi_{heavy}$  in (a)) for an off-time of 0.5 ms.

with increasing off-time, as measured by means of laser scans. This is probably due to radial diffusion of ions, an effect, which causes the pre-ionized volume to increase. The shorter the time between pulses the closer is the pre-ionized channel to the previous plasma volume. That means for short off-times, the effect of plasma expansion on the index of refraction can be neglected.

Although there is for larger off-times an increase in plasma diameter, as already discussed, the increase in the amplitude of the phase shift with increasing off-time seems to be due to an increased electron density rather than an increased plasma diameter. The higher electron density is related to the measured increased breakdown voltage.

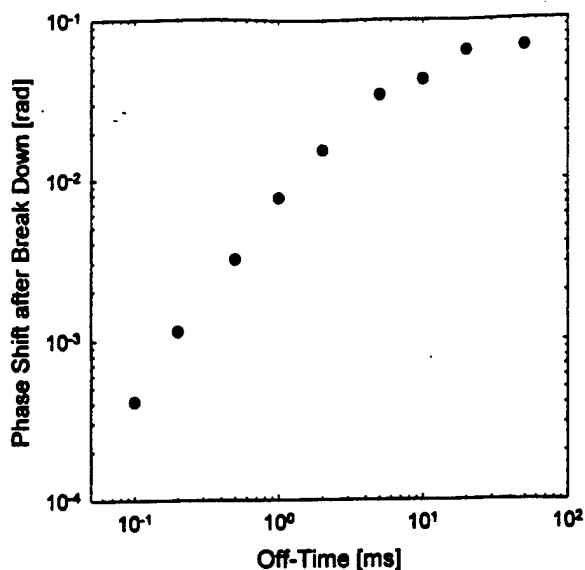


Figure 6. Phase shift caused by gas breakdown versus time between pulses (off-time) measured with the laser beam passing through the centre of the plasma column.

Although this voltage increase is not very pronounced, even small increases can cause considerably larger transient electron densities during breakdown. Again, by reducing the time between the applied voltage pulses, the phase shift caused by breakdown will approach a value which corresponds to the value of the electron density for dc operation of the atmospheric pressure glow discharge.

The temperature is the parameter which defines the slowly varying phases shift after breakdown. It is related to the gas density through the ideal gas law. The phase shift in steady state allows us to therefore to determine the gas temperature. For an evaluation of the absolute gas temperature, the off-time needs to be at least 50 ms (long compared with the time scale of a pressure wave in our plasma), to ensure, that the system approaches steady state. However, since the phase shift only provides us with the difference in temperature for breakdown and for steady state, and for short intervals the gas has not yet cooled down to room temperature, the value of the gas temperature obtained in this way will be too small. If the phase shift, on the other hand, is evaluated at long intervals between pulses where the gas has probably reached room temperature, the change in volume and electron density value will need to be taken into account for the calculation of the gas temperature from the phase shift. Any calculated temperature values are therefore subject to considerable errors. We only obtain values of the change in temperature or gas density.

For a given switch-off time, a change in the heavy particle density difference can be assigned to the electron density at ignition. In figure 7, the heavy particle density difference is plotted versus the electron density for different off-times. The shorter the off-time, the more the gas density approaches the dc value and so does the electron density. In order to obtain the value of the electron density in dc mode, the spline curve in figure 7 must be extrapolated to an off-time of zero, which is equivalent to a zero value in the heavy particle density

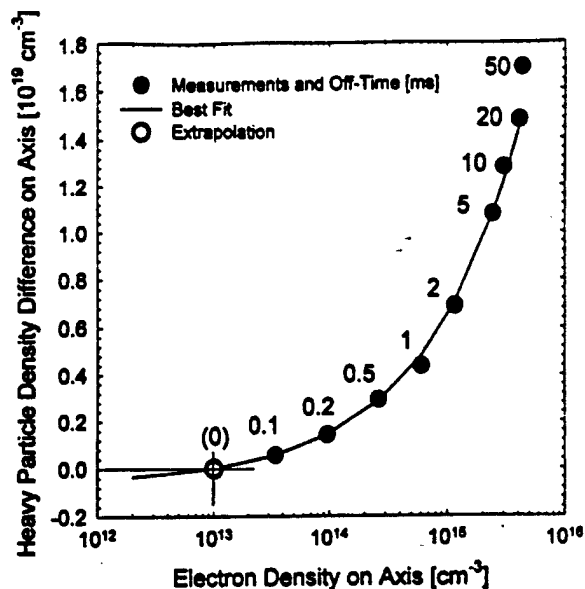


Figure 7. Electron density in the centre of the plasma column after breakdown versus the change in heavy particle density relative to their density for dc operation. The numbers along the curve indicate the off-time for the particular density results. The electron density in the dc mode was obtained by extrapolation of the spline curve to an off-time of zero.

difference. Using this spline curve, an electron density of  $10^{13} \text{ cm}^{-3}$  in the centre of the discharge was found for the dc mode.

The radial distribution of  $n_e$  can be calculated by applying the Abel inversion to the measured spatial distribution of the phase shift  $d\Phi(z)$  (insert figure 4). An Abel inversion is very sensitive to the accuracy of the values far away from the centre. Another method has therefore been used: a radial profile  $f(r)$  of a defined width was assumed, and the expected relative spatial profile  $d\Phi(z) = \int f(x^2 + z^2) dx$  was calculated and compared with the measured spatial profile. The type of the radial profile and its width was varied until the best fit of the spatial profiles (figures 4 and 5, electron and heavy particles, respectively) was obtained. For electrons the radial distribution is described best by a parabolic profile. The electron density  $n_e$  in the centre of the discharge is given by

$$n_e = d\Phi_{el} \frac{2(c^2 m_e \epsilon_0 4\pi^2)}{e^2 \lambda \int_{-\infty}^{+\infty} f_{el}(r) dr}$$

where  $f_{el}(r)$  is the radial profile normalized at the centre.  $d\Phi_{el}$  is the shift for a beam passing through the centre ( $z = 0$ ) of the discharge.

As in the case of the electron component, the profile of the value of the heavy particle density with the dc value subtracted was obtained through comparison with assumed radial profiles. For the heavy particles, a Gaussian profile turned out to provide the best fit. The gas temperature is related to the heavy particle density through the ideal gas law  $p = n_{heavy} kT$  with  $p$  being constant. The calculated relative radial gas temperature profile and the radial electron density profile are shown in figure 8.



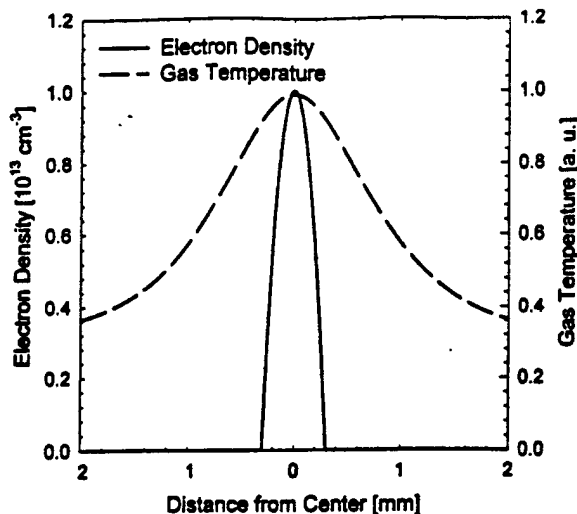


Figure 8. Radial electron density and temperature profile for a atmospheric pressure air plasma column with a length of 2 mm at a current of 10 mA and a sustaining voltage of 360 V.

## 6. Conclusion

The index of refraction of a direct current glow discharge plasma in atmospheric air was measured by means of  $\text{CO}_2$  laser interferometry. The contribution of electrons and heavy particles to the index of refraction was separated by utilizing the different time scales for electron generation and gas heating for the case that the discharge was operated in a pulsed mode. The initial rapid change in the index of refraction was assumed to be due to electron generation; with the following slower change being due to heavy particle density reduction caused by gas heating at constant pressure. In order to obtain information on the electron density and gas temperature for the direct current discharge, the time between pulses was continuously reduced, and the electron density values were extrapolated towards an inter-pulse duration of zero. The spatial distribution was obtained by shifting the laser laterally through the plasma column. The values of the index of refraction change along the line of sight were then converted into a radial profile by using a numerical inversion method. This method was shown to provide information on electron densities in a partially ionized air plasma with electron densities on the order of  $10^{13} \text{ cm}^{-3}$  with spatial variations in the  $100 \mu\text{m}$  range. The temperature could also be obtained, with the same spatial resolution with, however, less accuracy.

Similar results on the same type of discharge have been obtained with other diagnostic methods. The electron density in the centre of the plasma column, which was measured as  $10^{13} \text{ cm}^{-3}$ , is identical to that obtained by using measured current density and electrical field intensity values, and known values of the electron mobility [1]. The gas temperature values obtained through this method are comparable with those obtained by using emission spectroscopy of the second positive system of nitrogen [4]. The diagnostic technique described in this paper is suitable for the evaluation of a variety of partially ionized non-homogenous high-pressure plasmas. The range of electron densities is determined by the phase resolution. It was found to be  $0.01^\circ$  corresponding to a line integral of  $\int n_e dl = 5.8 \times 10^{11} \text{ cm}^{-2}$ . This value was obtained by replacing the plasma with an electric phase shifter and reducing the phase shift to a value where signal and noise became identical. Improvements of the phase resolution are possible by increasing the mechanical stability of the optical set-up. The temporal resolution is limited by the response time of the detector and/or the operation frequency of the acousto-optic modulator. In our case it was the acousto-optic modulator which limited the temporal resolution to 50 ns. The spatial resolution is determined by the waist of the focused laser beam through the discharge. It was measured as  $100 \mu\text{m}$  by using apertures of various diameters placed in the focal plane.

## Acknowledgments

This work was funded by the Air Force Office of Scientific Research in Cooperation with the DDR&E Air Plasma Ramparts MURI Program, and by the National Science Foundation (NSF). We appreciate the support of Old Dominion University, Norfolk, VA, USA, and the Institute for Low Temperature Plasmaphysics, Greifswald, Germany.

## References

- [1] Stark R H and Schoenbach K H 1999 *J. Appl. Phys.* **85** 2075
- [2] Stark R H and Schoenbach K H 1999 *Appl. Phys. Lett.* **74** 3770
- [3] Shi W and Schoenbach K H 1998 *Proc. IEEE Int. Conf. Plasma Science (Raleigh, NC, June 1998)* p 283
- [4] Block R, Laroussi M, Leipold F and Schoenbach K H 1999 *Proc. IEEE Int. Conf. Plasma Science (Monterey, CA, June 1999)* p 116
- [5] Schoenbach K H, Kunhardt E E, Laux C O and Kruger C H 1998 *Proc. IEEE Int. Conf. Plasma Science (Raleigh, NC, June 1998)* p 283
- [6] Duschin L A and Pawlitschenko O S 1973 *Plasmadiagnostik mit Lasern* vol 8 (Berlin: Akademie-Verlag).
- [7] Grothaus M G, Moran S L and Hardesty L W 1993 *9th IEEE Int. Pulse Power Conf. (Albuquerque, NM, 1993)* ed K Prestwich and W Baker p 475

# PHYSICS OF PLASMAS

Vol. 7, No. 5, Pt. 2, May 2000

## **Microhollow cathode discharge excimer lamps**

Karl H. Schoenbach, Ahmed El-Habachi, Mohamed M. Moselhy, Wenhui Shi,  
and Robert H. Stark

*Physical Electronics Research Institute, Department of Electrical and Computer Engineering,  
Old Dominion University, Norfolk, Virginia 23529*

pp. 2186-2191

## Microhollow cathode discharge excimer lamps\*

Karl H. Schoenbach,<sup>†,a)</sup> Ahmed El-Habachi, Mohamed M. Moselhy, Wenhui Shi, and Robert H. Stark

*Physical Electronics Research Institute, Department of Electrical and Computer Engineering, Old Dominion University, Norfolk, Virginia 23529*

(Received 15 November 1999; accepted 20 January 2000)

Microhollow cathode discharges are high-pressure, nonequilibrium gas discharges between a hollow cathode and a planar or hollow anode with electrode dimensions in the 100  $\mu\text{m}$  range. The large concentration of high-energy electrons, in combination with the high-gas density favors excimer formation. Excimer emission was observed in xenon and argon, at wavelengths of 128 and 172 nm, respectively, and in argon fluoride and xenon chloride, at 193 and 308 nm. The radiant emittance of the excimer radiation was found to increase monotonically with pressure. However, due to the decrease in source size with pressure, the efficiency (ratio of excimer radiant power to input electrical power), has for xenon and argon fluoride a maximum at  $\sim 400$  Torr. The maximum efficiency is between 6% and 9% for xenon, and  $\sim 2\%$  for argon fluoride. © 2000 American Institute of Physics. [S1070-664X(00)95105-X]

### I. INTRODUCTION

Excimer lamps are quasi-monochromatic light sources, which can be operated over a wide range of wavelengths in the ultraviolet (UV) and vacuum-ultraviolet (VUV). The operation of excimer lamps is based on the formation of excited molecular complexes (excimers) and the transition from the bound excimer state to a repulsive ground state. Examples for these complexes are rare-gas dimers and rare-gas-halogen exiplexes. The advantage of excimer lamps over other spectral lamps is their high-internal efficiency, which may reach values of up to 40%, when operated at high pressure.<sup>1</sup> The fact that it is a noncoherent radiation source allows us to scale the lamp to large size and to use it to irradiate (and treat) large areas. Applications for excimer lamps are UV curing and polymerization, UV oxidation, photo-chemistry, photo-deposition, photo-annealing, pollution control, to name only a few.<sup>2</sup>

In order to generate excimer radiation two conditions need to be satisfied: First, the electron energy distribution needs to contain a sufficient concentration of electrons with energies larger than the excitation energy of the excimer gas atoms. Secondly, since the formation of excimers is a three-body process, the pressure needs to be high, on the order of one atmosphere or higher. Both conditions can only be satisfied simultaneously in nonequilibrium plasmas. There are two ways to generate nonequilibrium plasmas: Operation at high-electric fields on such a short time scale that thermalization of the plasma is prevented, or operation on a small enough spatial scale, e.g., in the cathode fall of a gas discharge. The first concept is used in barrier (silent) discharges, discharges between dielectric covered electrodes separated by gas filled gaps of millimeter to centimeter

distance.<sup>3</sup> The second kind of nonequilibrium plasmas is found in plasma boundary layers, particularly the cathode fall of stable high-pressure discharges, such as corona discharges and high-pressure hollow cathode discharges. We have studied the latter type, hollow cathode discharges, with respect to the application as excimer source.

Hollow cathode discharges are gas discharges between a cathode, which contains a hollow structure, and an arbitrarily shaped anode.<sup>4</sup> At gas pressures such that the pressure,  $p$ , times cathode hole diameter,  $D$ , is on the order of Torr cm, the discharge develops in stages, dependent on the discharge current.<sup>5,6</sup> At low currents a "predischARGE" is observed, a glow discharge with a shape determined by the vacuum electric field. With increasing current, the plasma column formed along the axis of the cathode hole begins to serve as a virtual anode, causing a modification of the electric field distribution in the cathode hole. The initially axial electric field in the cathode plane changes into a radial one, and electrons, generated at the cathode, are accelerated radially towards the axis. They lose their energy in the cathode fall and in the negative glow, which for high values of  $pD$  is a ring shaped plasma layer adjacent to the cathode edge. For small values of  $pD$ , on the order of 1 Torr cm and less, the negative glow extends to the center forming a plasma cylinder.

When the discharge changes from an axial predischARGE into a radial discharge the sustaining voltage drops and the current increases: The discharge has a negative differential resistance. Although discharges in all current modes are hollow cathode discharges, generally the term "hollow cathode discharge" is used only for this mode. With increasing current the discharge voltage stays first constant, typical for a normal glow discharge, and then transfers into an abnormal glow discharge, characterized by a positive differential resistance.

Hollow cathode discharges are known for an electron energy distribution, which contains a high concentration of high-energy electrons. Using spectral diagnostics,<sup>7</sup> retarding

\*Paper SI2 5 Bull. Am. Phys. Soc. 44, 285 (1999).

<sup>†</sup>Invited speaker.

<sup>a)</sup>Electronic mail: schoenbach@ece.odu.edu

field analyzers,<sup>8</sup> and probes<sup>9</sup> electron energies well over 10 eV have been measured. But most of the studies have been performed in low-pressure hollow cathode discharges. Attempts to extend the range of pressure to higher values have been reported by White in 1958.<sup>10</sup> According to the White-Allis similarity law,  $V = V(pD, I/D)$ , where  $V$  is the sustaining voltage, and  $I$  is the discharge current, higher-pressure operation can be achieved by reducing the diameter,  $D$ , of the cathode hole.<sup>10,11</sup> The lowest value of  $pD$ , for which this law holds, is given by the condition that the mean free path for ionization must not exceed the hole diameter.<sup>12</sup> For argon, the minimum  $pD$  is, according to this condition, 0.026 Torr cm.<sup>5</sup> Empirical values for the upper limit in  $pD$  are 10 Torr cm for rare gases, less for molecular gases.<sup>13</sup> Based on the assumption, that electrons oscillating through the center between opposite cathode falls (pendulum electrons) are responsible for the "hollow cathode effect,"<sup>4,6</sup> the upper limit for  $pD$  can be determined by the condition that the distance between opposite cathodes must not exceed the lengths of the two cathode fall lengths plus the negative glow. This leads for argon to an upper limit in  $pD$  of slightly more than 1 Torr cm.<sup>14</sup>

Because of the required small size of the cathode opening for high-pressure operation we have coined the term "MicroHollow Cathode Discharges (MHCD)" for these discharges.<sup>5</sup> For atmospheric pressure discharges typical hole diameters should, according to the upper limit value for  $pD$ ,<sup>14</sup> be on the order of ten micrometers. However, this value is based on the assumption that the gas is at room temperature, a condition, which is not fulfilled in MHCDs. In these discharges the gas temperature may reach values of 2000 K, as shown for atmospheric pressure MHCDs in air.<sup>15</sup> Since the gas density, rather than the gas pressure is the relevant parameter in the similarity law for hollow cathode discharges, the temperature needs to be taken into account. If the effect of three-body collisions is neglected and the ideal gas law is applied the similarity law can be corrected for temperature dependence by multiplying the  $pD$  value with the ratio of actual gas temperature to room temperature. But even taking the relatively high-gas temperature of MHCDs into consideration, the diameter of the cathode opening should still be less than 100  $\mu\text{m}$  for hollow cathode discharge operation. However, stable hollow cathode discharges have been observed with cathode hole sizes as large as 250  $\mu\text{m}$  in xenon. These results indicate that at high  $pD$  values photon coupling rather than pendulum-electron coupling between opposite cathode falls is responsible for the observed negative differential resistance and the discharge stability.

## II. EXPERIMENTS

The electrode geometry for a single hole microhollow cathode excimer lamp as it is used in our experiments is shown in Fig. 1. The electrode geometry consists of two metal plates with circular opening, separated by a dielectric film. This geometry is a simplified version of hollow cathode discharge geometries where the cathode contains a cylindrical hole<sup>10</sup> or a cylindrical cavity.<sup>16</sup> Both, cathode and anode consist of 100  $\mu\text{m}$  thick molybdenum. In earlier experiments

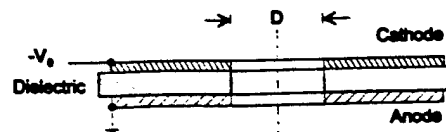


FIG. 1. Microhollow electrode geometry.

they were separated by a mica layer of 200  $\mu\text{m}$ . In more recent experiments we have used 100–250  $\mu\text{m}$  thick alumina ( $\text{Al}_2\text{O}_3$ ) because it withstands higher temperatures. The cylindrical holes in the cathode and the mica have been varied between 80 and 700  $\mu\text{m}$ .

Spectral measurements have been performed using a 0.5 m McPherson scanning monochromator, model 219, with a grating of 600 G/mm blazed at 150 nm, and by means of a 0.2 m McPherson monochromator, model 234/302, with a grating of 1200 G/mm. The discharge chamber with  $\text{MgF}_2$  or  $\text{LiF}_2$  windows was mounted directly at the inlet of the monochromator. The spectrally resolved radiation at the exit slit was detected with a photomultiplier tube after conversion to visible light, centered around 425 nm, by a sodium salicylate scintillator. With slits opening of 600  $\mu\text{m}$  the instrument resolution was  $\sim 3$  nm full width at half maximum (FWHM).

In addition to spectral measurements we have measured the spatial distribution of the excimer source by using a VUV imaging system which allows us to generate an image of the excimer source with a magnification of ten onto the cathode of a proximity focused image converter.<sup>17</sup> The emission from the fluorescent anode of the image converter is recorded by means of a charge coupled device (CCD) camera. Spectral resolution is obtained by using filters, which only allow the excimer radiation to pass.

## III. RESULTS

### A. Electrical characteristic and shape of excimer source

The dc (direct current) voltage characteristics of microhollow cathode discharges in rare gases show a distribution typical for hollow cathode discharges<sup>6</sup> even for  $pD$  values large compared to 1 Torr cm. A current-voltage characteristic for discharges in xenon at a pressure of 750 Torr is shown in Fig. 2(b). The hole diameter is 250  $\mu\text{m}$ ,  $pD$  is consequently 18.75 Torr cm. For low current the differential resistivity of the discharge is positive, as expected for a hollow cathode discharge in the predischARGE phase, where space charge effects (virtual anode) are not important. At a current of 4 mA the discharge enters a range with negative differential resistivity, the phase where it changes into a hollow cathode discharge with radial electric fields.

The source of the xenon excimer radiation, the microhollow cathode discharge plasma, as seen end-on through a band pass filter (maximum transmission of 24.4% at 170.9 nm and a FWHM of 26.8 nm) is only at low currents concentrated in the cathode hole [Fig. 2(a)]. The ring shaped region at the inner edge of the cathode opening represents the negative glow of the discharge. With increasing current, the excimer source extends into the area outside the hole,

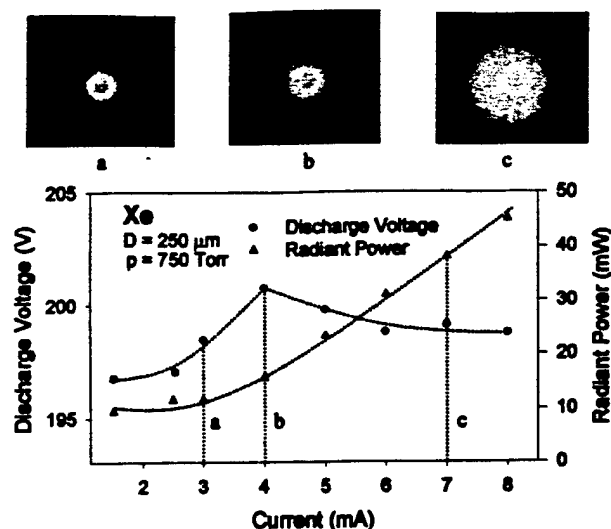


FIG. 2. (a) (upper part): End-on photographs of micro hollow cathode (250 μm) discharges in xenon at a pressure of 750 Torr for various currents. The photographs were taken through an optical filter, which allowed only the excimer radiation to pass. (b) (lower part): Current characteristic of the microhollow cathode discharges, and VUV radiant power dependent on current.

covering at a current of 7 mA and a pressure of 750 Torr the cathode surface over a distance of approximately four times the hole diameter. As with current, the size of the excimer source changes with pressure. At high pressure, as for small currents, the source is located in or close to the cathode opening, particularly at the inner edge of the cathode hole (Fig. 3). With reduced pressure the source extends more and more over the cathode surface.

## B. Spectral emission

Most of our excimer studies have focused on xenon, with its excimer emission peaking at 172 nm. A xenon spectrum for discharge operation with hollow electrodes of 100 μm diameter is shown in Fig. 4.<sup>18</sup> At 40 Torr, the 147 nm xenon resonance line, corresponding to transitions from the  $^3P_1$  state to the  $^1S_0$  ground state, dominates the emission spectra. There are some indications of the first continuum, which extends from the resonance line towards longer wave-

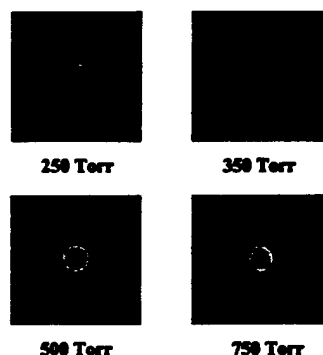


FIG. 3. End-on photographs of micro hollow cathode (250 μm) discharges in xenon at various pressures. A circle indicates the edge of the cathode opening. The photographs were taken through an optical filter, which allowed only the excimer radiation to pass.

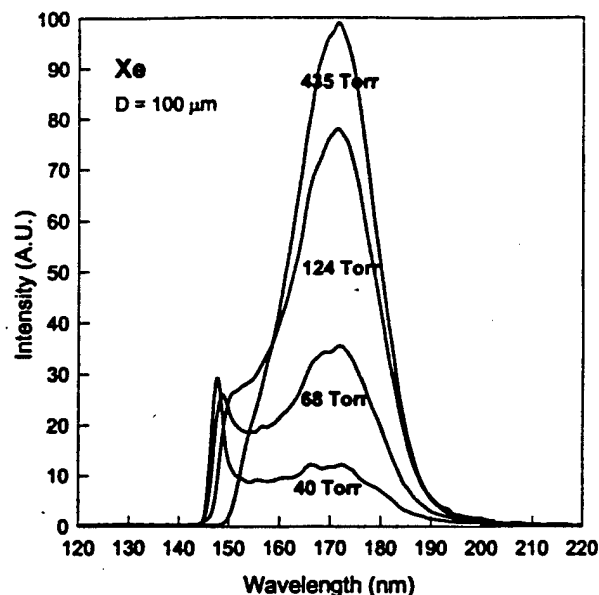


FIG. 4. VUV emission spectra of high-pressure micro hollow cathode discharges in xenon with gas pressure as variable parameter. The discharge voltage was 225 V ± 10 V, and the current was kept at 3.15 mA ± 0.15 mA.

length. The second excimer continuum peaking at 172 nm appears at higher pressures. At pressures greater than 300 Torr, it dominates the emission spectra up to the longest recorded wavelength of 800 nm. The second continuum results from transitions from the lowest vibrational level of singlet  $^1\Sigma$  and the triplet  $^3\Sigma$  excimer states to the repulsive ground state. Transitions from higher vibrational levels of these states correspond to the first excimer continuum. Besides of pressure, the excimer emission it depends on the discharge current. As shown in Fig. 2(b) it increases linearly with current above the transition into the hollow cathode mode.

Argon excimer emission has been studied in flowing gas with a gas flow of 380 sccm.<sup>19</sup> At low pressure, the spectrum over the range of 100–200 nm is dominated by Ar II lines, mostly transitions between states having a  $3s^2 3p^4 (^3P)$  ionic core. At high pressure the intensity of these lines is strongly reduced and the main spectral feature is the excimer line, peaking at 130 nm. The emission of the argon excimer radiation increases, as for xenon, with gas pressure, and with discharge current. The sustaining voltage,  $V$ , is approximately the same as for xenon (200 V).

The presence of an attaching gas in the gas mixture is considered a major obstacle for the generation of high-pressure dc glow discharges. High-pressure discharges in rare-gas-halide mixtures tend to constrict and become unstable in times on the order of ten nanoseconds. However, as in rare gases, microhollow cathode discharges could also be operated in rare-gas-halogen mixtures in a stable dc mode up to atmospheric pressure. Argon fluoride excimer emission with a maximum at 193 nm was recorded in a gas mixture consisting of 1% fluorine, 5% argon, and 94% helium.<sup>20</sup> The measured ArF excimer spectrum is shown in Fig. 5 for a pressure of 400 Torr. The line width at half intensity is just 3 nm, compared to 24 nm for Xe (Fig. 4). Similarly, xenon

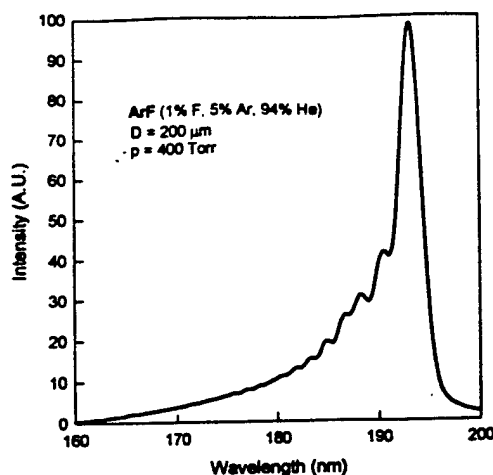


FIG. 5. Argon fluoride excimer emission spectrum of a dc microhollow cathode discharge operated in a gas mixture containing 1% of fluorine, 5% of argon, and 94% of helium at 400 Torr. The discharge voltage was 498 V, the current was 6 mA.

chloride excimer radiation was measured peaking at 308 nm, in a gas mixture consisting of 0.06% hydrogen chloride, 0.03% hydrogen, 1.5% xenon and neon as buffer gas. Discharge voltages were  $\sim 500$  V for discharges in ArF, and 180 V for XeCl discharges.

### C. Efficiency and radiant emittance

Measurements of the efficiency, the ratio of radiant power in the UV to input electrical power, have been performed for xenon and argon fluoride discharges. In order to determine the absolute values of the excimer emission two methods have been used.<sup>18</sup> One is based on comparing the discharge emission with that of calibrated UV sources: A Mercury vapor lamp (line emission at 185 nm) and a Deuterium lamp (continuum from 160 to 400 nm). A second one utilizes a calibrated radiometer. Both, for xenon and argon fluoride discharges, the efficiency was found to increase with pressure up to  $\sim 400$  Torr, where it reaches values of 6%–9% for xenon<sup>18</sup> and  $\sim 2\%$  for ArF, and then decreases again for higher pressure. Although the efficiency for ArF is less than that for Xe, the peak spectral radiant power at identical electrical power input is for ArF higher by a factor of 2 to 3 compared to Xe, due to the differences in line width (Figs. 4 and 5).

The decrease of the measured efficiency at higher pressure can be explained by the decrease in size of the excimer source with pressure (Fig. 3). The radiant emittance, the optical power emitted per surface element, increases with pressure. However, this increase does, at pressures greater than 400 Torr, not compensate for the reduction in size of the source. Consequently, the overall optical power (integral of radiant emittance over source area) decreases at higher pressures.

### D. Direct current versus pulsed operation

One of the special features of microhollow cathode excimer sources is their stability, which allows us to operate them in a direct current mode. However, in certain cases it

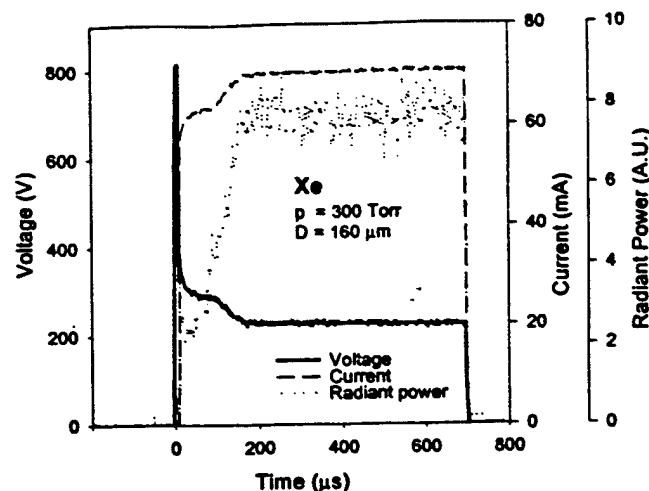


FIG. 6. Temporal development of the voltage, current, and radiant power of a discharge in xenon at 300 Torr.

could be an advantage to operate the discharges in a pulsed mode. This is particularly the case when high-radiant emittance is required. As known from dc measurements, the total optical power increases with current, however, at constant pressure the source size also increases [Fig. 2(a)]. The source area shrinks when the pressure is increased (Fig. 3). High-radiant emittance, therefore, requires both, high current and high pressure. The current for dc operation is limited by the thermal loading of the electrode structure to  $\sim 10$  mA per discharge. With pulsed operation thermal loading of the electrodes can be largely avoided. The limitation in current, and consequently in intensity, is for pulsed operation determined by the development of current driven instabilities, the glow-to-arc transition, rather than thermal processes affecting the electrodes.

We have studied the discharge in xenon under pulsed condition and were able to extend the current range to 80 mA before instabilities set in.<sup>21</sup> The temporal development of current, voltage, and excimer intensity of a discharge in xenon at a pressure of 300 Torr is shown in Fig. 6. Breakdown occurs at voltages between 700 V and 1 kV. A stable discharge phase is reached after times on the order of 100  $\mu$ s, dependent on discharge current.<sup>21</sup>

### E. Parallel operation

Industrial applications of microhollow cathode discharge excimer lamps require generally higher total optical power levels than achievable with single microhollow cathode discharges. The optical power of single xenon discharge reaches approximately hundred mW (at an efficiency of 6%–9%), consequently, the operation at the kW optical power level would require an array of more than  $10^4$  discharges.

It can be expected that in the current range where the  $V$ - $I$  characteristic of the microhollow cathode discharge has a positive slope, the Townsend region and the abnormal glow region,<sup>6</sup> parallel operation of microhollow cathode discharges can be achieved without ballasting the individual discharges. Operation of the discharge in the abnormal glow mode requires limiting of the cathode area, such that the

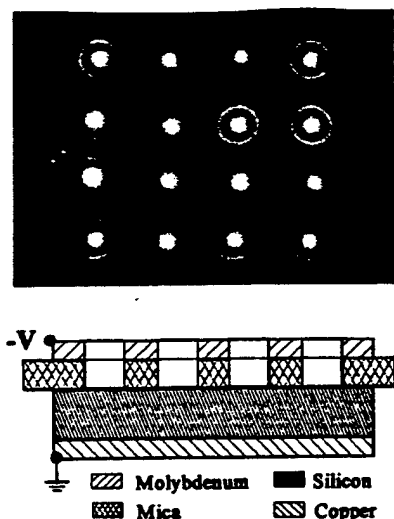


FIG. 7. Cross section of the electrode system, and end-on photograph of a discharge array in argon. The total current was 28 mA.

current density increases with increasing current. One way to limit the cathode area is to use blind holes in the cathode material instead of openings as shown in Fig. 1. Such geometry was utilized in earlier experiments,<sup>5</sup> and parallel operation could be demonstrated. A second method is to use a geometry as shown in Fig. 1, but to cover the cathode area with a dielectric, except the cylindrical surface of the cathode opening.<sup>22</sup> This method has allowed us to operate two microhollow cathode discharges in atmospheric pressure argon in parallel without individual ballast.

For discharges operating in modes where the slope of the current-voltage characteristics is negative, flat, or only slightly positive, it was not possible to obtain stable parallel dc operation consistently without ballasting the individual discharges. Individual ballasting is a reasonable approach for relatively small arrays. A method, which has allowed us to extend this method to large arrays, is the use of distributed resistive ballast.<sup>23</sup> This was achieved by using a semi-insulating material, in our case semi-insulating silicon, as anode material. The result of this experiment is shown in Fig. 7. The method allows us to generate arrays of microhollow cathode discharge excimer sources of any size, limited only by the thermal loading of the ballast resistor.

#### IV. DISCUSSION

One important condition for excimer formation in glow discharges is an electron energy distribution with a large concentration of electrons with energies greater than the excitation energy of the excimer gases. For argon, the lowest excited state is at 11.55 eV. Excimer emission using the same microhollow cathode geometry as shown in Fig. 1 has even been reported for neon,<sup>24</sup> where the lowest excited state is at 16.6 eV. The presence of electrons in hollow cathode discharges with energies greater than the energy required for populating the lowest excited states in rare gases is not surprising. It has been shown in various experiments that the electron energy distribution in such discharges contains a high concentration of electrons in the high-energy tail of the

distribution (for example, see Ref. 4). Measurements of the energy distribution of electrons accelerated in the cathode fall of a glow discharge have shown that even a beam component exists with electron energies comparable to the full cathode fall energy.<sup>8</sup>

The second condition for dc excimer sources, a stable, nonthermal discharge at high-neutral gas density (such that excimer formation, a three-body process, occurs at a higher rate than collisional or radiative decay of the excimer precursors) can, to our knowledge, only be fulfilled in corona discharges<sup>25</sup> and micro discharges, such as the MHCD. High-pressure glow discharges in plane parallel electrode geometries are prone to instabilities, particularly to glow-to-arc transitions, and can only be sustained for times on the order of ten nanoseconds.

The exceptional stability of hollow cathode discharges is assumed to be due to a coupling process between the two cathode falls, which face each other at a distance of  $D$ . For low  $pD$  values, it is the electrons which provide coupling between opposite cathode sheaths. The "pendulum" electrons generated at the cathode surface and accelerated in the cathode fall, gain enough energy to oscillate through the plasma on axis, which serves as a virtual anode. Whenever instabilities, characterized by locally increasing electron density, begin to form in the hollow cathode fall, the voltage across the cylindrical cathode fall is reduced. This causes a reduction in the concentration of pendulum electrons and consequently a reduced ionization rate in opposite cathode falls. This effect counters the growth of electron density, and would explain the excellent stability of hollow cathode discharges.

However, for values of  $pD$  exceeding 1 Torr cm (at room temperature), electron coupling between the opposite cathode falls becomes increasingly unlikely.<sup>14</sup> Still, hollow cathode discharges in xenon were shown to have a hollow cathode discharge phase with negative differential resistance even for temperature corrected  $pD$  values large compared to one Torr cm [Fig. 2(b)]. At high values of  $pD$ , it is assumed that photons provide the coupling between opposite cathode falls. Photoelectron emission from the cathode surfaces has been suggested by Little and von Engel<sup>26</sup> as a mechanism responsible for the hollow cathode effect. Experiments in argon between two parallel cathodes of variable distance seem to support this assumption.<sup>27</sup> An effect on discharge current and sustaining voltage was observed at "hollow" cathode distances large compared to the distance where the two negative glows merged. Merging occurred at a  $pD$  value close to 1 Torr cm, in agreement with computational results.<sup>14</sup> As in the case of electron coupling, the reduction in photoemission, caused by reduced cathode fall voltage due to the emergence of a local increase in electron density (instability) counters the growth of this instability.

The high energies of electrons accelerated in the cathode fall, and the excellent stability of microhollow cathode discharges are the important features for microhollow cathode discharge excimer lamps. An additional bonus is the fact that by increasing the current (abnormal glow) or by decreasing it (predischARGE) the discharge behaves like a resistor: A feature, which allows us to generate arrays of such discharges

with relatively simple means. Experiments in xenon indicate that in MHCD arrays an average radiant emittance of 50 W/cm<sup>2</sup> may be achievable.

The measured efficiency of 6%–9% for xenon excimer MHCD emitters is a factor of five below theoretical values.<sup>1,18</sup> The reason for the lower than expected efficiency is assumed to be the relatively high temperature of the plasma. Heating an excimer gas is known to reduce the excimer emission.<sup>28</sup> This is due to the reduction in gas density with increasing temperature at a fixed pressure, but also due to the fact that the rate coefficient of the three-body process, which leads to excimer formation, scales with  $T^{-0.5}$ .<sup>29</sup> Temperature measurements in microhollow cathode discharges have to date only been performed in atmospheric air, where temperatures of ~2000 K have been obtained.<sup>30</sup> Although the gas temperature in rare-gas microhollow cathode discharges is expected to be lower, it is probably still large enough to cause a strong reduction in efficiency. Cooling through gas flow is expected to increase the efficiency of MHCD excimer sources.

Barrier discharge excimer lamps have, probably to a large extent due to the lower plasma temperature, a higher efficiency than MHCDs. Whereas the highest measured internal efficiency in MHCDs is 9% for Xe, corresponding to an external efficiency of approximately half this value, external efficiencies of 10% have been measured in barrier discharge lamps, and even 20% seemed to be achievable.<sup>31</sup> However, the radiant emittance, which is stated in Ref. 31 as being in the range of 100 mW/cm<sup>2</sup> is considerably higher for MHCDs where an emittance of 10 W/cm<sup>2</sup> has been reached.

A particular feature of microhollow cathode discharges is the extreme dc power density in these discharge plasmas. Typical discharge voltages are ~200 V. Currents of up to 10 mA are reached in such discharges when operated dc, resulting in an electrical power for single discharges on the order of Watt. For high-pressure operation the plasma is concentrated in the cathode opening. The volume of cathode fall and negative glow, where most of the electrical energy is dissipated is assumed to be less than the volume determined by the cathode opening. For a 100  $\mu$ m thick, 100  $\mu$ m diam cathode opening the volume is 0.810<sup>-6</sup> cm<sup>3</sup>. The power density is consequently on the order of 10<sup>6</sup> W/cm<sup>3</sup>. In the pulsed mode, where we are able to reach 80 mA for millisecond time duration, the power density is expected to be even higher. With power densities that high conditions for lasing should be achievable when a multitude of such discharges is arranged in series. This opens the possibility to build cw (continuous wave) or quasi cw excimer microlasers, an exciting prospect for the future of microhollow cathode discharges.

## ACKNOWLEDGMENTS

This work is supported by the Department of Energy, the National Science Foundation, the Defense Advanced Research Projects Agency, and the Air Force Office of Scientific Research. The authors would also like to thank Dr. Jaeyoung Park, Los Alamos National Laboratory, for helpful discussions.

- <sup>1</sup>B. Gellert and U. Kogelschatz, *Appl. Phys. B: Photophys. Laser Chem.* **52**, 14 (1991).
- <sup>2</sup>See National Technical Information Service Doc. No. ADA357742INZ. (U. Kogelschatz, B. Eliasson, and W. Egli, *Proc. XXIII Intern. Conf. on Phenomena in Ionized Gases*, 1997, Inv. Papers, Paper C4-47.) Copies may be ordered from the National Technical Information Service, Springfield, VA, 22161.
- <sup>3</sup>U. Kogelschatz, *Pure Appl. Chem.* **62**, 1667 (1990).
- <sup>4</sup>G. Schaefer and K. H. Schoenbach, "Basic Mechanisms Contributing to the Hollow Cathode Effect" appearing in *Physics and Applications of Pseudosparks* (Plenum, New York and London, 1990), p. 55.
- <sup>5</sup>K. H. Schoenbach, R. Verhappen, T. Tessnow, F. E. Peterkin, and W. W. Byszewski, *Appl. Phys. Lett.* **68**, 13 (1996).
- <sup>6</sup>A. Fiala, L. C. Pitchford, and J. P. Boeuf, *Contr. Papers, XXII Conf. on Phenomena in Ionized Gases, Hoboken, NJ, 1995* (Stevens Institute of Technology, Hoboken, NJ, 1995), p. 191 (in the process of being registered with NTIS).
- <sup>7</sup>K. Fujii, *Jpn. J. Appl. Phys.* **16**, 1081 (1977).
- <sup>8</sup>P. Gill and C. E. Webb, *J. Phys. D: Appl. Phys.* **10**, 299 (1977).
- <sup>9</sup>V. S. Borodin and Yu. M. Kagan, *Sov. Phys. Tech. Phys.* **11**, 131 (1966).
- <sup>10</sup>A. D. White, *J. Appl. Phys.* **30**, 711 (1959).
- <sup>11</sup>D. J. Sturges and H. J. Oskam, *J. Appl. Phys.* **35**, 2887 (1964).
- <sup>12</sup>H. Helm, *Z. Naturforsch. A* **27a**, 1812 (1972).
- <sup>13</sup>J. W. Gewartkowski and H. A. Watson, *Principles of Electron Tubes* (Van Nostrand, Princeton, NJ, 1965), p. 561.
- <sup>14</sup>Karl H. Schoenbach, Ahmed El-Habachi, Wenhui Shi, and Marco Ciocca, *Plasma Sources Sci. Technol.* **6**, 468 (1997).
- <sup>15</sup>Rolf Block, Olaf Toedter, and Karl H. Schoenbach, *Proc. 30th AIAA Plasmadynamics and Lasers Conf., Norfolk, VA, July 1999* (American Institute of Aeronautics and Astronautics, Washington DC), paper AIAA-99-3434.
- <sup>16</sup>Jean-Pierre Boeuf and Leanne C. Pitchford, *IEEE Trans. Plasma Sci.* **19**, 286 (1991).
- <sup>17</sup>A. El-Habachi, M. Moselhy, and K. H. Schoenbach, *Bull. Am. Phys. Soc.* **44**, No. 4, 67 (1999).
- <sup>18</sup>Ahmed El-Habachi and Karl H. Schoenbach, *Appl. Phys. Lett.* **73**, 885 (1998).
- <sup>19</sup>Ahmed El-Habachi and Karl H. Schoenbach, *Appl. Phys. Lett.* **72**, 22 (1998).
- <sup>20</sup>Wenhui Shi, Ahmed El-Habachi, and Karl H. Schoenbach, *Bull. Am. Phys. Soc.* **44**, No. 4, 25 (1999).
- <sup>21</sup>M. Moselhy, A. El-Habachi, and K. H. Schoenbach, *Bull. Am. Phys. Soc.* **44**, No. 4, 29 (1999).
- <sup>22</sup>Masatoshi Miyake, Hikaru Takahashi, Koichi Yasuoka, and Shozo Ishii, *Conf. Record, IEEE Intern. Conf. Plasma Science, Monterey, CA, 1999* (Institute of Electrical and Electronics Engineers, Piscataway, NJ), p. 326.
- <sup>23</sup>W. Shi, R. H. Stark, and K. H. Schoenbach, *IEEE Trans. Plasma Sci.* **27**, 16 (1999).
- <sup>24</sup>P. Kurunczi, K. Becker, K. H. Schoenbach, and A. El-Habachi, *Conf. Record, 12th IEEE Intern. Conf. Plasma Science, Monterey, CA, 1999* (Institute of Electrical and Electronics Engineers, Piscataway, NJ), p. 143.
- <sup>25</sup>M. Salvermoser and D. E. Murnick, *Bull. Am. Phys. Soc.* **44**, No. 4 (1999).
- <sup>26</sup>P. F. Little and A. von Engel, *Proc. R. Soc. London, Ser. A* **224**, 209 (1954).
- <sup>27</sup>See National Technical Information Document No. ADA357742INZ. (Hajime Onoda, Masaki Yatsu, and Minoru Sugawara, *Contr. Papers, Vol. 2, XXIII Conf. on Phenomena in Ionized Gases, Toulouse, France, 1997* Paper II-68.) Copies may be ordered from the National Technical Information Service, Springfield, VA, 22161.
- <sup>28</sup>J. D. Ametep, J. Diggs, D. M. Manos, J. M. Kelley, *J. Appl. Phys.* **85**, 7505 (1999).
- <sup>29</sup>D. J. Eckstrom, H. H. Nakano, D. C. Lorents, T. Rothen, J. A. Betts, M. E. Leinhardt, D. A. Dakin, and J. E. Maenchen, *J. Appl. Phys.* **64**, 1679 (1988).
- <sup>30</sup>Robert H. Stark, Uwe Ernst, Mohamed El-Bandrawy, Christophe Laux, and Karl H. Schoenbach, *Proc. 30th AIAA Plasmadynamics and Lasers Conf., Norfolk, VA, July 1999* (American Institute of Aeronautics and Astronautics, Washington DC), paper AIAA-99-3666.
- <sup>31</sup>K. Stockwald and M. Neiger, *Contrib. Plasma Phys.* **35**, 15 (1995).



# Direct current glow discharges in atmospheric air

Robert H. Stark<sup>a)</sup> and Karl H. Schoenbach

*Physical Electronics Research Institute, Old Dominion University, Norfolk, Virginia 23529*

(Received 5 January 1999; accepted for publication 26 April 1999)

Direct current glow discharges have been operated in atmospheric air by using 100  $\mu\text{m}$  microhollow cathode discharges as plasma cathodes. The glow discharges were operated at currents of up to 22 mA, corresponding to current densities of 3.8 A/cm<sup>2</sup> and at average electric fields of 1.2 kV/cm. Electron densities in the glow are in the range from 10<sup>12</sup> to 10<sup>13</sup> cm<sup>-3</sup>. Varying the current of the microhollow cathode discharge allows us to control the current in the atmospheric pressure glow discharge. Large volume atmospheric pressure air plasmas can be generated by operating microhollow cathode discharges in parallel. © 1999 American Institute of Physics. [S0003-6951(99)01425-4]

Research on high-pressure glow discharges is motivated by applications such as instantly activated reflectors and absorbers for electromagnetic radiation, surface treatment, thin-film deposition, remediation and detoxification of gaseous pollution, and gas lasers. Many of these applications require the generation of air plasma at atmospheric pressure with electron densities exceeding 10<sup>11</sup> cm<sup>-3</sup>. One of the major obstacles in obtaining such a plasma are instabilities, particularly glow-to-arc transitions (GAT), which lead to the filamentation of the glow discharge in times short compared to the desired lifetime of a homogeneous glow. These instabilities generally develop in the cathode fall, a region of high electric field, which in self-sustained glow discharges is required for the emission of electrons through ion impact. Eliminating the cathode fall, by supplying the electrons by means of an external source, is therefore expected to extend the range of stable operation.

Recently, it has been shown that microhollow cathode discharges (MHCDs) serve as electron emitters for high-pressure glow discharges.<sup>1</sup> Microhollow cathode discharges are high-pressure, direct current glow discharges between closely spaced electrodes with an electrode opening of approximately 100  $\mu\text{m}$  and an electrode distance of about 200  $\mu\text{m}$ . Experiments in argon and xenon have shown that dc operation of microhollow cathode discharges in noble gases is possible at atmospheric pressure.<sup>2,3</sup> More recently, stable discharge operation has also been obtained in atmospheric pressure air.<sup>4</sup> When operated in the hollow cathode discharge mode electrons are extracted through the anode opening at moderate electric fields. These electrons support a stable plasma between the microhollow anode and a third positively biased electrode. Direct current glow discharges in argon at one atmosphere have been generated using this method.<sup>1</sup> As shown in the following, the microhollow cathode discharges can also be used to sustain dc glow discharges in atmospheric pressure air.

The electrode system used in our experiments consists of a microhollow electrode system and an additional electrode with variable distance of up to 10 mm from the microhollow anode. The electrode configuration and the experimental

setup are shown in Fig. 1. Also shown are photographs of the microhollow cathode discharge in air (end-on) and the MHCD sustained glow between hollow anode and third electrode (side-on). The pressure was, in this case, 10 Torr. The microhollow cathode discharge is generated between two plane-parallel electrodes with centered circular openings. The electrodes consist of 100- $\mu\text{m}$ -thin molybdenum foils and the cathode and anode hole diameter of the plasma cathode ranges from 80 to 100  $\mu\text{m}$ . The dielectric is alumina (Al<sub>2</sub>O<sub>3</sub>, 96% purity) of 250  $\mu\text{m}$  thickness and is placed as a spacer between the electrodes. The anode of the microhollow cathode geometry is on ground potential, the third electrode is biased positively with respect to the microhollow anode. It serves as anode for the microhollow cathode sustained (MCS) glow discharge. The sustaining voltage of the microhollow cathode discharge is in the range from 400 to 600 V depending on current, gas pressure, and gap distance. The MHCD current was limited to values of less than 22 mA dc to prevent overheating of the sample.

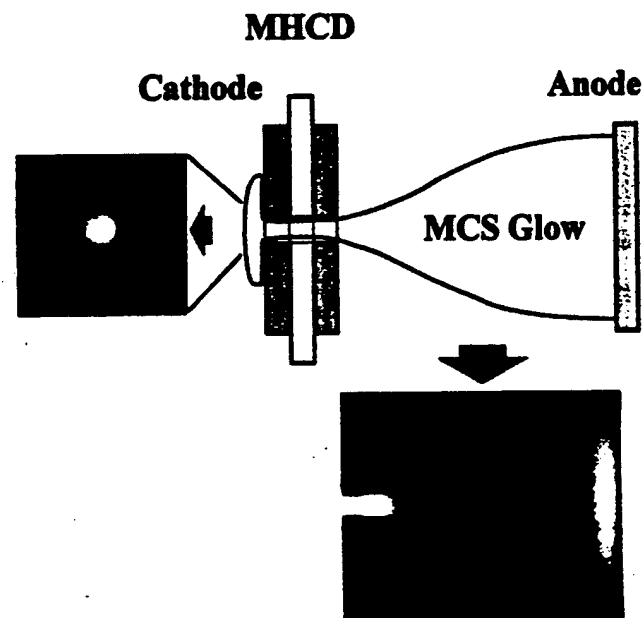


FIG. 1. Geometry of the microhollow electrode system with a third electrode and the appearance of the discharge plasma, end-on and side-on.

<sup>a)</sup>Electronic mail: stark@ece.odu.edu

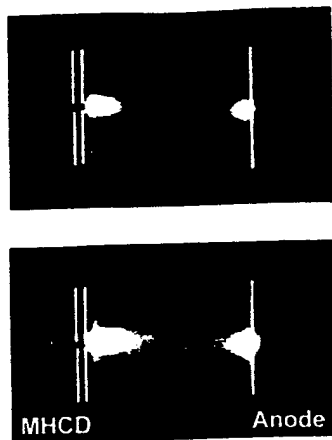


FIG. 2. MCS glow discharge in atmospheric air at two different current levels 8.7 and 22 mA, respectively, at 0.2 cm gap distance. Upper photograph:  $V_{\text{MHCD}} = 499$  V,  $I_{\text{MHCD}} = 8.9$  mA,  $V_{\text{MCS}} = 250$  V,  $I_{\text{MCS}} = 8.7$  mA. Lower photograph:  $V_{\text{MHCD}} = 409$  V,  $I_{\text{MHCD}} = 27.0$  mA,  $V_{\text{MCS}} = 238$  V,  $I_{\text{MCS}} = 22.0$  mA.

Since possible discharge instabilities like thermal instability or attachment instability<sup>5</sup> may occur on a time scale of microseconds and less, too fast to be observed with dc current and voltage monitors, we have in all measurements monitored the current and voltage by means of fast electrical probes and recorded the traces by means of a 400 MHz digital oscilloscope. In addition, the appearance of the dc discharge has been recorded by means of a charge-coupled device camera.

Figure 2 shows atmospheric pressure air discharges at two current levels of 8.7 and 22 mA, respectively. The air plasma is cylindrical with the diameter at the plasma cathode determined by the hole diameter (100  $\mu\text{m}$ ). At 8.7 mA the diameter increases to 430  $\mu\text{m}$  in the midplane of the discharge gap, and then shrinks again to approximately the cathode diameter at the third electrode. At 22 mA the diameter in the midplane is about 860  $\mu\text{m}$ . The current density is at the currents of 8.7 and 22 mA, and 6 and 3.8 A/cm<sup>2</sup>, respectively.

Figure 3 shows the development of the MCS air glow discharge current with increasing MHCD current at atmospheric pressure. The voltage at the third electrode was kept constant at  $V = 250$  V. The MCS glow discharge current is identical to the plasma cathode current above the minimum

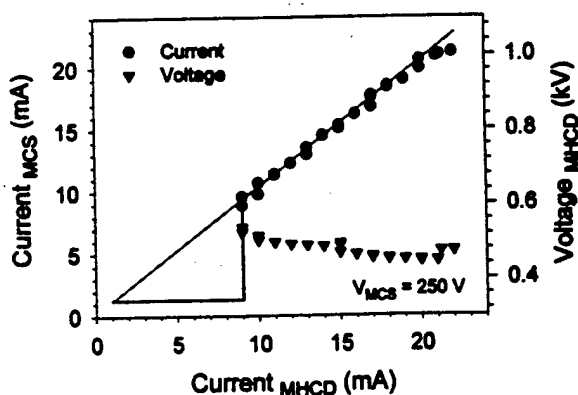


FIG. 3. MCS glow discharge current vs MHCD current and forward voltage vs current of the MHCD for constant voltage  $V_{\text{MCS}}$  at the third electrode.

sustaining current (8 mA) for the MCS discharge. The microhollow cathode discharge acts as a constant current source for the air glow. In this mode the forward voltage in the microhollow cathode discharge, which serves as the plasma cathode, decreases slightly with current (Fig. 3). Small variations in the MHCD voltage cause, therefore, large swings in the electron current, and consequently, the current in the air glow.

The electron density  $n_e$  can be estimated from the electrical parameters of the discharge, the electric field  $E$ , the current density  $j$ , and the electron mobility  $\mu_e$ :

$$n_e = j / (E \mu_e e), \quad (1)$$

with  $e$  being the electron charge and  $\mu_e$  obtained from

$$(\mu_e p) T_0 = 0.45 \times 10^6 \text{ (cm}^2 \text{ Torr/V s)}. \quad (2)$$

This equation holds for air<sup>5</sup> at room temperature  $T_0$ . Recent measurements showed that the gas temperature  $T$  in air glow discharges at currents of approximately 10 mA is close to 2000 K.<sup>4</sup>

In order to take this elevated gas temperature into account, it was assumed that  $\mu_e p$  depends linearly on  $T$ :

$$(\mu_e p)_T = T / T_0 (\mu_e p)_{T_0}. \quad (3)$$

Assuming that the electric field in the discharge is given as the anode voltage divided by the gap distance, and that the current density at midplane is the current divided by the cross section of the discharge at this plane, the electron density at this position can be estimated. The cross section of the discharge was obtained from Fig. 2, by considering the radius, where the intensity decreased to half of the maximum intensity, as the effective discharge radius. For  $p = 760$  Torr,  $j = 3.8$  A/cm<sup>2</sup> and  $E = 1.2$  kV/cm, and  $T = 2000$  K, the estimated electron density at midplane is  $5 \times 10^{12}$  cm<sup>-3</sup>.

In air, the main electron-loss process is electron attachment to oxygen. The energy density required to sustain a discharge in such an attaching gas is given as

$$P = n_e W_{\text{ion}} / \tau, \quad (4)$$

where  $n_e$  is the electron density,  $W_{\text{ion}}$  the effective ionization energy, and  $\tau$  is the average lifetime of the electrons. At concentrations of  $10^{13}$  cm<sup>-3</sup>, in atmospheric air,  $\tau$  is 10 ns.<sup>6</sup> Assuming that the effective ionization energy is 50 eV, the power density required for the sustenance of an atmospheric air plasma with electron densities of  $5 \times 10^{12}$  cm<sup>-3</sup> is 4 kW/cm<sup>3</sup>. Assuming that the average electric field in the glow is 1.2 kV/cm, and the current density at midpoint between the electrodes is approximately 3.8 A/cm<sup>2</sup>, the experimentally obtained power density is 4.6 kW/cm<sup>3</sup>, a value which is close to the theoretical value.

Although the plasma volume in this experiment is still only cubic millimeters, the described method allows us to scale it up to larger values. In the longitudinal direction this can be achieved by extending the electrode gap, which requires increasing the applied voltage. In the transverse direction large volume plasma operation can be achieved by superimposing microhollow cathode discharge supported glows through parallel operation.<sup>7</sup> The possible individual control of each of the discharge elements permits us to gen-

erate any desired plasma pattern in the transverse plane. A limiting factor is the power density, which at this point would prevent us from generating large volume plasmas. However, experimental results with combustion-assisted glow discharges in air indicate that the power can be reduced by orders of magnitude.<sup>8</sup> Experiments with combustible additives and additives with low ionization potential are underway.

This work was funded by the Air Force Office of Scientific Research in Cooperation with the DDR&E Air Plasma Ramparts MURI Program.

- <sup>1</sup>R. H. Stark and K. H. Schoenbach, *J. Appl. Phys.* **85**, 2075 (1999).
- <sup>2</sup>K. H. Schoenbach, A. El-Habachi, W. Shi, and M. Ciocca, *Plasma Sources Sci. Technol.* **6**, 468 (1997).
- <sup>3</sup>A. El-Habachi and K. H. Schoenbach, *Appl. Phys. Lett.* **73**, 7 (1998).
- <sup>4</sup>R. Block, O. Toedter, and K. H. Schoenbach, *Bull. Am. Phys. Soc.* **43**, 1478 (1998).
- <sup>5</sup>Y. P. Raizer, *Gas Discharge Physics*, 2nd ed. (Springer, Berlin, Germany, 1991).
- <sup>6</sup>R. J. Vidmar, *IEEE Trans. Plasma Sci.* **18**, 733 (1990).
- <sup>7</sup>W. Shi, R. H. Stark, and K. H. Schoenbach, *IEEE Trans. Plasma Sci.* **27**, 16 (1999).
- <sup>8</sup>E. Kunhardt, Stevens Institute of Technology (private communication).

# Parallel Operation of Microhollow Cathode Discharges

Wenhui Shi, Robert H. Stark, and Karl H. Schoenbach

**Abstract**—Parallel operation of dc microhollow cathode discharges in argon at pressures up to several hundred torr was obtained without individual ballast at low currents, where the slope of the current-voltage characteristic is positive. By using semi-insulating silicon as anode material, we were able to extend the range of stable operation over the entire current range, including that with negative differential resistance. This opens the possibility to utilize microhollow cathode discharge arrays in flat panel lamps.

**Index Terms**—Gas discharges, glow discharges, light sources.

THE dc voltage-current ( $V$ - $I$ ) characteristics of microhollow cathode discharges show three distinct modes of operation: the Townsend mode at low currents, followed by the hollow cathode discharge mode, with negative differential conductance, and at high currents a mode with a  $V$ - $I$  characteristic which resembles that of an abnormal glow discharge [1], [2]. It is expected that in the current range where the  $V$ - $I$  characteristic has a positive slope, the Townsend region and the “abnormal glow” mode, stable, parallel operation of microhollow cathode discharges can be achieved without ballasting the individual discharges.

In order to confirm this hypothesis experimentally two holes of 100  $\mu\text{m}$  diameter each, separated by 100  $\mu\text{m}$ , were drilled through 100  $\mu\text{m}$  thick molybdenum foils, which served as electrodes, and a 200  $\mu\text{m}$  thick mica spacer. Electrical and optical measurements were performed in argon at pressures of up to 800 torr. The discharges were ignited by increasing the applied voltage up to a value where one of the two gaps broke down. By increasing the current, the optical emission from this first discharge became more intense and the plasma began to extend over the surface of the molybdenum cathode. When the plasma reached the second hole the second discharge turned on.

The  $V$ - $I$  characteristics of the individual discharges, taken in the phase where only one of the discharges was running, show the typical shape of the Townsend mode and hollow cathode discharge mode (Fig. 1). The third mode, the abnormal glow mode, was avoided in these dc experiments because of concern about thermal damage of the electrode system. Previously performed pulsed experiments in this current range had demonstrated parallel discharge operation [3]. With both discharges on, which in the hollow cathode mode could be obtained for short periods of time (seconds) only, the measured current is approximately the sum of the currents of the two

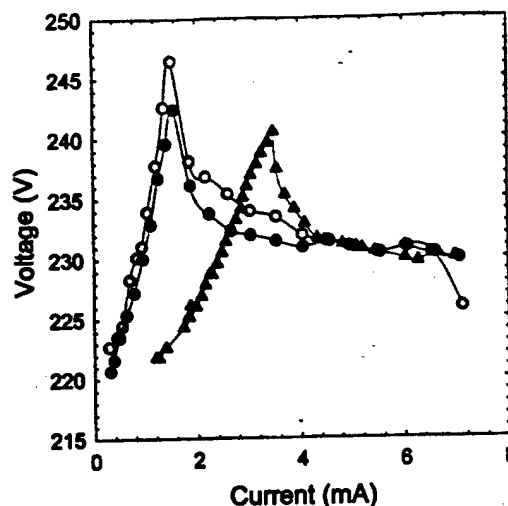


Fig. 1. The current-voltage characteristics of each of the two hollow cathode discharges (circles) in a two-hole configuration and the current-voltage characteristic of the two-hole discharge array (triangles). The gas was argon at a pressure of 400 torr.

individual discharges. This indicates relatively weak coupling between the discharges in this electrode configuration.

The relative intensities of the discharges depend on the range of operation. In the range where the differential resistance of the single discharge is positive, the intensities in the two holes were comparable (Fig. 2, upper photograph). The discharges in this mode were stable, except for sporadically occurring current fluctuations. Such fluctuations caused quenching of one of the two discharges if their average differential resistance was less than 10 V/mA, and if the positive differential resistance range extended over a current range of less than 1 mA. Where the  $V$ - $I$  slope is negative or flat one discharge dominated (Fig. 2, lower photograph). Only rarely were discharges with approximately equal intensity observed, but even then they were stable only for seconds.

In order to obtain parallel operation over the entire dc current range, particularly where the discharge  $V$ - $I$  characteristic is flat or has a negative slope, the discharges need to be individually ballasted. For large arrays, with possibly thousands of discharges this becomes technically challenging. Instead of ballasting each discharge by means of a resistor we have explored the use of distributed resistive ballast for stable operation of multiple discharges in flat panels. This can be achieved by using a semi-insulating material, e.g., a semi-insulating semiconductor, as electrode material. A cross section of an electrode system with the anode made of semi-insulating silicon is shown in Fig. 3. Silicon had been used before as electrode material [4], however, not for the purpose of ballasting the discharges.

Manuscript received July 15, 1998; revised November 16, 1998. This work was funded by DOE, Advanced Energy Division and AFOSR in cooperation with the DDR&E Air Plasma Ramparts MURI Program.

The authors are with the Physical Electronics Research Institute, Old Dominion University, Norfolk, VA 23529 USA (e-mail: schoenbach@ece.odu.edu).

Publisher Item Identifier S 0093-3813(99)02424-8.

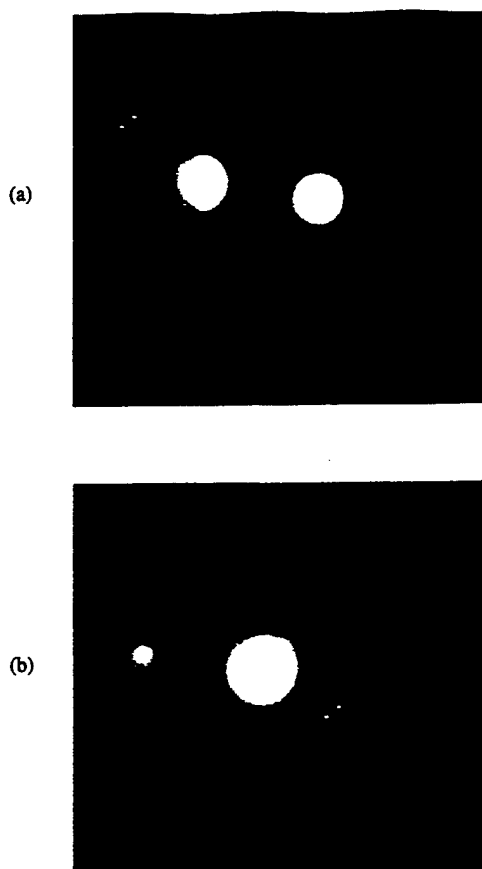


Fig. 2. End-on photograph of two dc discharges operating in the Townsend mode at a current of 2 mA (a) and in the hollow cathode discharge mode with 6 mA (b). The photographs, which were taken with a charge-coupled device camera, are overexposed to show the plasma outside the holes.

In order to obtain data on the optimum parameters of the resistive material required for stable operation of two parallel discharges, the distributed resistor was simulated by a network of two ballast resistors in series with the discharges, and a variable coupling resistor connecting the two discharges. Based on the experimental results, a semi-insulating silicon wafer of 300  $\mu\text{m}$  thickness and a resistivity of 1200  $\Omega\text{cm}$  was chosen as anode and connected to the electrode system in the way shown in Fig. 3. Sixteen holes, with a diameter of 500  $\mu\text{m}$  each, were drilled through cathode and mica layer. An end-on photograph shows the resulting dc discharges at a pressure of 28 and 62 torr, respectively. With increasing pressure the plasma changes from columnar to ring shaped [5]. We were able to operate all sixteen discharges, dc, up to 100 torr in argon. By reducing the hole size to 100  $\mu\text{m}$  the pressure range for full sixteen-hole operation could be extended to 300 torr.

The experiments demonstrated that parallel operation of dc microhollow cathode discharges can be obtained by using distributed resistive ballast. This relatively simple method allows us to operate large arrays of discharges, e.g., for use as flat panel excimer lamp. A 12 W flat panel Xe excimer lamp with 1 W optical power at 172 nm would require 20 parallel microhollow cathode discharges, each operated at a voltage

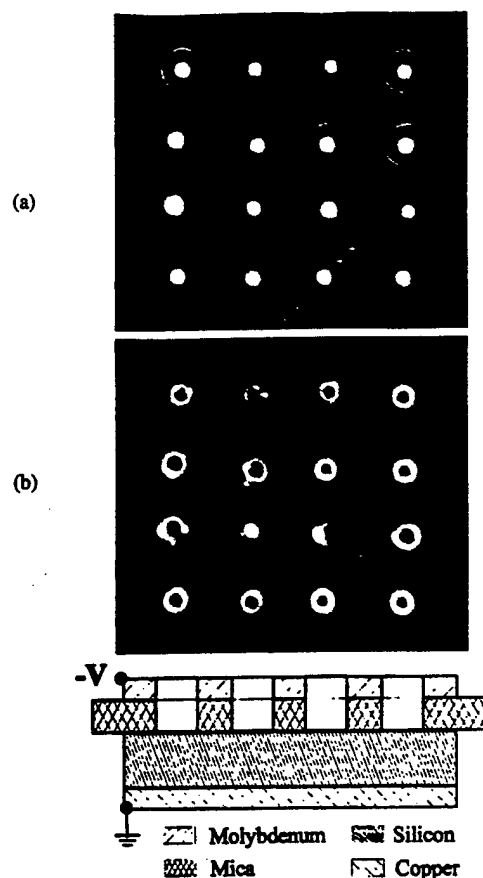


Fig. 3. Cross section of the electrode system and end-on photographs of the 16-discharge array in argon at 28 torr (a) and 62 torr (b). Currents were 28 and 25 mA, respectively.

of 200 V and a current of 3 mA with an efficiency (optical power/electrical power) of 8% [6].

#### ACKNOWLEDGMENT

The authors would like to thank A. V. Phelps of JILA for his suggestions which led to the distributed ballast experiment.

#### REFERENCES

- [1] K. H. Schoenbach, C. A. Verhappen, T. Tessnow, F. E. Peterkin, and W. W. Byszewski, "Microhollow cathode discharges," *Appl. Phys. Lett.*, vol. 68, no. 1, pp. 13–15, 1996.
- [2] A. Fiala, L. C. Pitchford, and J. P. Boeuf, "Two-dimensional, hybrid model of glow discharge in hollow cathode geometries," in *Proc. XXII Conf. Phenomena Ionized Gases*, Hoboken, NJ, 1995, vol. 4, pp. 191–192.
- [3] K. H. Schoenbach, T. Tessnow, and R. Verhappen, "High pressure hollow cathode discharges," in *Conf. Record, IEEE ICOPS*, Boston, MA, 1996, p. 229.
- [4] J. W. Frame, D. J. Wheeler, T. A. DeTemple, and J. G. Eden, "Microdischarge devices fabricated in silicon," *Appl. Phys. Lett.*, vol. 71, no. 9, pp. 1165–1167, Sept. 1997.
- [5] K. H. Schoenbach, A. El-Habachi, W. Shi, and M. Ciocca, "High pressure hollow cathode discharges," *Plasma Sources Sci. Technol.*, vol. 6, pp. 468–477, 1997.
- [6] A. El-Habachi and K. H. Schoenbach, "Generation of intense excimer radiation from high-pressure hollow cathode discharges," *Appl. Phys. Lett.*, vol. 73, no. 7, pp. 885–887, Aug. 1998.

# Direct current high-pressure glow discharges

Robert H. Stark and Karl H. Schoenbach<sup>a)</sup>

*Physical Electronics Research Institute, Old Dominion University, Norfolk, Virginia 23529*

(Received 22 July 1998; accepted for publication 13 November 1998)

Stabilization and control of a high-pressure glow discharge by means of a microhollow cathode discharge has been demonstrated. The microhollow cathode discharge, which is sustained between two closely spaced electrodes with openings of approximately 100  $\mu\text{m}$  diam, serves as plasma cathode for the high-pressure glow. Small variations in the microhollow cathode discharge voltage generate large variations in the microhollow cathode discharge current and consequently in the glow discharge current. In this mode of operation the electrical characteristic of this system of coupled discharges resembles that of a vacuum triode. Using the microhollow cathode discharge as plasma cathode it was possible to generate stable, direct current discharges in argon up to atmospheric pressure, with estimated electron densities in the range from  $10^{11}$  to  $10^{12}\text{ cm}^{-3}$ . The recently demonstrated parallel operation of these discharges indicates the potential of this technique for the generation of large volume plasmas at high gas pressure through superposition of individual glow discharges. © 1999 American Institute of Physics. [S0021-8979(99)07304-1]

## I. INTRODUCTION

Research on high pressure glow discharges is motivated by applications such as instantly activated reflectors and absorbers for electromagnetic radiation, surface treatment, thin film deposition, remediation and detoxification of gaseous pollution, and gas lasers. The two basic methods which can be used to generate large volumes of weakly ionized gas at high (atmospheric) pressure are: (1) external ionization (by means of photons or charged particles); and (2) internal ionization, the generation of electrons and ions in a self-sustained gas discharge.

Generally the efficiency of external ionization is rather low, and therefore the cost of such a method relatively high. Methods to generate large volumes of ionized gas at high pressure have therefore concentrated on ionization mechanisms where the energy required for the ionization is drawn from electrical energy. Examples of this kind of mechanism are radio frequency (rf) and microwave discharges, barrier discharges, and pulsed corona discharges where the discharge is sustained by alternating or pulsed fields, and steady state discharges where the discharge is driven by a direct current (dc) power source.

Much of the efforts in generating stable glow discharges at high pressure have focused on preventing the onset of instabilities in the regions near the electrodes,<sup>1</sup> particularly in the cathode region. These are the regions of higher electric field and consequently higher power density compared to the positive column of the discharge. This region is therefore the cradle of instabilities which lead to constrictions and arc formation in the discharge.

The glow-to-arc transition (GAT), the development of a highly conductive channel which shorts out the glow discharge, shows the first visible evidence near the cathode.<sup>2</sup> Other instabilities which may develop in the positive column

of discharges in electronegative gases, such as the attachment instability, are generally more benign than the GAT.

Segmentation of the cathode, and ballasting the individual discharge resistively has been used to prevent the onset of the GAT instability in atmospheric pressure glow discharges.<sup>1</sup> The current density in the bulk of the glow discharge is known to increase linearly with pressure ( $j_{\text{bulk}} \propto p$ ), whereas the current density in the cathode layer for normal mode operation increases quadratically with pressure ( $j_{\text{cl}} \propto p^2$ ). In order to make the conditions in the bulk and at the cathode compatible, the current cross section at the cathode needs to be reduced with increasing pressure. This was achieved by using pins as individual cathodes with cross sections small compared to the area of the cathode segment.<sup>3</sup> The onset of bulk instabilities can be prevented by flowing air with such a speed through the discharge that the plasma is replaced by cold air on a time scale small compared to the inverse of the growth rate of bulk instabilities.

Another way of eliminating the conditions for GAT in the cathode fall region of a glow discharge is to eliminate the cathode fall, that means to provide the electrons rather than through ion impact at the cathode, through external sources. This requires replacing the cathode by an externally controlled electron emitter. Besides of offering the possibility to adjust the electron emission to the large volume glow discharge, this approach also keeps the thermal losses in the cathode, which in case of resistive ballast are substantial, at a minimum and reduces the requirements for cooling. Experimental studies on the use of microhollow cathode discharges as plasma cathodes have been performed in argon and the results are reported in this article.

## II. CONCEPT OF MICROHOLLOW CATHODE SUSTAINED GLOW DISCHARGES

Hollow cathode discharges are glow discharges between a cathode, which contain some kind of a hollow and an arbitrarily shaped anode. Similarity laws<sup>4</sup> indicate that the dis-

<sup>a)</sup>Electronic mail: schoenb@rolls-royce.eng.odu.edu

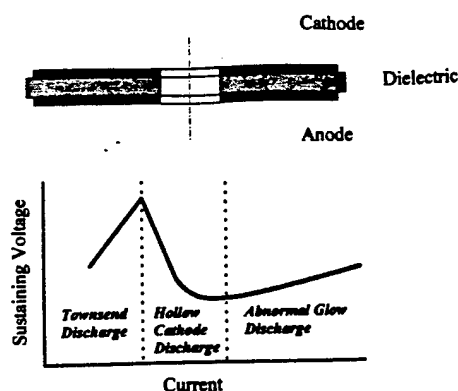


FIG. 1. (top): Geometry of microhollow electrode system with a center borehole. (bottom): Voltage-current characteristic of microhollow electrode discharges (current scale is logarithmic).

charge voltage is constant for constant  $p \cdot D$ , where  $p$  is the pressure of the fill gas and  $D$  the diameter of the cathode hole. Experiments in argon and xenon have shown that dc operation of hollow cathode discharges in noble gases is possible at atmospheric pressure, if the diameter of the cathode hole is reduced to values on the order of  $100 \mu\text{m}$ .<sup>5,6</sup> Recent results indicate that stable discharge operation can also be obtained in atmospheric pressure air.<sup>7</sup> The geometry of the microdischarge system is shown in Fig. 1 (top). The electrode system consists of two plane-parallel electrodes with a center borehole in each electrode. As spacer between the electrodes, mica with a thickness of approximately  $200 \mu\text{m}$  is used. The electrode aperture is on the order of  $100 \mu\text{m}$  in diameter. A molybdenum foil of  $100 \mu\text{m}$  thickness is used as electrode material. The currents drawn by a single discharge have for our electrode system been limited to  $7 \text{ mA}$  due to thermal loading. This value corresponds to an average current density of  $120 \text{ A/cm}^2$  in the  $100\text{-}\mu\text{m}$ -diam cathode hole area.

The voltage-current ( $V$ - $I$ ) characteristic of hollow cathode discharges shows three distinct ranges of operation [Fig. 1 (bottom)]. The resistive  $V$ - $I$  characteristic at low current, with an exponential increase in current with voltage, indicates that the discharge in this mode is a Townsend discharge.<sup>8</sup> A schematic sketch of the discharge in this mode is shown in Fig. 2 (left part). Here it is assumed that the product of pressure,  $p$ , times the electrode gap,  $d$ , is less than the  $p \cdot d$  value in the minimum of the Paschen curve. The discharge therefore develops along a path, from the outer face of one electrode to the outer face of the second one, rather than the shortest possible path, along the dielectric. At higher pressure, or larger gap between the electrodes, respectively, where this condition is not satisfied, the discharge develops inside the electrode cavity and assumes a hollow cylindrical shape.<sup>9</sup>

With increasing current, the conductivity of the discharge column inside the electrode cavity increases and it forms a virtual anode [Fig. 2 (right part)]. The electric field begins to change from a mainly axial to a more radial field concentrated at the cathode (cathode fall). The axial field is reduced to values required to compensate for electron losses

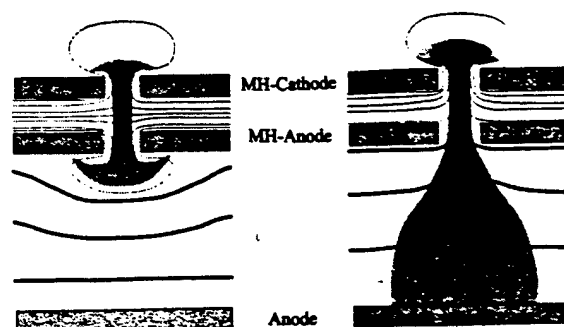


FIG. 2. (left part): Sketch of the microhollow cathode discharge in the Townsend mode and potential distribution in the three-electrode system. (right part): Sketch of the microhollow cathode discharge sustained glow discharge with the MHCD operating in the hollow cathode discharge mode. Also shown is the potential distribution. Because of the change in the potential distribution, the electric field generated by the third electrode becomes comparable to the electric field of the MHCD in the anode aperture and a discharge develops in the space between the MHCD and the third electrode.

in the virtual anode (positive column). The formation of this strong radial field at the cathode perimeter causes a fraction of electrons generated at the cathode through ion impact to gain such energy that they oscillate through the axis region, unloading much of their energy through ionizing collisions in this region. This hollow cathode effect leads to an increase in current with simultaneous decay in voltage [negative differential conductivity, Fig. 1 (bottom)]. With further increase in current, the normal hollow cathode glow discharge expands over an increasing area at the cathode surface. However, since discharge expansion to areas beyond the circumference of the cathode hole is related to a lengthening of the discharge path, the discharge voltage rises (abnormal glow discharge). This effect which is shown in the  $V$ - $I$  characteristics of the discharges at high current [Fig. 1 (bottom)], was also obtained in modeling results.<sup>10</sup>

Extraction of electrons from the microhollow cathode discharge (MHCD) by means of a third, positively biased electrode on the anode side of the MHCD geometry requires that the electric field generated by the third electrode is on the same order as the field in the MHCD. When operated in the Townsend mode, where typical electric fields in the hollow cathode structure are on the order of  $10 \text{ kV/cm}$ , this would require very high voltages applied to this third electrode which is placed at distance large compared to the gap of the MHCD. Therefore the third electrode, if biased at a moderate voltage, is not expected to have any influence on its operation [Fig. 2 (left part)].

However, when the hollow cathode discharge transfers in the mode where the axial electric field is replaced by a radial one, the electric field generated by the third electrode only needs to be on the order of that in a positive column, typically  $100 \text{ V/cm}$  to affect the hollow cathode discharge. The potential in the hollow anode plane is then similar to that of an electron lens. The electrons in the hollow electrode rather than drifting to the microhollow anode are rerouted to the third electrode. Consequently it is expected that the MHCD acts as an electron source for a larger volume glow

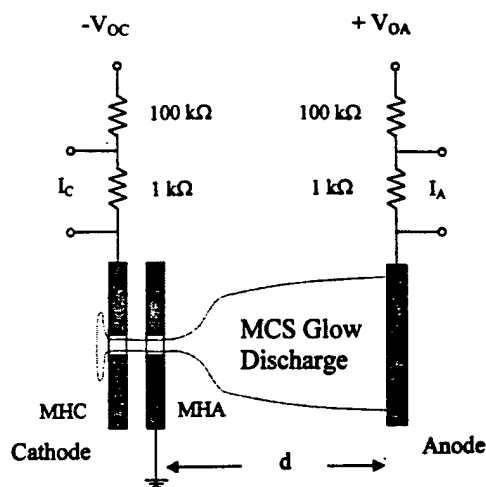


FIG. 3. Electrode configuration and electrical circuit.

discharge between the hollow anode and the third electrode when operated in the hollow cathode mode.

In the resistive current ranges (ranges where the slope of the  $V$ - $I$  characteristic is positive) hollow electrode discharges can be operated in parallel without or at least with small ballast. For being used as electron source, as discussed in the previous paragraph, the relevant range of operation would be that at high current, where the discharge resistance increases [abnormal glow discharge, Fig. 1 (bottom)]. Experimental results<sup>11</sup> indicate that parallel operation of microhollow cathode discharges can be achieved in this range of current densities in excess of  $100 \text{ A/cm}^2$ .

### III. EXPERIMENTAL SETUP

The electrode system, which is placed in a stainless steel chamber, consists of a microhollow electrode system (see Fig. 1) and an additional (third) electrode with variable distance from the microhollow electrodes. The vacuum and gas handling system allows us to operate the discharge in the range from millitorr up to atmospheric pressure. Two windows provide optical access to the discharge, side on and end on. A charge coupled device camera with video recording system is used to record the appearance of the discharge.

The electrode configuration and electrical arrangement of the setup is shown in Fig. 3. The electrode on the very left serves as microhollow cathode (MHC) for the MHCD. The anode of the microhollow cathode geometry is on ground potential. The plasma cathode current is measured by recording the voltage across a  $1 \text{ k}\Omega$  resistor in the microhollow cathode discharge circuit. The third electrode, also made of molybdenum, is positively biased. It serves as anode for the microhollow cathode sustained (MCS) glow discharge. Its distance from the microhollow anode,  $d$ , can be varied between 0 and 10 mm. As for the MHCD, a  $100 \text{ k}\Omega$  resistor is used to limit the discharge current in the MCS glow discharge, which is measured by means of a resistor of  $1 \text{ k}\Omega$ . The applied voltages at both, the microhollow cathode and the third electrode are limited to values of 800 V, determined by the voltage feed throughs in our discharge chamber. The sustaining voltage of the microhollow cathode discharge is in



FIG. 4. Side-on view of the microhollow cathode discharge in argon at 160 Torr with the third electrode unbiased.

the range from 100 to 400 V depending on current and gas pressure. The microhollow cathode discharge current was limited to 7 mA to prevent overheating of the sample.

The discharges were operated in the dc mode. Since possible discharge instabilities may occur on a time scale of microseconds and less, too fast to be observed with dc current and voltage monitors, we have, in all measurements, monitored the current and voltage by means of fast electrical probes and recorded the traces on a 400 MHz digital oscilloscope.

Before each experiment the chamber was evacuated to  $10^{-4}$  Torr, then filled with argon (spectroscopic grade with impurities less than 0.000 01%) at the desired pressure. Argon was chosen because in previous experiments stable microhollow cathode discharges in this gas have been obtained up to atmospheric pressure.<sup>9</sup> The argon pressure in this experiment was varied between 40 and 760 Torr. Two procedures have been used to study the effect of a MHCD on a MCS glow discharge:

At constant pressure and electrode geometry, (1) the bias potential was kept constant and the MHCD current was varied slowly by increasing or decreasing the sustaining voltage, and (2) the MHCD current was kept constant and the potential at the third electrode was varied slowly by increasing or decreasing the bias voltage.

### IV. EXPERIMENTAL RESULTS

With the third electrode unbiased the MHCD may develop (statistically) in one of the two modes: (a) an umbrella shaped plasma layer develops at the anode side of the MHCD system; and (b) the MHCD plasma does not extend into the electrode space; only a plasma layer at the circumference of the anode aperture is visible.

An example of the anode plasma extended into the anode backspace is shown in Fig. 4. The side-on photograph shows three areas of high intensity. The area of highest intensity in the center represents the plasma column, the outer areas the edges of the plasma layer at the anode surface. Although the mechanism of the MHCD formation is not yet understood, it will be shown that it is irrelevant for the use of the MHCD as plasma cathode, and we have consequently not paid much attention to this phase.



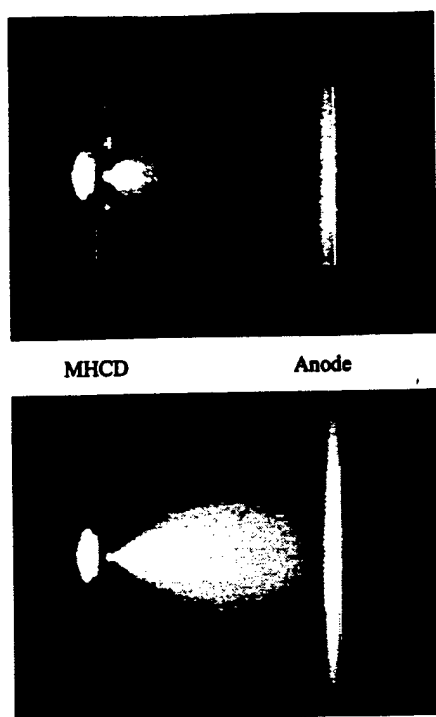


FIG. 5. (top): Side-on view of the MHCD and the predischage in argon at 160 Torr at a voltage of 66 V applied to the third electrode. ( $V_{\text{MHCD}} = 289$  V,  $I_{\text{MHCD}} = 1.09$  mA,  $I_{\text{MCS}} = 0.42$  mA.) (bottom): Side-on view of the MHCD and the MCS glow discharge for 77 V anode potential. ( $V_{\text{MHCD}} = 259$  V,  $I_{\text{MHCD}} = 1.27$  mA,  $I_{\text{MCS}} = 1.27$  mA.) The gap between plasma cathode and anode is 0.5 cm.

With increasing bias potential,  $V_A$ , at the third electrode (anode), the current flow to this electrode increases exponentially, but is still small compared to the MHCD current. In this phase, the *predischage* phase, a luminous plasma develops in the space between plasma cathode and anode [Fig. 5 (top)]. Although the umbrella like structure of the MHCD anode is still present in this mode, electrons originating from the center of the MHCD are carried increasingly—with increasing  $V_A$ —to the third electrode. Eventually, at a certain threshold voltage the plasma umbrella becomes detached from the MHCD anode [Fig. 5 (bottom)] and a bell shaped discharge column is formed. In this mode, the MCS *glow* mode, the current in the MCS glow is identical with the MHCD current.

Besides the dependence on the applied voltage,  $V_A$ , the appearance of the glow between MHCD and anode is also determined by the microhollow cathode discharge current. This is shown in Fig. 6. The solid curve in Fig. 6 correspond to the threshold values of MHCD current and anode potential where the transition from the predischage to the MCS glow is observed. The dashed vertical line in Fig. 6 represents the mode of operation where the glow between plasma cathode and anode is controlled by  $V_A$ , at constant MHCD current. The dashed horizontal line in Fig. 6 represents a mode of operation where the MCS glow discharge is controlled by the current in the microhollow cathode discharge, with the anode voltage,  $V_A$ , kept constant. Point A represents the transition from the predischage to the MCS glow discharge for both cases.

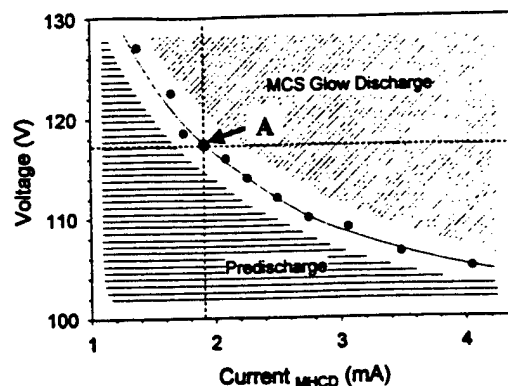


FIG. 6. Range of operation of the predischage and the MCS glow discharge in argon at 160 Torr.

The development of the current in the glow between plasma cathode and third electrode (anode) with increasing microhollow cathode current (along a horizontal line as shown in Fig. 6:  $V_A = \text{constant}$ ) and the corresponding  $V-I$  characteristic of the MHCD are shown in Fig. 7. Up to a MHCD current of 3 mA the current in the glow discharge is small compared to the MHCD current. This is the predischage phase, where the axial MHC electric field in the microhollow geometry exceeds the external field. At the current threshold value in the two fields, the internal and the external fields become comparable and the current is completely rerouted from the microhollow anode to the third electrode.

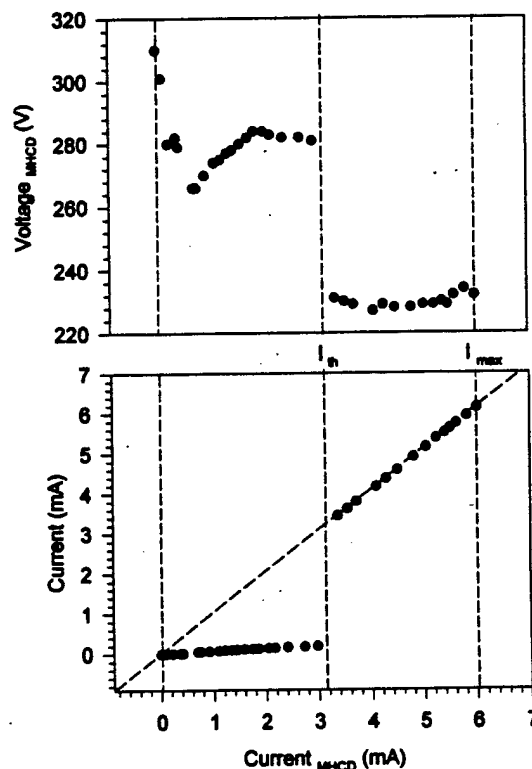


FIG. 7. MHCD voltage (top) and current measured at the anode (bottom) vs MHCD current at a constant anode potential of 100 V (argon,  $p = 160$  Torr). The transition at  $I_{th}$  corresponds to a point on the solid curve in Fig. 6.

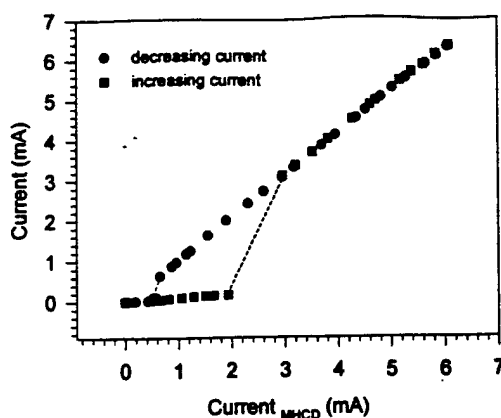


FIG. 8. Hysteresis in the transition from predischARGE to MCS glow discharge.

This means, that the MHCD current and the MCS glow discharge current become identical. This switching effect is correlated with a sudden drop in the MHCD voltage. The results depicted in Fig. 7 were obtained by varying the MHCD current from low to high values. By changing the current from high to low values, the transition from high current mode to the low current mode occurs at much lower values of the MHCD current (Fig. 8).

The upper limit in MCS glow discharge current and voltage, respectively, is determined by the onset of the GAT. Then the discharge current rises by several orders of magnitude. Simultaneously the forward voltage drops to a few tens of volts. The  $V$ - $I$  characteristics in Figs. 7 and 8 were obtained for discharges in argon at 160 Torr and an electrode gap of 5 mm. The pressure could be increased to 1 atm without reaching the threshold value for the GAT. A side-on photograph of a dc discharge in argon at 1 atm is shown in Fig. 9 between electrodes, which are 2 mm apart. The plasma is bell shaped, with its diameter at the plasma cathode determined by the hole diameter (100  $\mu$ m). Its diameter increases to 2 mm at the anode. Assuming that the electric field,  $E$ , in this discharge is given as the anode voltage divided by the gap distance, and that the current density,  $j$ , at midplane is

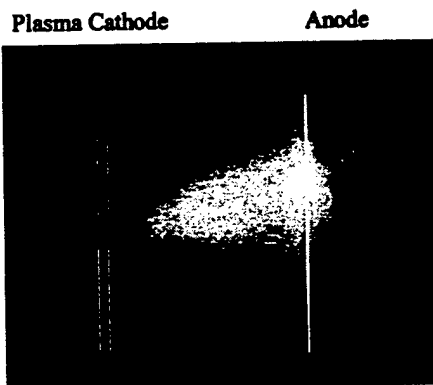


FIG. 9. MCS glow discharge in argon at atmospheric pressure with an anode potential of 213 V. The gap between plasma cathode and anode is 0.2 cm. ( $V_{MHCD}$  = 169 V,  $I_{MHCD}$  = 470  $\mu$ A,  $I_{MCS}$  = 500  $\mu$ A.)

the current divided by the cross section of the discharge at this plane, the electron density at this position can be estimated

$$n_e = j / (E \mu_e e),$$

with the electron mobility,  $\mu_e$ , being  $0.33 \times 10^6$  ( $\text{cm}^2 \text{Torr/V s}$ ) for argon.<sup>1</sup>

For  $p$  = 760 Torr,  $j$  = 0.05 A/cm<sup>2</sup>, and  $E$  = 1 kV/cm the estimated electron density at midplane is  $7 \times 10^{11} \text{ cm}^{-3}$ . The cross section of the discharge was obtained from Fig. 9, by considering the radius, where the intensity dropped to half of the maximum intensity, as effective discharge radius.

## V. DISCUSSION

Hollow cathode discharges operate at low current in a Townsend mode, where in an electrode configuration as shown in Fig. 2 (left part) the electric field is dominantly axial. With increasing current they transfer into the hollow cathode mode with high radial electric fields in the cylindrical cathode fall of the discharge. The axial field in the plasma column, which serves as a virtual anode in this case, is rather small. When the hollow cathode discharge operates in this mode external fields generated by a third, positively biased electrode in front of hollow anode can penetrate into the electrode cavity and force the hollow cathode current to flow to the third electrode [Fig. 2 (right part)]. The hollow cathode discharge serves then as electron source for a glow discharge between hollow anode and the third electrode. The hollow cathode system can then be considered as plasma cathode, the third electrode as anode of a MCS glow discharge.

In the plasma cathode sustained glow discharge the cathode fall is eliminated. This is of great importance for the stability of the glow discharge. The cathode fall, a region of high electric field, is generally the cradle of instabilities. Stability is particularly an issue for high-pressure glow discharges, where GATs, emerging from the cathode fall region, are limiting the lifetime of these plasmas to times on the order of microseconds and less. Since in the plasma cathode sustained glow discharge the generation of electrons occurs in the hollow cathode discharge, the glow discharge is stable as long as the hollow cathode discharge is stable, providing that the conditions in the main discharge are such that bulk instabilities are avoided.

It was shown in earlier studies that a stable, high-pressure operation of hollow cathode discharges could be achieved by reducing the cathode hole in the hollow cathode geometry to submillimeter diameter.<sup>6</sup> In argon and xenon these microhollow cathode discharges have been operated, dc, up to and even exceeding atmospheric pressure with cathode hole diameters of 100  $\mu$ m.<sup>6,9</sup> When used in the three-electrode system as described in this article, we were able to obtain a stable, dc, MCS glow discharge in argon at atmospheric pressure. Electron densities in this glow discharge were estimated to be  $7 \times 10^{11} \text{ cm}^{-3}$  in the midplane of the main glow discharge.

The volume of the MCS atmospheric pressure discharge is in our experiment still on the order of cubicmillimeter.

However, it should be easy to extend the discharge in axial direction by increasing the applied voltage, as long as the electric field in the discharge is kept below the threshold field for GATs. Extending the discharge in radial direction requires multihole operation, where individual MCS glow discharges are operated in parallel. Experiments in argon at pressures of so far up to 300 Torr have shown that multihole operation of MHCDs is possible. Sixteen discharges have been ignited and sustained in a dc mode by using distributed resistive ballast.<sup>11</sup>

Besides stabilizing a high-pressure glow discharge, the MHCD may also serve as a current valve for the glow discharge. As shown in Fig. 7, the MHCD current determines the glow discharge current at a constant voltage across the main glow discharge gap. The MHCD current on the other hand can easily be controlled by the MHCD voltage. Small variations in this voltage cause large swings in current. The microhollow cathode sustained glow discharge behaves consequently similar as a *vacuum triode*: Small changes in the control voltage cause large changes in the plate (anode) current. This feature of the MCS glow discharge can be used to generate patterns by individually controlling discharges in discharge arrays.

Another feature of the MCS glow discharge, the threshold current required for its onset, opens the possibility to switch a large volume glow discharge on with small voltage swings. By operating the discharge system just below the threshold for onset of the MCS glow discharge (Fig. 7), only a small voltage pulse is required to turn the main discharge on. Once in the on state, it will stay there, even when the voltage pulse is turned off, because of the hysteresis of the main discharge (Fig. 8).

The concept of microhollow cathode discharge sustained high-pressure glow discharges can be applied to any gas. One of the most important gases with applications such as surface treatment and exhaust treatment is air. First results of experiments in air indicate that the stabilizing effect of microhollow cathode discharges on high-pressure glow discharges works also for high-pressure discharges in molecular and electronegative gases.

## ACKNOWLEDGMENT

This work was solely funded by the Air Force Office of Scientific Research (AFOSR) in cooperation with the DDR&E Air Plasma Ramparts MURI program.

- <sup>1</sup>Y. P. Raizer, *Gas Discharge Physics* (Springer, Berlin, 1991), Chap. 13.
- <sup>2</sup>R. R. Mitchel, L. J. Denes, and L. E. Kline, *J. Appl. Phys.* **49**, 2376 (1978).
- <sup>3</sup>A. P. Napartovich, Yu. S. Akishev, XXI International Conference on Phenomena in Ionized Gases, 1993, Bochum, Germany, Proc. III, p. 207.
- <sup>4</sup>D. J. Sturges and H. J. Oakam, *J. Appl. Phys.* **35**, 2887 (1964).
- <sup>5</sup>A. El-Habachi and K. H. Schoenbach, IEEE International Conference on Plasma Science, Rayleigh, NC, 1998, p. 125.
- <sup>6</sup>A. El-Habachi and K. H. Schoenbach, *Appl. Phys. Lett.* **72**, 22 (1998).
- <sup>7</sup>R. Block, O. Toedter, and K. H. Schoenbach, *Bull. APS* **43**, 1478 (1998).
- <sup>8</sup>J. D. Cobine, *Gaseous Conductors* (Dover, New York, 1958), p. 144.
- <sup>9</sup>K. H. Schoenbach, A. El-Habachi, W. Shi, and M. Ciocca, *Plasma Sources Sci. Technol.* **6**, 468 (1997).
- <sup>10</sup>A. Fiala, L. C. Pitchford, and J. P. Boef, Proceedings of the XXII International Conference on Phenomena in Ionized Gases, Hoboken, NJ, 1995, Contr. Papers 4, p. 191.
- <sup>11</sup>W. Shi, R. H. Stark, and K. H. Schoenbach, *IEEE Trans. Plasma Sci.* (to be published).

# **Publications in Conference Proceedings**



**AIAA 2000-2417**

**Experiments and Simulations of DC and  
Pulsed Discharges in Air Plasmas**

M. Nagulapally, G.V. Candler  
University of Minnesota  
Minneapolis, MN

C.O. Laux, L. Yu, D. Packan, C.H. Kruger  
Stanford University  
Stanford, CA

R. Stark, K.H. Schoenbach  
Old Dominion University  
Hampton, VA

**31st AIAA Plasmadynamics  
and Lasers Conference**

**19-22 June 2000 / Denver, CO**

# Experiments and Simulations of DC and Pulsed Discharges in Air Plasmas

Manoj Nagulapally\*

Graham V. Candler\*\*

*Department of Aerospace Engineering and Mechanics  
University of Minnesota, Minneapolis MN 55455*

Christophe O. Laux†

Lan Yu\*

Denis Packan\*

Charles H. Kruger‡

*Department of Mechanical Engineering  
Stanford University, Stanford CA 94305*

Robert Stark†

Karl H. Schoenbach\*\*

*Department of Electrical and Computer Engineering  
Old Dominion University, Hampton VA 23529*

## Abstract

Experiments were conducted with atmospheric air plasmas at temperatures around 2000 K in order to increase the electron number density to approximately  $10^{13} \text{ cm}^{-3}$  by means of an applied DC discharge and an electric pulse in parallel to the DC discharge. The DC discharge produces a stable region of elevated electron number density, in agreement with two-temperature kinetics calculations. In the pulsed experiments at the end of the 10 ns pulse, the ionization level was measured to be about  $10^{13}$  electrons/cm<sup>3</sup>. Following the pulse, the electron number density decreased to  $10^{12} \text{ cm}^{-3}$  in approximately 12  $\mu\text{s}$ , in good agreement with the chemical kinetics model. This result suggests that elevated electron number densities of the order of  $10^{13} \text{ cm}^{-3}$  can be maintained in low temperature air plasmas by means of repetitively pulsed discharges. In this paper, we present results of the DC and pulsed experiments, as well as two-dimensional CFD simulations of the DC experiments. The computational model uses the Stanford two-temperature chemical kinetics model for the plasma, as well as finite-rate models for vibration-electronic energy relaxation and electron translational energy relaxation. The computational results are in good agreement with the measured electron concentration, temperatures, and cathode fall.

## Introduction

There has been considerable interest in recent years in finding methods for reducing the power budget required to generate large volumes of atmospheric pressure air plasmas at modest temperatures below 2000 K with electron number densities of the order of  $10^{13} \text{ cm}^{-3}$ . These reactive air plasmas potentially have numerous applications based on their medical, biological, environmental, electromagnetic, and aerodynamic effects. In order to increase the electron number density without significantly heating the gas, the energy must be added in a targeted fashion. One method is to apply the energy addition to the free electrons by means of an imposed electrical discharge. This approach was successfully demonstrated at Stanford in a series of experiments in atmospheric pressure air at temperatures between 1800 and 3000 K. In these experiments, a DC electric field was applied to flowing air plasmas with initial electron concentration corresponding to the chemical equilibrium value at the corresponding temperature. These experiments showed that it is possible to obtain stable diffuse glow discharges with electron number densities of up to  $2 \times 10^{12} \text{ cm}^{-3}$ , which is up to six orders of magnitude higher than in the absence of the discharge. This value corresponds to the maximum current that can be drawn from the 250 mA power supply used in the experiments. In principle, the electron number density could be increased to higher values approaching  $10^{13} \text{ cm}^{-3}$  with a power supply capable of delivering more current. The diffuse discharges are approximately 3.5 cm in length and 3.2 mm in diameter. No significant degree of gas heating was observed, as the measured gas temperature remained within a few

\* Graduate Research Assistant, Student Member AIAA

\*\* Professor, Senior Member AIAA

† Senior Research Scientist, Member AIAA

‡ Professor and Vice Provost, Dean of Research and Graduate Policy, Member AIAA

hundred Kelvin of its value without the discharge applied. The measured power budget was found to be in good agreement with modeling predictions based on a zero-dimensional model of plasma chemistry coupled with an electric discharge model over the entire range of our measurements. For electron number densities of  $10^{13} \text{ cm}^{-3}$ , the predicted power budget is approximately  $20 \text{ kW/cm}^3$ .

Because the power budget for DC electron heating is too high for the practical use of air plasmas in large-scale applications, methods to reduce the power budget are being explored at Stanford. Based on the predictions of our chemical kinetics and electrical discharge models, it was found that a repetitively pulsed electron heating strategy could provide significant power budget reductions. The basis of the pulsed heating strategy is to leverage the finite recombination time of electrons and to increase the ionization efficiency by using voltage pulses of duration much shorter than the recombination time. Significant increases in ionization efficiency can be obtained by using short electric pulses with peak voltages moderately larger than for the case of DC electron heating. These high voltage pulses significantly enhance the tail of the electron energy distribution function, thereby increasing the rate of ionization relative to vibrational excitation by electron impact, which is the dominant channel for inelastic power losses in the DC discharges investigated.

In this paper, we present a summary of the DC and pulsed experimental results along with numerical simulations of the DC experiments. The calculations are being used to quantify the effect of a DC discharge on the electron concentration in the atmospheric pressure air plasma and to refine our fundamental understanding of ionization kinetics.

### Experimental Approach

All experiments described here were conducted with the experimental set-up shown in Figure 1. The device consists of two parts, a gas preheater and a discharge region. The gas preheater comprises a 50 kW radio-frequency inductively-coupled plasma torch operating at a frequency of 4 MHz, a cold gas injection ring, and a water-cooled mixing test-section with an inner diameter of 2 cm and a length of 18 cm. The temperature of the plasma at the exit of the 2 cm diameter torch nozzle is about 5000 K and its velocity is about 100 m/s. The plasma then enters a test-section where it is cooled to the desired temperature by mixing with an adjustable amount of cold air injected into the plasma stream through a radial mixing ring. At the exit of the mix-

ing test-section the air flow is close to local thermodynamic equilibrium (LTE) conditions. Finally, a 1 cm exit diameter converging nozzle is mounted at the exit of the mixing test-section. This nozzle is used to control the velocity, hence the residence time, of the flow within the discharge region. For the pulsed discharge experiments, the centerline temperature, flow velocity, and mass flow rate at the entrance of the discharge region were approximately 2300 K, 440 m/s and 4.9 g/s, respectively.

The discharge region consists of two platinum pin electrodes of 0.5 mm diameter held along the axis of the air stream by two water-cooled  $\frac{1}{16}$ " stainless-steel tubes placed crosswise to the plasma flow. The bottom electrode is mounted on the copper nozzle and the upper electrode is affixed to a Lucite ring itself mounted on a vertical translation stage in order to provide adjustable interelectrode distance. Several platinum pins (diameter 0.02") can be inserted into the discharge region to measure the voltage at various locations along the axis of the discharge in order to determine the electric field. The interelectrode distance was set to 3.5 cm for the DC discharge experiments, and 1.2 cm for the combined pulsed/DC discharges.

The electric pulse was generated with a pulse forming line system developed at Old Dominion University by Stark and Schoenbach. The pulse shape was approximately rectangular, with maximum voltage of 10 kV and duration 10 ns. In the pulsed experiments, a DC discharge of 2 kV and 150 mA was applied in parallel to the pulse in order to pre-ionize the plasma at an electron number density of approximately  $6.5 \times 10^{11} \text{ cm}^{-3}$ . In all experiments presented here, the bottom electrode was biased to negative potentials and the top electrode was connected to ground.

## Experimental Results

### DC Discharge Experiments

Figure 2 a photograph of the air plasma plume in the region between the two electrodes without the discharge applied. Figure 3 shows the same region with the DC discharge Applied between the electrodes. In these DC experiments, the interelectrode distance was 3.5 cm, the discharge current 200 mA, and the voltage applied across the electrodes was 5.2 kV. The bright region in Figure 3 corresponds to the discharge-excited plasma. The discharge diameter is approximately 3.5 mm and the electron concentration was determined from electrical conductivity measurements to be approximately  $2 \times 10^{12} \text{ cm}^{-3}$ . Without the discharge applied, the centerline rotational temperature along the axis of the flow decreases from 2300 K immediately

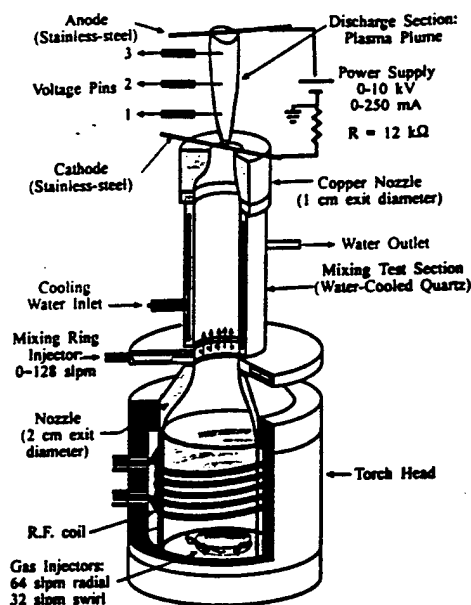


FIGURE 1. Schematic of the Stanford Plasma Torch, showing the location of the discharge section.

above the cathode (bottom electrode) to 2020 K at the anode. With the discharge applied, the measured rotational temperature remains approximately constant at a value of 2300 K along the axis of the discharge region. Thus the applied discharge does not noticeably increase the temperature of the plasma. The cathode fall voltage of the DC discharge was measured from the potential difference between the cathode and a voltage pin placed at a distance of 0.2 mm downstream of the cathode. The measured value of 290 V is in excellent agreement with the cathode fall voltage reported in the literature for glow discharges.<sup>1</sup>

The measured electrical discharge characteristics for this case as well as several additional experimental conditions at plasma temperatures ranging from 1800 to 2900 K are shown in Figure 4. The solid curves in Figure 4 correspond to the predicted discharge characteristics in atmospheric pressure air plasmas at temperatures of 2000 and 3000 K, respectively. A detailed description of the theory underlying these predicted discharge characteristics was presented in Ref. 2. Good agreement is obtained between the measured and predicted discharge characteristics over a range of experiments spanning more than three orders of magnitude in current density. The current density corresponding to an electron number density of  $10^{13} \text{ cm}^{-3}$  is indicated by the dashed line in the figure. The predicted current density  $j$  and electric field  $E$  required to generate  $10^{13}$  electrons/cm<sup>3</sup> in 2000 K atmospheric pressure air are equal to 17 A/cm<sup>2</sup> and 1.4 kV/cm. The corresponding power budget,  $jE$ , is therefore approximately 24 kW/cm<sup>3</sup>.



FIGURE 2. Air plasma at 2000 K without discharge.



FIGURE 3. Air plasma at 2000 K with DC discharge. The measured electron number density in the bright central region is approximately  $2 \times 10^{13} \text{ cm}^{-3}$ .

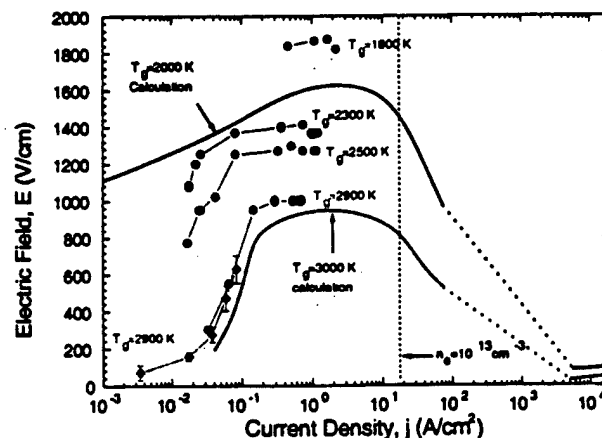


FIGURE 4. Measured and predicted electrical discharge characteristics in atmospheric pressure air plasmas generated by DC electric discharges.



### Pulsed Discharge Experiments

As discussed in the previous section, the power budget required to sustain elevated electron number densities with DC electric discharges is too high for practical applications with large volume air plasmas. We have therefore explored new strategies to reduce the power budget required to sustain superionized air plasmas. Our investigations have focused on an approach based on pulsed electron heating. The basis of the pulsed heating strategy is to leverage the finite recombination time of electrons and to increase the ionization efficiency by using short electric pulses with peak voltages moderately larger than for the case of DC electron heating. These high voltage pulses significantly enhance the tail of the electron energy distribution function, thereby increasing the rate of ionization relative to vibrational excitation by electron impact, which is the dominant channel for inelastic power losses in the DC discharges investigated.

This strategy is illustrated in Figure 5. Short voltage pulses are applied intermittently to increase the

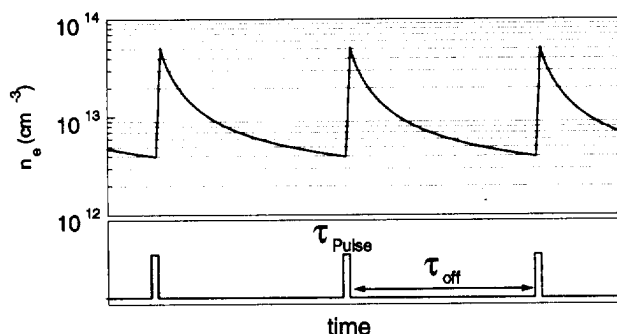


FIGURE 5. Predicted electron number density for a repetitively pulsed discharge.

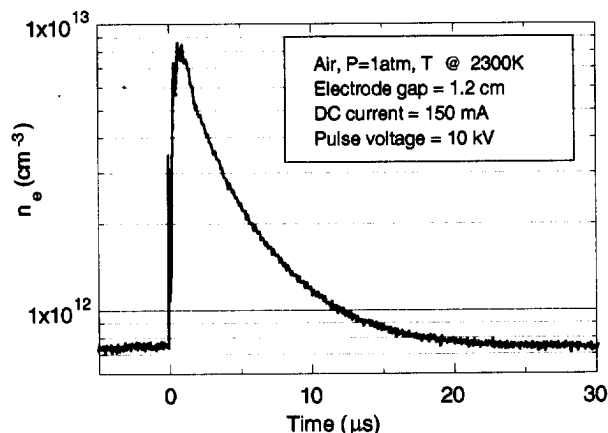


FIGURE 6. Electron number density as a function of time for the pulsed discharge experiment.

electron number density. The decay rate between pulses is governed by electron recombination processes. The average electron number density obtained with this system depends on the pulse duration, the interval between two consecutive pulses, and the pulse voltage.

In order to test the pulsing scheme, experiments were conducted at Stanford University in collaboration with Old Dominion University. These experiments employed a pulse forming line, designed and built at Old Dominion University, capable of generating a short duration (10 ns) rectangular electric pulse with peak voltages that can be varied in the range 0-16 kV. In order to experimentally simulate a repetitively pulsed discharge, the initial elevated electron number density resulting from the "previous" pulse in a repetitive discharge was created using a DC discharge operated in parallel with the pulse. These experiments enabled us to determine the voltage required to increase the electron number density to approximately  $10^{13} \text{ cm}^{-3}$  with a 10 ns ionizing pulse as well as the recombination time of electrons after the end of the pulse.

In order to determine the effect of the pulse on the plasma, the electrical resistance of the plasma was measured as a function of time from the voltage across the electrodes and the current flowing through the plasma. The electron number density can be obtained from the resistance measurements if the area of the discharge is known. This area was obtained from optical measurements of the light emitted by the plasma during pulse excitation and found to be approximately the same as the DC discharge diameter of 3.2 mm. The electron number density measured in this manner is shown in Figure 6. The electron number density increases from the initial value of  $6.5 \times 10^{11} \text{ cm}^{-3}$  to a peak of  $10^{13} \text{ cm}^{-3}$ , then decays to  $1 \times 10^{12} \text{ cm}^{-3}$  in approximately  $12 \mu\text{s}$ . The average measured electron number density over the  $12 \mu\text{s}$  duration is  $2.8 \times 10^{12} \text{ cm}^{-3}$ . With careful accounting for the background elevation of the electron temperature and the fact that the gas is flowing during the experiment, the two-temperature kinetic model has been shown to agree very well with the experimental results.

### Power Budget

We can now estimate the power reduction afforded by repetitively pulsed electron heating in comparison with DC electron heating. We consider here a repetitively pulsed discharge starting from an initial electron number density of  $10^{12} \text{ cm}^{-3}$ . The electron number density is increased to  $10^{13} \text{ cm}^{-3}$  with a 10 ns rectangular voltage pulse. The electron temperature required to produce  $10^{13}$  electrons/ $\text{cm}^3$  in 10 ns is calculated to be 32,900 K, corresponding to a field of 4 kV/cm. The

gas temperature is assumed to be 2000 K. In order to simulate the case of a repetitive discharge without background DC electron heating, we consider that the electron temperature is equal to 2000 K throughout the recombination phase. The time predicted for the electrons to recombine to the initial value of  $10^{12} \text{ cm}^{-3}$  is  $8.7 \mu\text{s}$ . The calculated average electron number density over the entire cycle is approximately  $2.6 \times 10^{12} \text{ cm}^{-3}$ .

From the results shown in Fig. 4, the current density and electric field required to sustain an electron number density of  $2.6 \times 10^{12} \text{ cm}^{-3}$  using DC electron heating are  $4.5 \text{ A/cm}^2$  and  $1600 \text{ V/cm}$ , respectively. The volumetric power for the DC case is then

$$P_{\text{DC}} \simeq 4.5 \text{ A/cm}^2 \times 1600 \text{ V/cm} = 7.2 \text{ kW/cm}^3$$

For the repetitively pulsed system, the average current density during the ionization phase can be calculated from Ohm's law and the predicted electron number density evolution. For the present case, the peak current density at the end of the pulse is approximately  $30 \text{ A/cm}^2$  and the average current density during the pulse  $10.5 \text{ A/cm}^2$ . The average power during the 10 ns pulse is then  $10.5 \text{ A/cm}^2 \times 4.0 \text{ kV/cm} = 42 \text{ kW/cm}^3$ . The total power over one pulse cycle is obtained by multiplying this value by the duty cycle of the pulser, here equal to  $(10 \text{ ns})/(8.7 \mu\text{s}) = 1.15 \times 10^{-3}$ . The power requirement for the repetitive pulsed discharge is then

$$P_{\text{Pulsed}} \simeq 42 \text{ kW} \times 1.15 \times 10^{-3} = 48 \text{ W/cm}^3$$

Thus the power budget reduction afforded by the repetitively pulsed discharge in comparison with the DC discharge is a factor of 150.

The optimal power budget that can be achieved with a pulse of given duration  $\tau_1$  in air at a given gas temperature depends on the minimum and maximum electron number densities in each pulse ( $n_{e,\text{min}}$  and  $n_{e,\text{max}}$ ), the concentrations of heavy species, the electric field during (or equivalently the electron temperature imposed by) the pulse, the interval between pulses  $\tau_2$ , and the desired average electron number density in the repetitive discharge. From analysis of the full 38-reaction mechanism for the case of ionization with a pulse  $\tau_1 = 10 \text{ ns}$ , we find that the dominant chemical reactions during the ionization phase are the electron impact ionization of  $\text{O}_2$  and  $\text{N}_2$ . Shortly after the end of the ionization phase, the dominant ion becomes  $\text{NO}^+$  as a result of fast charge transfer and charge exchange reactions. Thus for the recombination phase, we consider that the dominant reaction is the dissociative recombination of  $\text{NO}^+$ . Based on

these observations, the electron number density evolution during the ionization and recombination phases can be approximated as

$$\begin{aligned} \left. \frac{dn_e}{dt} \right|_{\text{ionization}} &\simeq k_{\text{ion},\text{N}_2} n_e n_{\text{N}_2} + k_{\text{ion},\text{O}_2} n_e n_{\text{O}_2} \\ &\simeq k_{\text{ion}} n_e N \end{aligned}$$

and

$$\left. \frac{dn_e}{dt} \right|_{\text{recombination}} \simeq -k_{\text{DR},\text{NO}^+} n_e n_{\text{NO}^+} \simeq k_{\text{DR}} (n_e)^2$$

where the rate coefficients of electron impact ionization of  $\text{N}_2$  and  $\text{O}_2$  (which depend on the electron temperature  $T_e$ ) and the rate coefficient for dissociative recombination of  $\text{NO}^+$  are taken from Ref. 2.

The ratio  $R$  of the power required to produce a given average electron number density  $n_e^*$  with a repetitively pulsed discharge relative to the power required to produce the same electron number density with a DC discharge can be expressed as

$$R = \frac{(\sigma E^2)_{\text{DC}}}{(\sigma E^2)_{\text{Pulse}}} \times \frac{\tau_1 + \tau_2}{\tau_1}$$

Using the electron energy equation and Ohm's law (see Ref. 2),  $R$  can be approximated by

$$R \simeq \frac{n_e^*}{\langle n_e \rangle_{\text{ion}}} \frac{[T_{e,\text{DC}}]^{3/2}}{[T_{e,\text{Pulse}}]^{3/2}} \times \frac{\tau_1 + \tau_2}{\tau_1}$$

where  $\langle n_e \rangle_{\text{ion}}$  stands for the average electron number density during the ionization phase of the pulse.

By solving the electron number density rate equations, analytical expressions can be obtained for  $\langle n_e \rangle_{\text{ion}}$  and  $\tau_2$  as a function of  $\tau_1$ ,  $T_e$ , and the various rate coefficients. Assuming that the duration  $\tau_2$  of the recombination phase is much longer than the ionization phase  $\tau_1$ , we obtain

$$R \simeq \frac{k_{\text{ion}}(T_e) N}{k_{\text{DR}} n_e^*} \times \frac{\alpha^2 e^\alpha}{(e^\alpha - 1)^2} \times \left( \frac{T_{e,\text{DC}}}{T_{e,\text{Pulse}}} \right)^{3/2}$$

where  $\alpha \equiv k_{\text{ion}} N \tau_1$ . Additional expressions can also be obtained for  $\tau_2$  and for the minimum and maximum electron number densities of the repetitive pulsed discharges.

Figure 7 shows the power reduction factor, minimum and maximum electron number densities, and interval between pulses as a function of the pulsed electron temperature to maintain an average electron number density of  $2.6 \times 10^{12} \text{ electrons/cm}^3$  with a 10 ns repetitively pulsed discharge in 2000 K atmospheric pressure air. It can be seen that there exists an optimum electron temperature of 27,000 K for maximum power budget reduction by a factor of 220.

The corresponding optimal parameters are minimum and maximum electron number densities of  $1.3 \times 10^{12}$  and  $6.1 \times 10^{12} \text{ cm}^{-3}$ , respectively, and interval between pulses of 8 microseconds. For an electron temperature of 32,900 K corresponding to the case analyzed in the previous section, we find that the predicted power budget reduction is by a factor of 190, which is consistent with the factor of 150 predicted by the more refined analysis presented earlier. This type of analysis is thus useful to optimize repetitive pulsing strategies. It should be noted that care should be exercised in extrapolating the above power budget reduction expression to the case of pulses shorter than 10 ns because the ionization phase may be affected by additional reactions at shorter pulse durations.

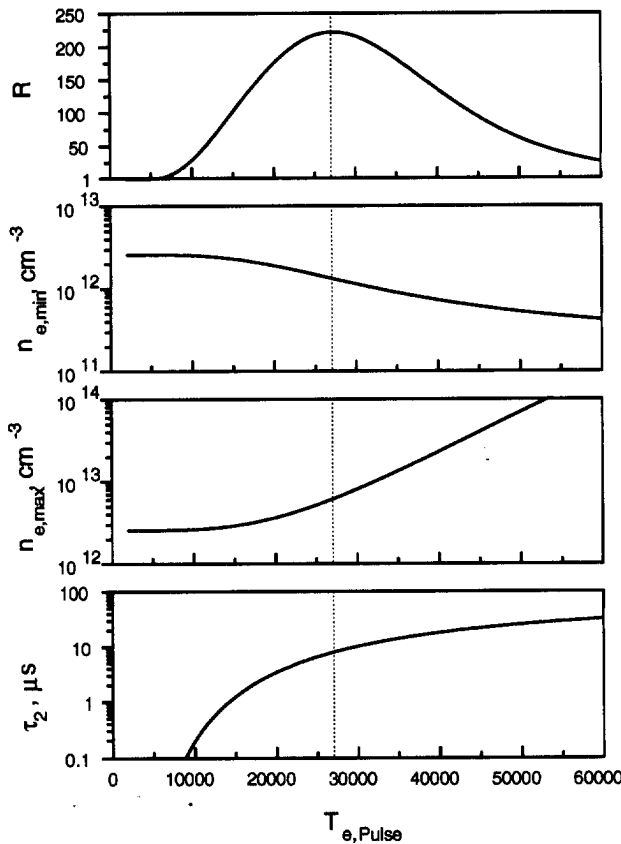


FIGURE 7. Power reduction factor afforded by pulsed vs. DC discharges to maintain an average electron number density of  $2.6 \times 10^{12} \text{ electrons/cm}^3$  in 2000 K atmospheric pressure air, as a function of the pulsed electron temperature. Also shown are the minimum and maximum electron number densities, and interval between pulses. All calculations are for a pulse duration of 10 ns.

### Numerical Simulations

In this section we discuss our numerical simulations of the DC discharge experiments. The main extension of previous work<sup>3</sup> involves the modeling of the discharge region.

### Conservation Equations

The DC discharge flow field is described by the Navier-Stokes equations that have been extended to include the effects of nonequilibrium thermochemistry. We solve separate mass conservation equations for each of the 11 chemical species present, as well as conservation equations for the radial, axial and swirl direction momenta. The energy of the flow is modeled by solving a total energy conservation equation, a vibration-electronic energy conservation equation, and an electron energy conservation equation.

Here we focus on the electron energy conservation equation because the variation of the electron temperature is the most important effect in these flows. We have

$$\frac{\partial E_e}{\partial t} + \nabla \cdot ((E_e + p_e)(\mathbf{u} + \mathbf{v}_e)) = -\nabla \cdot \mathbf{q}_e - n_e e \tilde{\mathbf{E}} \cdot \mathbf{u} - Q_{h-e} - Q_{v-e} + w_e e_e,$$

where  $\mathbf{q}_e = -k_e \nabla \cdot T_e$ , is the flux of electron energy. The conductivity of electron temperature,  $k_e$  is taken from Mitchner and Kruger.<sup>4</sup>  $Q_{h-e}$ , the heavy particle-electron energy transfer rate, is

$$Q_{h-e} = n_e \sum_h 3k(T_e - T) \left( \frac{m_e}{m_h} \right) \delta_{eh} \nu_{eh}.$$

The vibrational-electron energy transfer rate,  $Q_{v-e}$  is from Ref. 5. The electric field,  $\tilde{\mathbf{E}}$ , may be expressed in terms of the electron pressure,  $p_e$ , and current density,  $\mathbf{j}$ , and the electrical conductivity,  $\sigma$ , as

$$-n_e e \tilde{\mathbf{E}} \cdot \mathbf{u} = \nabla p_e \cdot \mathbf{u} + \frac{\mathbf{j}^2}{\sigma}$$

In the above equations,  $w_e$  is the chemical source term for the electrons,  $\delta_{eh}$ , is the nonelastic energy factor and  $\nu_{eh}$ , is the average frequency of collisions between electrons and heavy particles. For the experimental conditions, the ions have negligible concentrations, and the collision frequency is well approximated by

$$\nu_{eh} = \frac{p}{kT} g_e Q_{en},$$

where  $g_e = \sqrt{8kT_e/\pi m_e}$  is the electron thermal speed and  $Q_{en}$  is the average cross-section taken to be  $10^{-15} \text{ cm}^2$ .

### Discharge Model

To model the discharge region shown in Fig. 3, we generalize the channel model suggested by Steenbeck.<sup>1</sup>

At an infinitesimal time after the discharge is ignited, the current is vanishingly small everywhere except within the discharge region between the electrodes. The current at each axial,  $x$ , location is then

$$i = 2\pi \int_r \sigma E r dr \approx 2\pi E \int_r \sigma r dr,$$

where  $E$  is assumed to be only a function of  $x$ .

The current is controlled experimentally, and thus is a prescribed parameter. By imposing this current conservation at every location along the axis of the discharge, the field  $E(x)$  can be determined from the above equation. Now, we can apply the field to the electron energy equation in the form of the Joule heating source term. The discharge then spreads and attains a steady shape as a result of diffusive processes.

As mentioned earlier, the pin electrodes are placed cross-wise to the plasma flow. Since the stainless steel tubes carrying the electrodes do not significantly disturb the flow, the flow around the electrodes is not modeled. However, the effect of the cathode is considered by injecting a flux of electrons from a region that corresponds to the location of the cathode. This flux is calculated from the total current in the discharge and the effective area of the cathode.

### Numerical Method

Under the conditions of the DC discharge experiments, the energy relaxation processes are very fast relative to the fluid motion time scales and the chemical kinetic processes. To handle this large disparity in characteristic time scales, we would usually use an implicit time integration method.<sup>6</sup> However, for this problem a complete linearization of the problem is itself very expensive. (We solve 17 conservation equations, and the cost of evaluating the Jacobians and inverting the system scales with the square of the number of equations.) Therefore we linearize only those terms that are relatively fast, which results in a simple and inexpensive semi-implicit method that very substantially reduces the cost of the calculations.

The relatively fast terms are the internal energy relaxation and the Joule heating terms in the source terms for the three energy equations. Therefore, we split the source vector,  $W$ , into these terms,  $W_{\text{fast}}$ , and all of the other terms,  $W_{\text{slow}}$ . The conservation equations are then written as

$$\frac{\partial U}{\partial t} + \frac{\partial F}{\partial x} + \frac{1}{r} \frac{\partial rG}{\partial r} = W_{\text{fast}} + W_{\text{slow}},$$

where  $U$  is the vector of conserved variables,  $F$  is the axial direction flux vector and  $G$  is the radial direction flux vector. We then linearize  $W_{\text{fast}}$  in time

$$W_{\text{fast}}^{n+1} = W_{\text{fast}}^n + C_{\text{fast}}^n \delta U^n + O(\Delta t^2)$$

where  $C_{\text{fast}}$  is the Jacobian of  $W_{\text{fast}}$  with respect to  $U$ , and  $\delta U^n = U^{n+1} - U^n$ . Because of the form of  $W_{\text{fast}}$ ,  $C_{\text{fast}}$  is a simple matrix that can be inverted analytically. Then the solution is integrated in time using

$$\delta U^{n+1} = \left( I - \Delta t C_{\text{fast}}^n \right)^{-1} \left( \Delta t (W_{\text{fast}}^n + W_{\text{slow}}^n) - \Delta t \left( \frac{\partial F^n}{\partial x} + \frac{1}{r} \frac{\partial rG^n}{\partial r} \right) \right)$$

This approach increases the stable time step by a factor of 50 compared to an explicit Euler method. This results in a very large reduction in the computer time required to obtain a steady-state solution.

A two-block grid is used to facilitate the implementation of the boundary conditions. The first grid block represents the nozzle section, and the second grid block represents the discharge region as well as a portion of the open air which acts as a large constant-pressure exhaust reservoir at one atmosphere.

The inflow boundary conditions are set by choosing the inflow static pressure to give the experimental mass flow rate of 4.9 g/s. The inflow is assumed to be in LTE at the measured temperature profile. This results in a consistent representation of the inflow conditions. The boundary conditions along the test-section surface are straight-forward. The velocity is zero at the surface, the temperature is specified, and the normal-direction pressure gradient is zero. We assume that the metallic surface is highly catalytic to ion recombination. Otherwise, the surface is assumed to be non-catalytic to recombination for neutrals.

The computation is initialized as follows: first, the inflow conditions are specified as above. Then the test-section and reservoir are all initialized at atmospheric pressure, and at each axial location the temperature profiles and chemical concentration profiles are set identical to the inflow boundary profiles. Once a converged solution is obtained for the flow in LTE, the discharge is ignited by injecting a flux of electrons at the cathode and applying the Joule heating source term to the energy equations. Then a steady-state solution for the DC discharge is obtained.

### Thermochemical and Transport Properties

We use the Stanford two-temperature 11-species, 38-reaction chemical kinetics model for air plasmas.<sup>1</sup> Transport properties are computed via mixing rules<sup>7</sup> from curve-fitted transport properties of individual species in the air plasma.<sup>8</sup> The electrical conductivity is taken from Ref. 2.

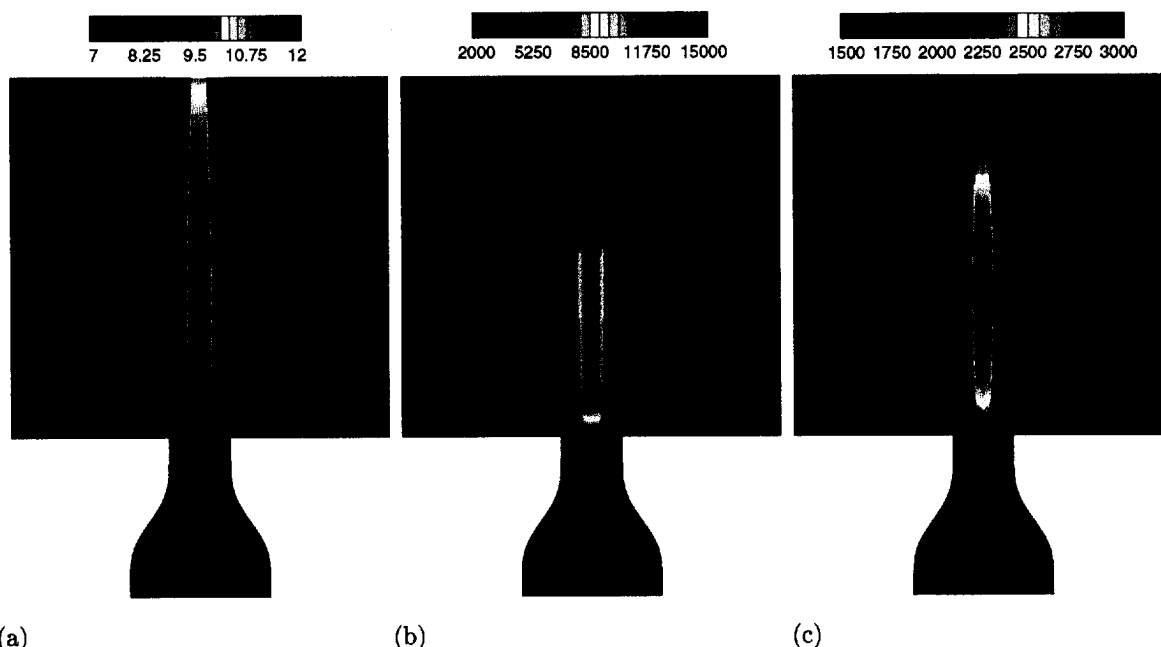


FIGURE 8.  $\log_{10}$  of the electron number density (a); electron Temperature (b); and translational temperature contours in the discharge region.

### Computational Results

In this section we present numerical simulations of the DC discharge experiment. Figure 8a shows the  $\log_{10}$  of the electron number density contours in the computational domain. The DC discharge region can be observed in this figure. This is the bright region where the electron number density is several orders of magnitude higher than in the region upstream of the cathode where there is no discharge. It can be observed that the electron number density is slightly higher than  $10^{12} \text{ cm}^{-3}$  in most of the discharge region. This is in good agreement with the experimental measurements for the electron number density. The electron number density falls off gradually downstream of the anode region. The shape of the discharge is similar to that observed in the photograph of the discharge in Fig. 3. The photograph also shows that the discharge is constricted at the cathode and diffuses radially outward, away from the cathode. The simulations capture this behavior.

Figure 8b plots the electron temperature contours in the computational domain. It shows that the electron temperature is about 12,000 K in the discharge region. The computed electron temperatures are consistent with the experimental predictions. Figure 8b also shows that the electron temperature drops off sharply just downstream of the anode because the electrons rapidly equilibrate with the heavy particles due to their strong coupling with the heavy species.

Figure 8c shows contours of the translational tem-

perature in the domain. It shows that the temperature in the discharge is about 3000 K in the discharge region. The computed temperatures are generally higher than the experimental measurements. Previous simulations of the Stanford University plasma torch experiments showed a similar over-prediction in the translational temperature. This indicates that the flow model used in the simulations may be missing an energy transport mechanism.

Figure 9 plots the axial variation of the centerline electron number density and the temperatures along with the experimental values. This figure quantitatively shows the variation of the electron concentration and the three temperatures along the centerline of the discharge. From the figure it can be seen that the electron number density remains slightly above  $10^{12} \text{ cm}^{-3}$  in the discharge region. It falls off gradually downstream of the anode. The computed electron temperature is very high in the cathode region and falls to about 12,000 K in most of the discharge region, which is close to the two-temperature kinetic model prediction. As observed in the contour plot for the electron temperature, the electron temperature falls off abruptly in the region downstream of the anode. The translational temperature increases from about 2200 K at the cathode to about 3000 K in the discharge region. This is higher than the measured translational temperature. However, the computed vibrational temperature is slightly lower than the experimentally measured value.

Figure 10 plots the radial profiles of the electron number density at two locations in the discharge. Near the cathode it can be seen that the diameter of the discharge is small and the electron number density is elevated in a region which is nearly equal to that of the cathode area. Near the center of the discharge the electron density is more diffuse and the diameter of the discharge is about 4 mm, which compares well with the experimentally observed diameter.

Figure 11 plots the computed potential along the centerline of the discharge. The computed potential is nearly linearly increasing with a finite cathode fall of about 300 V. The experiments indicate 290 V.

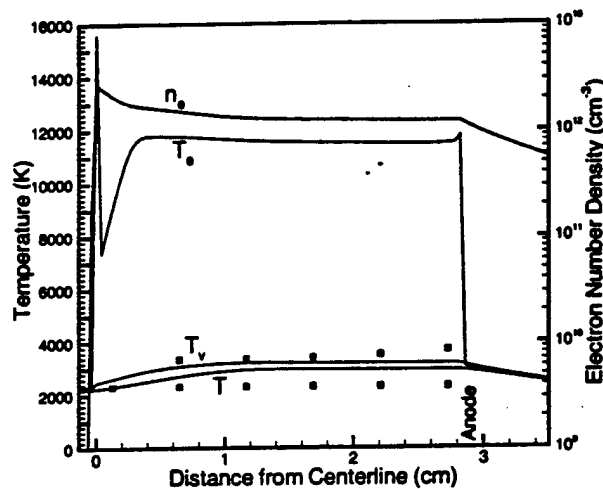


FIGURE 9. Computed electron number density and temperatures along the DC discharge centerline. Symbols denote experimentally measured values.

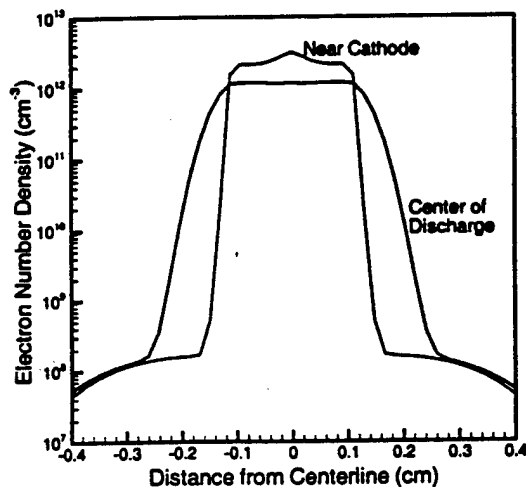


FIGURE 10. Computed radial profiles of electron number density

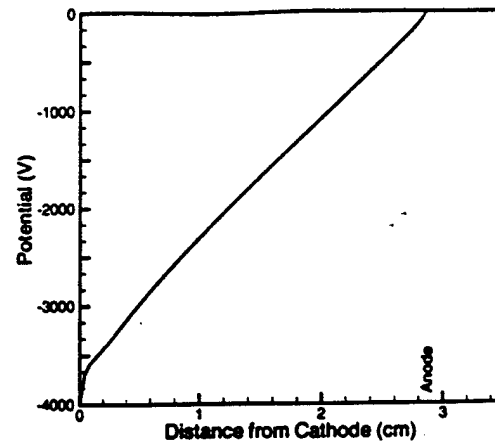


FIGURE 11. Axial variation of the potential along the centerline

### Conclusions

The present work demonstrates that stable, diffuse discharges with electron number densities approaching  $10^{13} \text{ cm}^{-3}$  at gas temperatures below 2000 K can be produced in atmospheric pressure air. This result stands in sharp contrast with the widespread belief that these diffuse discharges cannot exist without arcing instabilities or high levels of gas heating. The experiments also show that the power required to sustain an ionization level of  $10^{13} \text{ cm}^{-3}$  with a DC discharge is close to  $20 \text{ kW/cm}^3$ . Repetitively pulsed electron heating strategies were investigated as a way to reduce the power consumption. The experimental and modeling results presented here demonstrate that the power consumption can be dramatically reduced, by over two orders of magnitude, through the use of 10 ns pulsed electrical discharges with pulse characteristics tailored to match the ionization and recombination reaction times. A computational fluid dynamics code for the simulation of flowing nonequilibrium air plasmas including the presence of a DC discharge was developed and compared to the DC experiments conducted at Stanford University. The code uses a detailed two-temperature chemical kinetic mechanism, along with appropriate internal energy relaxation mechanisms. The discharge region was modeled by generalizing the channel model of Steenbeck, and a new semi-implicit time integration method was developed to reduce the computational cost. The computational results show good agreement with the experimental data, however the heat loss is more rapid in the experiment than predicted by the computations. Work is being carried out to fully understand this discrepancy. The code will be extended to handle the modeling of the pulsed discharges under investigation.

### Acknowledgments

This work was funded by the Director of Defense Research & Engineering (DDR&E) within the Air Plasma Ramparts MURI program managed by the Air Force Office of Scientific Research (AFOSR). Computer time was provided by the Minnesota Supercomputing Institute.

### References

- <sup>1</sup> Raizer, Y.P., *Gas Discharge Physics* Springer, New York, pp. 278-279, 1991.
- <sup>2</sup> Laux, C., Pierrot, L., Gessman, R. and Kruger, C.H., "Ionization Mechanisms of Two-temperature Plasmas," *30th AIAA Plasmadynamics and Lasers Conference, AIAA 99-3476*, Norfolk, VA, June. 1999
- <sup>3</sup> Nagulapally, M., D. Kolman, G.V. Candler, C.O. Laux, R.J. Gessman, and C.H. Kruger, "Numerical Simulation of Nonequilibrium Nitrogen and Air Plasma Experiments," *29th AIAA Plasmadynamics and Lasers Conference, AIAA 98-2665*, Albuquerque, NM, June 1998.
- <sup>4</sup> Mitchner, M. and C.H. Kruger, *Partially Ionized Gases*, Wiley, New York, pp. 92-94, 1973
- <sup>5</sup> Lee, J-H., "Electron-Impact Vibrational Relaxation in High-temperature Nitrogen," *30th Aerospace Sciences Meeting and Exhibit AIAA 92-0807*, Reno, NV, January. 1992
- <sup>6</sup> Candler, G.V. and R.W. MacCormack, "The Computation of Hypersonic Ionized Flows in Chemical and Thermal Nonequilibrium," *J. Thermophysics Heat Transfer*, Vol. 5, No. 3, pp. 266-273, July 1991.
- <sup>7</sup> Wilke, C.R., "A Viscosity Equation for Gas Mixtures," *J. Chem. Phys.*, Vol. 18, No. 4, p. 517, Apr. 1950.
- <sup>8</sup> Gupta, R.N., Yos, J.M., Thompson, R.A., and Lee, K.-P., "A Review of Reaction Rates and Thermodynamic and Transport Properties for an 11-Species Air Model for Chemical and Thermal Nonequilibrium Calculations to 30,000 K," *NASA RP-1232*, Aug. 1990.

## OPTICAL DIAGNOSTICS FOR NON-THERMAL HIGH PRESSURE DISCHARGES

Rolf Block, Mounir Laroussi, Frank Leipold, and Karl H. Schoenbach  
Physical Electronics Research Institute/Applied Research Center  
Old Dominion University  
12050 Jefferson Ave.  
Newport News, VA 23606

### Abstract

Two important parameters of high pressure, non-thermal plasmas are the gas temperature and the electron density. Optical emission spectroscopy and laser interferometry have been used to obtain these parameters in a dc atmospheric pressure hollow cathode discharge in air. Temperatures at and below 2000K and electron densities of approximately  $10^{16} \text{ cm}^{-3}$  have been measured. The two diagnostic methods are a subset of techniques developed to characterize non-thermal, high pressure plasmas in a newly established test facility at Old Dominion University.

### 1. Introduction

Non-thermal, high pressure plasmas have recently been used in novel emerging applications such as excimer light sources [1], surface modification of polymers [2], biological decontamination [3], and air plasma ramparts [4,5]. Each of these applications requires a specific set of plasma parameters. Diagnostic techniques applicable for high-pressure plasmas are required to adequately characterize the discharge. In this paper, we concentrate on a spectroscopic method, which yields information on the rotational structure of the second positive system of nitrogen for gas temperature measurement, and on interferometric methods using IR or microwave sources for electron density measurement. The experimental setups are presented, and results obtained on plasma generated with a microhollow cathode discharge are discussed.

### 2. Temperature Measurement

Optical emission spectroscopy allows us to determine plasma parameters such as electron density (through Stark broadening measurements) and gas temperature measurements. We have particularly concentrated on the gas temperature diagnostics in non-equilibrium plasmas in air. The rotational structure of the second positive system of nitrogen (transitions from the electronic



C-state to the B-state) contains information on the rotational temperature. Because of the low energies needed for rotational excitation and the short transition times, molecules in the rotational states and the neutral gas molecules are in equilibrium. Consequently, the rotational temperature provides also the value of the neutral gas temperature.

The 0-0 band of the second positive system of molecular nitrogen, modeled as a rigid rotor, has been simulated with the rotational temperature as variable parameter. In order to determine the plasma temperature, the simulated spectra are compared with the measured one. This comparison requires that the instrument profile (FWHM) of the spectrograph has to be taken into account. This is done by convoluting the computed line spectra with the appropriate Gauss function. Such simulated spectra for an FWHM=0.02nm are shown in fig. 1 for three temperatures [6]. The curves are shifted vertically for a better separation.

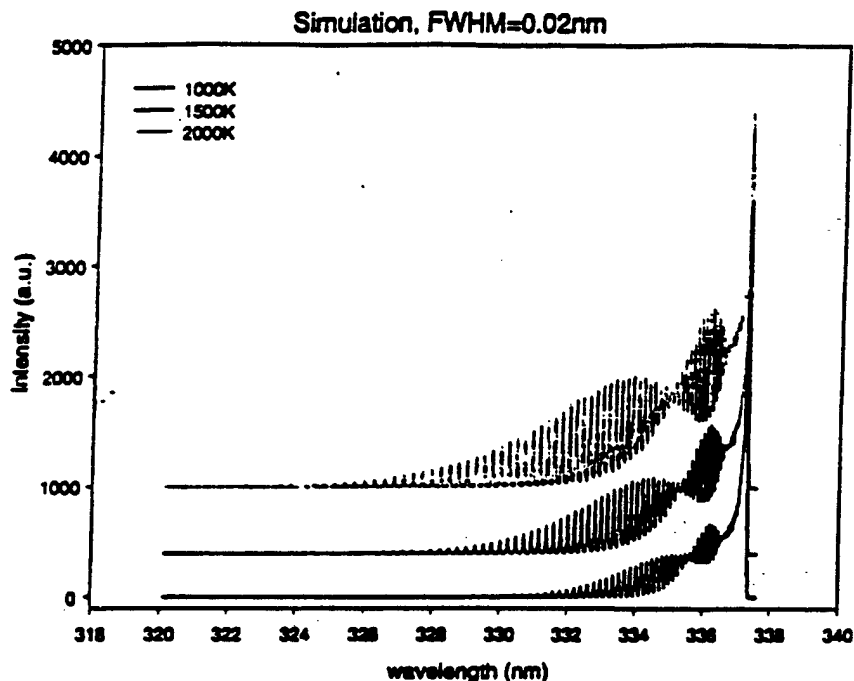


Fig. 1: Simulated spectra of molecular nitrogen

Generally, resolving the rotational structure requires a monochromator with very high resolution. A 0.5m imaging monochromator/spectrograph with a 3600 g/mm grating (with 240nm blaze wavelength) was used as dispersing element. Dual exit ports offer the versatility of mounting two different detectors at the same time. One exit port is equipped with an exit slit and a photomultiplier. The second port will be used for a fast light-intensified CCD-camera (25mm micro channel plate with photocathode, gating speed down to 200ps, adjustable in 100ps steps), which allows temporally resolved spectroscopic measurements.

Fig. 2 shows a measured spectrum of a microhollow cathode discharge (MHCD) in room air at atmospheric pressure. A MHCD is a direct current, high pressure glow discharge between two closely spaced electrodes, which contain circular openings [7]. The electrodes are separated by an insulator (mica or alumina). In this experiment we used 100 $\mu$ m thick molybdenum

across the electrodes was 500V, the discharge current was 12mA. The measurement profile of the spectrograph was measured with a mercury lamp (line at 361nm) as FWHM=0.02nm. A comparison with simulated spectra resulted in a temperature of  $T=1500\text{K}$ .

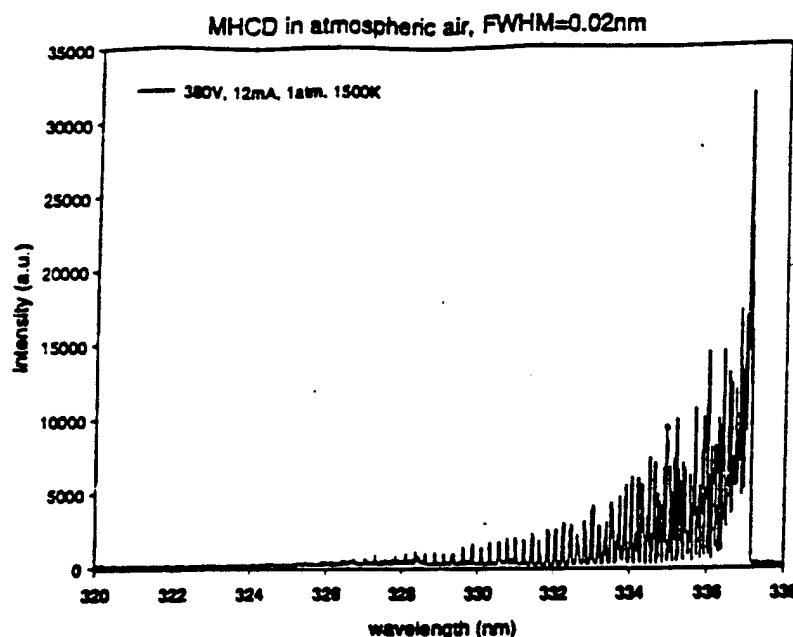


Fig. 2: Measured spectrum of a MHCD in atmospheric air.

The nitrogen line at 337.1nm (within the second positive system of nitrogen) is the line with the highest intensity and therefore easy to measure. This diagnostic can also be used in other gas mixtures, if the application allows the addition of small amounts of nitrogen.

### 3. Electron Density Measurement

#### 3a. Infrared Interferometry

The interferometer is designed as a heterodyne Mach-Zehnder interferometer. The source is a  $\text{CO}_2$ -laser operating at  $10.6\mu\text{m}$ . Figure 3 shows the experimental setup.

The laser beam is split in two beams. One beam passes through the plasma, while the second beam passes along a reference path, where it undergoes a frequency shift of 40 MHz applied by an acousto-optic modulator. Using a beam splitter, the two beams are allowed to interfere and produce two signals, only one of which has the beat frequency of 40 MHz. This signal is then compared to the driver signal of the acousto-optic modulator (which also has a frequency of 40 MHz). The phase shift is then converted to a voltage by a phase detector. The resolution of the interferometer was about 0.01 degree.

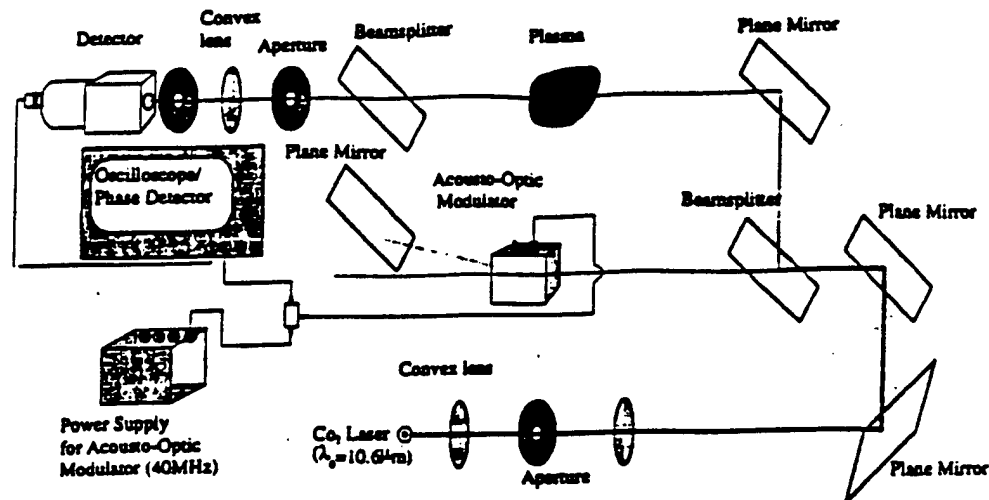


Fig. 3: IR-Interferometer for electron density measurement

The above-described technique is best applied to a pulsed system, with pulse repetition rate of few kilohertz. This enables the separation of the phase shift caused by the electrons from the phase shift caused by mechanical movement and thermal drifts. This method was applied to plasma generated by a microhollow cathode discharge in atmospheric pressure room air, using a sample with the same dimensions (100 $\mu\text{m}$  thick molybdenum electrodes, separated by 125 $\mu\text{m}$  thick alumina sheet, with 100 $\mu\text{m}$  holes). The voltage between the electrodes was 390V, the discharge current was 12mA. The plasma was 100 $\mu\text{m}$  wide and 400 $\mu\text{m}$  long. Electron densities on the order of  $10^{16} \text{ cm}^{-3}$  were measured. In order to provide evidence that the laser does not affect the plasma in the micro cavity, experiments with varying laser intensity have been performed. Fig. 4 shows that the electron density measurements are independent of the laser beam power.

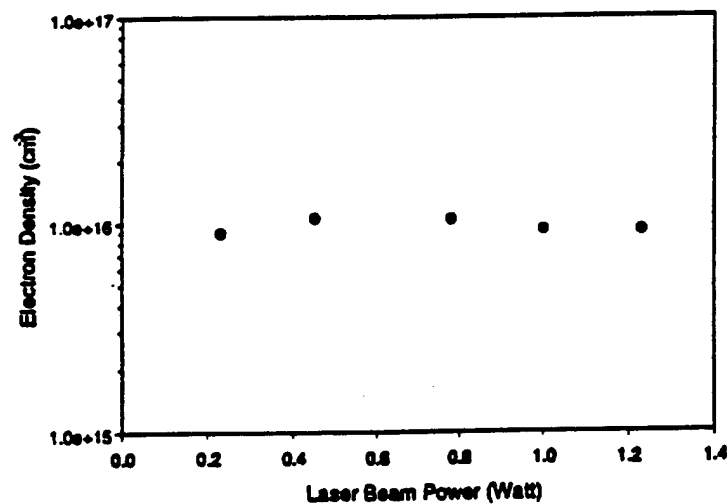


Fig. 4: Electron density versus laser beam power

### 3b. Microwave Interferometry

In order to extend the range of electron density measurements to lower values, a microwave interferometer is being developed. The increase in wavelength allows us to expand the diagnostic range down to  $10^{12} \text{ cm}^{-3}$ , however on the expense of spatial resolution. Figure 5 shows the interferometer design we adopted for our experiments.

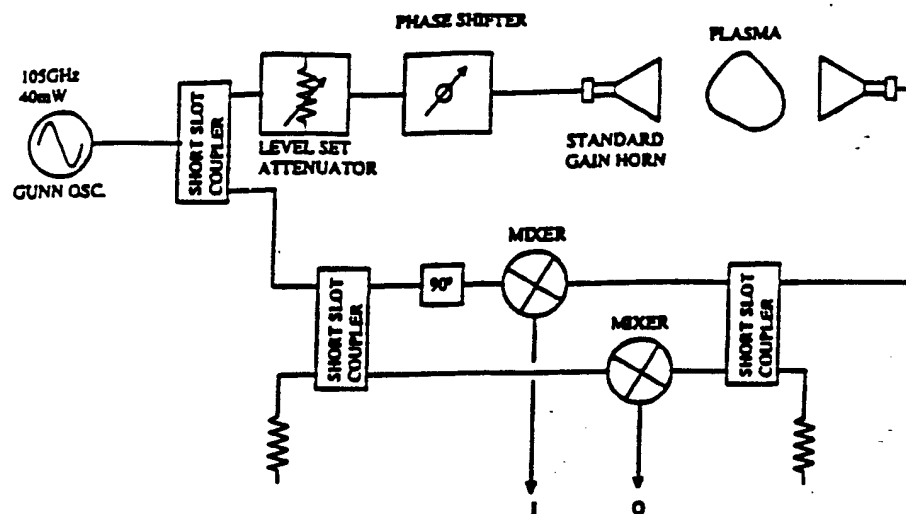


Fig. 5: Microwave Interferometer for number density measurement

The microwave interferometer, or phase bridge, shown above operates as follows. A microwave signal generated by a Gunn diode oscillator is divided in two equal portions by a Short Slot Coupler. One portion is transmitted through the plasma. The second portion is channeled to a second power divider which splits the signal to drive the LO input of the I-Q mixers. The signal transmitted by the plasma is also split in two portions, which drive the RF inputs of the I-Q mixers. Since both the LO and RF inputs of the mixers are at the same frequency, a DC signal is obtained at the IF output of the mixers. Calibration of the bridge is achieved by setting the Level Set Attenuator to the maximum attenuation position, measuring the DC offset of the mixers, varying the Phase Shifter through  $360^\circ$ , and recording the DC voltage at the IF output of the mixers. The measurement is repeated for varying level of attenuation. This set of data is then used to analyze actual phase shifts undergone by the microwave signal with the plasma ON. The accuracy of the measurement is determined by the resolution of the voltage measurements.

### Conclusion

Spectroscopic measurements of the structure of the second positive system of nitrogen allow us to accurately determine the background gas temperature in nonthermal plasmas. Our method was used on a microhollow cathode discharge. Temperatures at and below 2000 K were measured. Infrared and microwave interferometry allow us to obtain information on the electron

discharge plasma, we measured electron densities close to  $10^{10} \text{ cm}^{-3}$ . A specially designed microwave interferometer will allow us to measure electron densities down to about  $10^{12} \text{ cm}^{-3}$ .

The diagnostic techniques presented in this paper are a part of a test facility for high pressure, non-thermal plasmas. This test facility allows to study large volume plasmas over a large pressure range in a standardized discharge cell. The facility also includes electrical (large bandwidth scopes for current-voltage measurements) and optical (high speed CCD camera to study the development of instabilities) diagnostics.

### Acknowledgement

This work was funded by the US Air Force Office of Scientific Research in Cooperation with the DDR&E Air Plasma MURI Program.

### References

- [1] Ahmed El-Habachi and Karl H. Schoenbach, "Generation of Intense Excimer Radiation from High-Pressure Hollow Cathode Discharges", *Appl. Phys. Lett.* **73**, (1998), 885.
- [2] F. Massines, C. Mayoux, R. Messaoudi, A. Rabehi, and P. Segur, "Experimental Study of an Atmospheric Pressure Glow Discharge: Application to Polymers Surface Treatment", *Proc. Int. Conf. Gas Discharges & their Applications*, 1992, 730.
- [3] M. Laroussi, "Sterilization of Contaminated Matter with an Atmospheric Pressure Plasma", *IEEE Trans. Plasma Sci.*, **24**, (1996), 1188.
- [4] M. Laroussi, "Interaction of Microwaves with Atmospheric Pressure Plasmas", *Int. J. IR & Millimeter Waves*, **16**, (1995), 2069.
- [5] Robert H. Stark and Karl H. Schoenbach, "A Novel Plasma Cathode for High Pressure Glow Discharges", *J. Appl. Phys.*, **85**, (1999), 2075.
- [6] Rolf Block, Olaf Toedter and Karl H. Schoenbach, "Temperature Measurement in Microhollow Cathode Discharges in Atmospheric Air", *Bull. APS*, **43**, October 1998, 1478.
- [7] Karl H. Schoenbach, Ahmed el-Habachi, Wenhui Shi and Marco Ciocca, "High Pressure Hollow Cathode Discharges", *Plasma Sources, Science and Technology*, **6**, (1997), 468.



**AIAA-99-3666**

## **Direct Current Glow Discharges in Atmospheric Air**

**Robert H. Stark, Uwe Ernst<sup>1</sup>, Mohamed El-  
Bandrawy, Christophe O. Laux<sup>2</sup>, and  
Karl H. Schoenbach**

**Physical Electronics Research Institute  
Old Dominion University, Norfolk, VA 23529**

**<sup>1</sup> University of Erlangen, Germany**

**<sup>2</sup> Stanford University**

**30th Plasmadynamics and Lasers Conference  
28 June - 1 July, 1999 / Norfolk, VA**

# Direct Current Glow Discharges in Atmospheric Air

Robert H. Stark, Uwe Ernst<sup>1</sup>, Mohamed El-Bandrawy, Christophe O. Laux<sup>2</sup>, and

Karl H. Schoenbach

Physical Electronics Research Institute

Old Dominion University, Norfolk, VA 23529

## Abstract

Direct current glow discharges have been operated in atmospheric air by using microhollow cathode discharges as plasma cathodes. The glow discharge gap was varied between 2 mm and 10 mm. The differential electric field strength, necessary to support the air glow, was found to be about 1.2 kV/cm at current densities on the order of 3.8 A/cm<sup>2</sup>. The electron density is 10<sup>12</sup>-10<sup>13</sup> cm<sup>-3</sup> in the midplane of the discharge gap. The neutral gas temperature was measured by emission spectroscopy of the excited rotational states of the N<sub>2</sub> molecule (C-M transition) and was found to be approximately 2000 K. The glow discharge current can be controlled by varying the current of the plasma cathode. Parallel operation of the filamentary glow discharge allows the generation of large volume glows in atmospheric air.

## Introduction

Research on high pressure glow discharges is motivated by applications such as instantly activated reflectors and absorbers for electromagnetic radiation, surface treatment, thin film deposition, remediation and detoxification of gaseous pollution, and gas lasers. The majority of these applications require the generation of air plasma at atmospheric pressure. If used as plasma rampart its gas temperature should be less than 2,000 K; the air plasma should have a lifetime of at least 10 ms, and electron densities should be on the order of 10<sup>13</sup> cm<sup>-3</sup>.

One of the major obstacles in obtaining such a plasma are instabilities, particularly glow-to-arc-transitions (GAT), which lead to the filamentation of the glow discharge in times short compared to the desired lifetime of a homogeneous glow. These instabilities generally develop in the cathode fall, a region of high electric field, which in self sustained discharges is required for the emission of electrons through ion impact. Eliminating the cathode fall, by supplying the electrons by means of an external source, is therefore expected to extend the range of stable operation.

---

<sup>1</sup> University of Erlangen, Germany

<sup>2</sup> Stanford University, USA

## Microhollow Cathode Discharge as Electron Emitter

Microhollow cathode discharges (MHCDs) are gas discharges between closely spaced ( $\approx 100\mu\text{m}$ ) electrodes with circular openings with diameters on the same order as the electrode gap. Reducing the size of the electrode opening to the range of  $100\mu\text{m}$  and below, stable glow discharge operation has been achieved at atmospheric pressure and above in noble gases [1,3]. When operated in the hollow cathode discharge mode electrons can be extracted through the anode opening at moderate electric fields. These electrons support a stable plasma between the microhollow anode and a third electrode (anode).

### Atmospheric Pressure Glow Discharges in Air

This concept of using the plasma generated by a microhollow cathode discharge as electron source for high-pressure glow discharges has been applied to discharges in air [2]. We were able to generate a direct current glow in atmospheric pressure air with electron densities on the order of  $10^{13}\text{ cm}^{-3}$ . A photograph of the discharge and the electrode geometry, taken with a charge coupled device (CCD) camera, is shown in Fig. 1. Generally, the electrodes consist of  $100\mu\text{m}$  thick molybdenum foils, and the diameter of the electrode opening ranges from  $80$  to  $100\mu\text{m}$ . The dielectric is alumina,  $100$ - $250\mu\text{m}$  in thickness. The third electrode, also made of molybdenum, is placed at a distance of several millimeters up to one centimeter in front of the plasma cathode and is biased positively. The stable air glow develops between the MHCD (plasma cathode) and the third electrode.

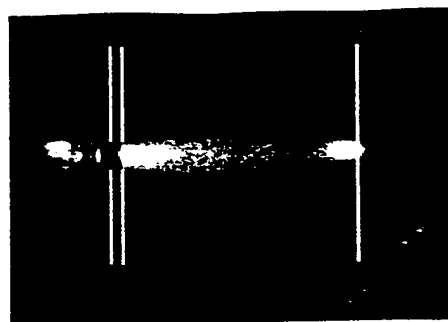


Fig. 1 Side-on photography of the discharge in 1 atmosphere in air. (Gap distance  $D = 2\text{ mm}$ )

The value of the neutral gas temperature was obtained through emission spectroscopy of the excited rotational states of the  $\text{N}_2$  molecule (C-M transition, [7]). A  $0.5\text{ m}$  scanning monochromator (McPherson) was used to record the emission spectra in a range between  $320\text{ nm}$  and  $338\text{ nm}$ . The width of the entrance and exit slit was  $30\mu\text{m}$ . The measured rotational spectra were then compared with the modeled one [8].

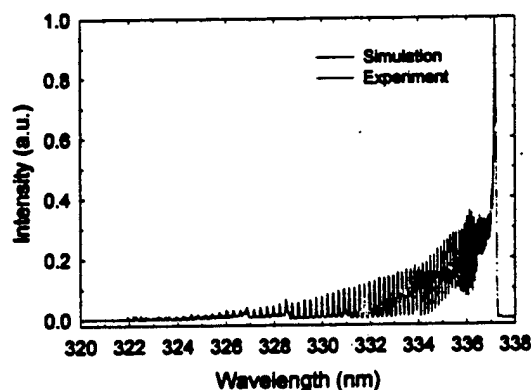


Fig. 2 Rotational spectra of Nitrogen (C-M transition, second positive system) for an atmospheric air glow ( $I = 8\text{ mA}$ ). The calculated spectra [8] fits best with the measured one for a rotational temperature of  $2400\text{ K}$ .



Fig. 2 shows a calculated spectrum and a measured spectrum in the mid plane of the discharge gap for a discharge in atmospheric pressure air. The gap distance was 2 mm and the discharge current was kept constant at 8 mA. The comparison of the calculated spectra with the measured spectra shows good agreement for a rotational temperature of 2400 K. The accuracy is better than 25 K. At 2 mm gap distance there was no significant change in gas temperature along the discharge axis and we have therefore concentrated on the measurement of the gas temperature in midplane of the discharge gap for various current and additives of helium, respectively.

The results of these measurements are shown in Fig. 3 and Fig. 4. At currents between 5 mA and 14 mA the gas temperature rises from 2200 to 2800 K. At current less than 8 mA, the gas temperature decreases linearly with current and the differential change of temperature with current is constant:

$$dT/dI = 66.6 \text{ (K/mA)} \quad (4)$$

The lower limit in current is given by the minimum current required to support stable dc glow discharge operation in atmospheric pressure air, which in this case is at approximately 4-5 mA.

In order to lower the gas temperature, an additive with high thermal conductivity (helium) was used (Fig. 4). The total pressure was 1 atm and the discharge current was kept constant at 8 mA. The decrease in temperature by adding up to 30% of helium can be described by the following relation:

$$dT/dp_{\text{partial}}(\% \text{He}) = -13.3 \text{ (K/p}_{\text{partial}}(\% \text{He})) \quad (5)$$

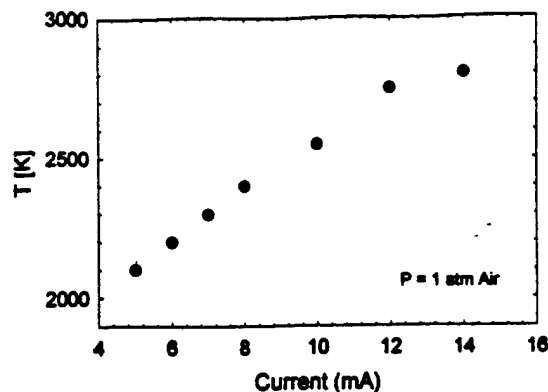


Fig. 3 Gas temperature for various glow discharge currents in 1 atmosphere air.

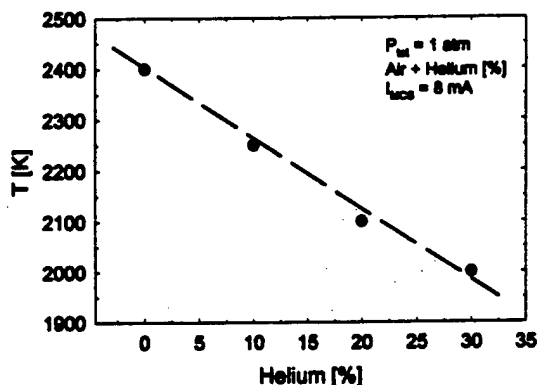


Fig. 4 Gas temperature for various partial pressure of helium in an atmospheric pressure air discharge.

For application as plasma rampart, the gas temperature needs to be lower than 2000 K. This can be achieved, either by operating the discharge at lower current or by adding helium. Assuming, that equation (5) holds also for discharge currents lower than 8 mA, the gas temperature can be estimated by using (4) and (5). E.g. at 5 mA discharge current and 20% helium as additive, the gas temperature of the atmospheric pressure air/helium discharge would be about 1930 K, which would satisfy the requirement in temperature for plasma ramparts. Experiments

indicate that the discharge current can be reduced further by reducing the gap distance of the supporting microhollow cathode discharge, allowing us to operate even pure air discharges at temperatures below 2000 K.

Based on Ohm's law, the electron density  $n_e$  in the plasma column can be estimated from the current density  $j$ , and the electron drift velocity  $v_e$ , which is dependent on the reduced electric field  $E/N_T$ :

$$j = e \cdot n_e \cdot v_e (E/N_T), \quad (1)$$

with  $e$  being the electron charge and  $N_T$  being the neutral particle density at a temperature  $T$ :

$$N_T = T_0/T \cdot N_0 \quad (2)$$

$N_0$  is the neutral particle density at  $T_0 = 273$  K. The electron drift velocity in air as function of the reduced electric field strength is [4]:

$$v_e = 5 \cdot 10^6 \text{ cm/s} \quad (3)$$

for a reduced electric field strength of  $32 \cdot 10^{-17} \text{ Vcm}^2$ . Measurements of the neutral gas temperature by emission spectroscopy of the rotational spectrum of the excited states of the  $N_2$  molecule in air (C-M transition) have indicated a temperature close to 2000 K. Assuming that the average electric field is the voltage across the discharge gap, divided by the gap distance and the current density is the current divided by the crosssection of the discharge in mid plane, the electron density at mid plane of the glow was estimated to be  $5 \cdot 10^{12} \text{ cm}^{-3}$ . For this calculation the average electric field was 1.2 kV/cm, obtained for a 2 mm gap, and the electron drift velocity was  $5 \cdot 10^6$

cm/s at 2000 K gas temperature. At increasing discharge current, values of  $10^{13} \text{ cm}^{-3}$  can be achieved.

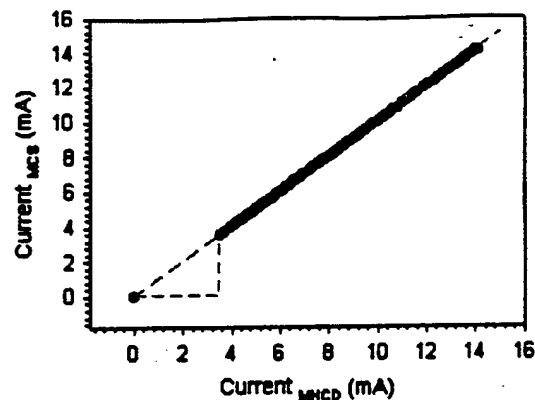


Fig. 5 Current in a 1 atmosphere glow discharge versus microhollow cathode discharge current.

Above a threshold value, the current in the glow is completely determined by the current of the microhollow cathode discharge [1]. In Fig. 5 the air glow discharge current versus MHCD current is shown. The glow discharge current is identical to the plasma cathode current. The microhollow cathode discharge acts consequently as a constant current source for the air glow. The current-voltage characteristic of the microhollow cathode discharge is such that small variations in the MHCD voltage cause large swings in the electron current, and consequently the current in the air glow; an effect which is analogous to that of a vacuum triode.

Although the plasma volume in this experiment is still on the order of  $\text{mm}^3$ , the described method allows us to scale it to larger values. In longitudinal direction this can be achieved by extending the electrode gap, which requires to increase the applied voltage. In transverse direction large volume plasma

operation can be achieved by superimposing microhollow cathode discharges supported glows through parallel operation [5]. Individual control of each of the discharge elements is possible and permits to generate any desired plasma pattern in the transverse plane.

A limiting factor for use as plasma rampart is the power consumption in the glow, which can be estimated from the electrical parameters. Assuming the average electric field in the glow to 1.2 kV/cm (approximated from a 2mm discharge), and the current density at midpoint between the electrodes to approximately 4A/cm<sup>2</sup>, the power density is 5 kW/cm<sup>3</sup>. This value agrees with estimates which are based on carrier lifetimes and average ionization energies [6]. For application as plasma rampart the power consumption is high and at this point would prevent us from generating large volume plasmas. However, experimental results with combustion assisted glow discharges in air indicate that the power can be reduced by orders of magnitude. A second approach to reduce power consumption is adding of gases with low ionization potential.

## References

- [1] Robert H. Stark and Karl H. Schoenbach, J. Appl. Phys., 85, 2075 (1999)
- [2] Robert H. Stark and Karl H. Schoenbach, Appl. Phys. Lett. Vol. 74, No. 25, 21. June 1999
- [3] Ahmed El-Habachi and Karl H. Schoenbach Appl. Phys. Lett., 73, 885 (1998)
- [4] J.W. Gallagher, E.C. Beaty, J. Dutton, and L.C. Pitchford, J. Phys. Chem. Ref. Data 12, 109 (1983)

- [5] Wenhui Shi, Robert H. Stark, and Karl H. Schoenbach, IEEE Trans. Plasma Science, 27, 16 (1999)
- [6] R. J. Vidmar, IEEE Trans. Plasma Science 18, 733 (1990)
- [7] R. Block, O. Toedter, and K. H. Schoenbach, AIAA-99-3434, this meeting
- [8] Christophe O. Laux, Richard J. Gessman, and Charles H. Kruger, "Measurements and Modeling of the Absolute Radiative Emission of Air Plasmas between 190 and 800 nm", to be submitted to JQSRT, Summer 1999

## Acknowledgement

This work was funded by the Air Force Office of Scientific Research in Cooperation with the DDR&E Air Plasma Ramparts MURI Program.



**AIAA 99-3434**

**Gas Temperature Measurements in High Pressure  
Glow Discharges in Air**

Rolf Block, Olaf Toedter and Karl H. Schoenbach  
Old Dominion University  
Norfolk, VA

**30th Plasmadynamics and Lasers Conference  
28 June - 1 July, 1999 / Norfolk, VA**

For permission to copy or republish, contact the American Institute of Aeronautics and Astronautics  
1801 Alexander Bell Drive, Suite 500, Reston, VA 20191

## GAS TEMPERATURE MEASUREMENTS IN HIGH PRESSURE GLOW DISCHARGES IN AIR

Rolf Block, Olaf Toedter, and Karl H. Schoenbach\*

Physical Electronics Research Institute/Applied Research Center  
Old Dominion University, Norfolk, VA, 23529/Newport News, VA 23606

### ABSTRACT

The temperature of the neutral particles in weakly ionized air can be determined by measuring the rotational spectrum of the 0-0 band within the second positive system of nitrogen and comparing it with simulated spectra. This diagnostic technique has been applied to direct current microhollow cathode discharges in atmospheric air. Temperatures in the range from 1700K to 2000K have been measured over a discharge current range from 4mA to 12mA. The rotational spectra of nitrogen were simulated using a simple model, which can easily be implemented. The simplicity compensates for the loss in accuracy (~10%), which can be achieved with more sophisticated models.

### INTRODUCTION

High-pressure glow discharges are nonequilibrium discharges: The temperature of the heavy particles is generally much less than the electron temperature. Applications for high pressure glow discharges range from gas lasers, remediation and detoxification of gaseous pollution, biological decontamination, surface treatment and thin film deposition, to their use as plasma ramparts. These are atmospheric pressure air plasmas, which serve as shields against strong electromagnetic radiation, and can be activated on a time scale of less than microseconds.

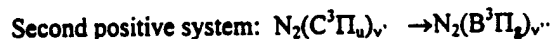
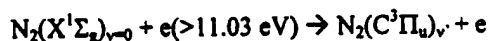
Of the plasma parameters which need to be known in order to determine the use of the air plasmas as ramparts two are of utmost importance: the electron density and the gas temperature. The electron density determines the frequency range where the shield is effective; the gas temperature should be below 2000K in order to prevent thermal loading of the system which is to be protected. A method, which allows us to obtain the temperature of the heavy particles in air, is based on

the measurement of the rotational state distribution in the second positive system of nitrogen, which involves transitions from the electronic C-state to the B-state. Due to the low rotational excitation energies and the short transition times (~0.6ns) the temperature relaxation between rotationally excited molecules and the neutral gas is very fast. Consequently, the rotational temperature provides a value for the neutral gas temperature, too.

Measurements of the rotational temperature are performed by means of emission spectroscopy. The measured spectrum depends on the thermal distribution of the rotationally excited states, the probability for the optical transitions, and the line shape function of the spectral system. In order to obtain information on the rotational (gas) temperature, the measured spectrum is compared to a simulated spectrum.

### SIMULATION OF THE N<sub>2</sub> SPECTRUM

The 0-0 band of the second positive system of molecular nitrogen has been simulated with the rotational temperature as variable parameter. Nitrogen, which is with 80% the major gas component in air, contributes to more than 98% of the UV emission in low temperature glow discharges. The strongest transition group in nitrogen is the so-called second positive system, which involves transitions from the electronic C-state to the B-state.



$$\lambda(v'=0 \rightarrow v''=0) = 337.1 \text{ nm}$$

The diatomic molecule of nitrogen is modeled as a symmetric top (rigid rotator). With the quantum number of both vibrational states being zero, the total frequency of a transition is described as the sum of the frequencies of the electronic transition and the difference between two rotational states. For the three branches P ( $\Delta J = +1$ ),

- Professor, Department of Electrical and Computer Engineering  
Copyright © 1999 The American Institute of Aeronautics and Astronautics Inc. All rights reserved.

Q ( $\Delta J=0$ ), and R ( $\Delta J=-1$ ),  $J$  being the rotational quantum number, this can be written as<sup>1</sup>:

$$P: \nu_{\Omega,J}^P = \nu_0 + F_{\Omega,J'-1} - F_{\Omega,J} \quad \text{with } \Omega = 0,1,2$$

$$Q: \nu_{\Omega,J}^Q = \nu_0 + F_{\Omega,J'} - F_{\Omega,J} \quad \text{with } \Omega = 1,2$$

$$R: \nu_{\Omega,J}^R = \nu_0 + F_{\Omega,J'+1} - F_{\Omega,J} \quad \text{with } \Omega = 0,1,2$$

where  $\nu_0$  is called the band origin or the zero line and  $F_{\Omega,J}$  the term values of the rotational states. For the triplet system of nitrogen (total rotational momentum projection  $\Omega=0,1,2$ ) these values can be estimated using the semiempirical equation of Budó<sup>2</sup>:

$$F_{0,J'} = B_v \left( J'(J'+1) - \sqrt{Z_1} - 2Z_2 \right) - D_v \left( J' - \frac{1}{2} \right)^4$$

$$F_{1,J'} = B_v \left( J'(J'+1) + 4Z_2 \right) - D_v \left( J' + \frac{1}{2} \right)^4$$

$$F_{2,J'} = B_v \left( J'(J'+1) + \sqrt{Z_1} - 2Z_2 \right) - D_v \left( J' + \frac{3}{2} \right)^4$$

with  $B_v$  and  $D_v$  being the rotational constants obtained from reference<sup>3,4</sup>. Equations for the values  $Z_1$  and  $Z_2$  as a function of the spin-orbit coupling constant  $Y_v$  are shown below:

$$Z_1 = Y_v(Y_v - 4) + \frac{3}{4} + 4J'(J'+1)$$

$$Z_2 = \frac{1}{3Z_1} \left( Y_v(Y_v - 1) - \frac{4}{9} - 2J'(J'+1) \right)$$

$Y_v$  takes the transition for increasing  $J'$  from Hund's case (a) to Hund's case (b) into account. Values can be found in references<sup>3,6</sup>. This set of equations allows us to determine the frequencies of the optical transitions.

The temperature dependent population of the rotational states for  $J'$  as well as  $J''$  is determined by the Boltzmann distribution:

$$f_J = \frac{N_{v,J}}{N_v} = \frac{(2J+1) \exp\left\{-\frac{hcB_v J(J+1)}{kT}\right\}}{\sum_{J=0}^{\infty} (2J+1) \exp\left\{-\frac{hcB_v J(J+1)}{kT}\right\}}$$

where  $(2J+1)$  is the degeneracy of the quantum state  $J$  and  $B_v$  is a rotational constant depending on the vibrational state. The infinite sum can be approximated by an integral, and the population of the rotational states can be described as:

$$f_J = \frac{hcB_v}{kT} (2J+1) \exp\left(-J(J+1) \frac{B_v hc}{kT}\right).$$

The intensity of each upper rotational level can be expressed, apart from a constant, as the product of the Boltzmann distribution  $f_j$  and a line-strength factor  $S_{J'}$ , which defines the distribution over the P, Q and R branches. The precise formulae for the line strengths of

a symmetric top for absorption, which are valid whether or not thermal equilibrium exists, were first given by Hönl and London<sup>7</sup>:

$$S_{J'}^P = \frac{(J'+1+\Omega)(J'+1-\Omega)}{J'+1}$$

$$S_{J'}^Q = \frac{(2J'+1)\Omega^2}{J'(J'+1)}$$

$$S_{J'}^R = \frac{(J'+\Omega)(J'-\Omega)}{J'}$$

The relative intensity of a spectral line is the product of the thermal distribution in the upper excited state and the Hönl-London factors:

$$I_{rel} = S_{J'} \cdot f_J$$

These formulas allow us to calculate the relative rotational line spectrum (wavelengths and intensities) of molecular nitrogen. In order to compare the measured spectrum with computed spectra, line-broadening effects have to be taken into account. Natural line broadening can be neglected compared to the instrumental FWHM. The instrument profile is measured using a low-pressure mercury lamp. In the last simulation step the computed line spectrum is convoluted with a Gaussian distribution with the FWHM determined in the calibration measurement. Results of the simulation of the line at 337.1 nm within the second positive system of nitrogen for an instrumental FWHM=0.025 nm at several temperatures, are shown in fig. 1. The curves are shifted vertically for a better separation.

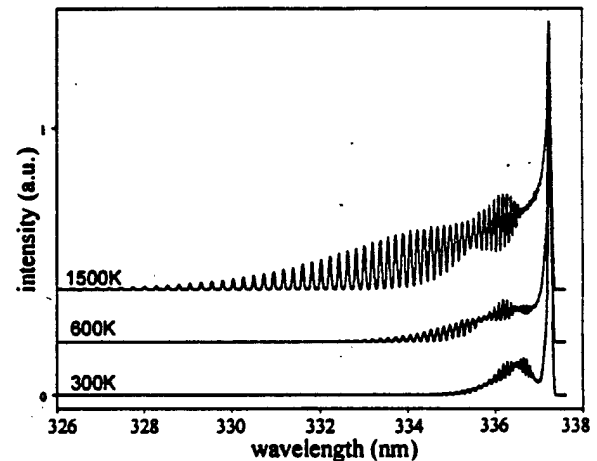


Fig. 1: Simulated (0-0) band of the second positive system of nitrogen at 300K, 600K and 1500K.

The diagnostic method has been applied to microhollow cathode discharges<sup>8</sup> in atmospheric air.

## EXPERIMENTAL RESULTS

Microhollow cathode discharges (MHCDs) are direct current, high pressure glow discharges between two closely spaced electrodes, which contain circular openings. In this experiment two 100  $\mu\text{m}$  thick circular molybdenum electrodes were used, which were separated by a 130  $\mu\text{m}$  thick alumina layer. A laser drilled hole through the sample had a cathode hole diameter of 170  $\mu\text{m}$ . The anode hole diameter is smaller. Experiments have shown that the anode geometry does not affect the discharge considerably; the anode hole could even be omitted. In order to keep the capacitance of the electrodes small, the cathode had a much smaller diameter than the anode. Details of the sample are shown in fig. 2.

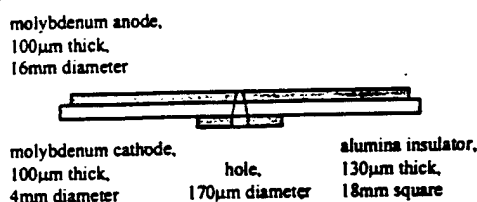


Fig. 2: Microhollow cathode geometry

The electrical circuit and the experimental setup are shown in fig. 3.

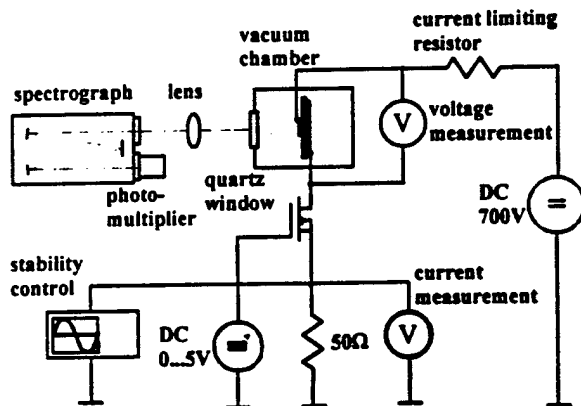


Fig. 3: Experimental setup

The Mosfet acts as a constant current source. The constant drain current can be adjusted by changing the dc gate voltage. The discharge is ignited by

momentarily raising the drain supply voltage. The sample is mounted in a stainless steel vacuum chamber.

A 0.5m Czerny-Turner spectrograph with a 3600 grooves/mm grating blazed at 240nm is used to record the emission spectrum. A photomultiplier with a spectral range of 180nm – 900nm is attached to the output slit. The electrical signal of the photomultiplier is recorded via a 16bit AD converter card. The instrumental FWHM was determined using the lines at 365nm and 312nm of a low-pressure mercury lamp; a resolution of 0.24Å was achieved. A measured spectrum from 300nm to 450nm of the discharge in atmospheric pressure dry air is shown in fig. 4. It shows the second positive system of nitrogen with the strongest line at 337.1nm.

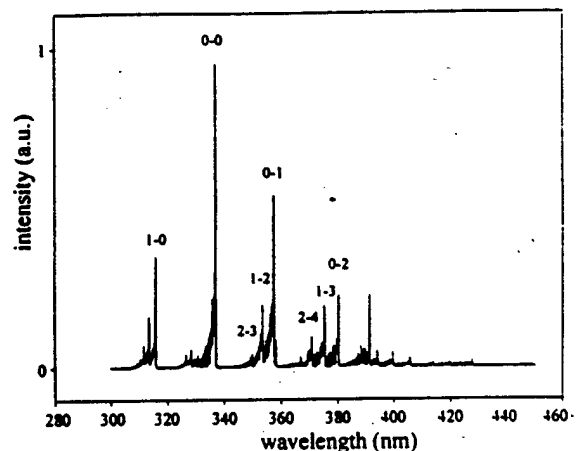


Fig 4: Emission spectrum of MHCD in atmospheric air

Rotational spectra of microhollow cathode discharges at atmospheric pressure in dry air as well as normal room air have been measured for various discharge currents. In order to prove that a thermal steady state is reached, measurements were repeated over time. Starting 10 minutes after igniting the discharge and adjusting the current to 4mA, 3 consecutive measurements in intervals of 10 minutes have been performed. Then the current was adjusted to 8mA and finally to 12mA, with the same measurement procedure for each current. Results for dry air are shown in fig. 5. The spectra are normalized and vertically shifted for a better separation.

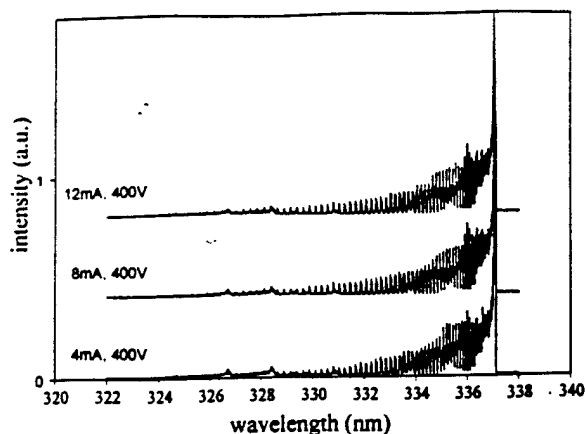


Fig. 5: Measured rotational spectra of MHCDs in dry air at atmospheric pressure.

With increasing temperature, higher rotational states are excited. In order to determine the highest temperature in the plasma, only the higher rotational states for wavelengths below 330nm were compared with the computed spectra. With increasing discharge currents from 4mA to 8mA and to 12mA the highest gas temperature increases from 1700K to 1900K and to 2000K. Although the power is doubled from 4mA to 8mA (the voltage is constant) and increased again by a factor of 1.5 from 8mA to 12mA, the temperature changes only by about 15%. This is probably due to the fact that with increasing power the plasma volume increases, so that the power density is only slightly changed.

The same measurements have been performed for room air (humid air). The results show the same behavior, with slightly smaller temperature changes (highest and average temperature) over the discharge current.

## CONCLUSION

The neutral gas temperature in weakly ionized air can be estimated by a comparison of measured and simulated spectra of the (0-0) band of molecular nitrogen. The  $N_2$  molecule was modeled as a rigid rotator, which allows a very easy implementation. However, the simplified model causes a loss in accuracy especially at higher temperatures. One measurement on a microhollow cathode discharge at a high temperature has shown that for temperatures up to 2000K the accuracy is about 10%. Our estimated

temperature was found to be lower by this fraction, compared to the results of a more sophisticated model<sup>9</sup>. This derivation from actual values is expected to be less for lower temperatures.

## ACKNOWLEDGEMENTS

This work was supported by the U.S. Air Force Office of Scientific Research in cooperation with the DDR&E Air Plasma Ramparts MURI program, and by the Department of Energy, Advanced Energy Division.

## REFERENCES

- <sup>1</sup> Herzberg, G., "Molecular Spectra and Molecular Structure, Volume I: Spectra of Diatomic Molecules", D. van Nostrand Company, Inc, Princeton, New Jersey, 1950.
- <sup>2</sup> Budó, A., "On the triplet-band term formulas for the general intermediate case and their application to the  $B^3\Pi$  and  $C^3\Pi$  terms of the  $N_2$  molecule", Z. Physik. 96, 1935, p. 219.
- <sup>3</sup> Roux, F., Michaud, F., and Vervloet, M., "High-resolution Fourier spectrometry of  $14N_2$ : Analysis of the (0-0), (0-1), (0-2), (0-3) bands of the  $C^3\Pi_u-B^3\Pi_g$  system", Can. J. Phys. 67, 1998, p. 143.
- <sup>4</sup> Roux, F., Michaud, F., and Verloet, M., "High-resolution Fourier spectrometry of  $14N_2$  violet emission spectrum: Extension of the analysis of the  $C^3\Pi_u-B^3\Pi_g$  system", J. Mol. Spec. 158, 1993, p. 270.
- <sup>5</sup> Lofthus, A., and Krupenie, P.H., "The spectrum of molecular nitrogen". J. Phys. Chem. Ref. Data, 6, 1977.
- <sup>6</sup> Herzberg, G., and Buettendbender, G., "Ueber die Struktur der zweiten positive Stickstoffgruppe und die Praedissoziation des  $N_2$ -Molekuels", Annalen der Physik, 21, 1935, p. 577.
- <sup>7</sup> Hönl, H., and London, F., Z. Physik 33, 1925, p. 803.
- <sup>8</sup> Schoenbach, K. H., El-Habachi, A., Shi, W., and Ciocca, M., "High Pressure Hollow Cathode Discharges", Plasma Sources Science and Technology, 6, 1997, p. 468.
- <sup>9</sup> Laux, Christophe, Stanford University, Thermosciences Division, Stanford, CA: private communication.



# **Abstracts of Conference Presentations**

# ICOPS<sub>2000</sub>



**IEEE Conference Record – Abstracts**

**The 27th IEEE International Conference  
on Plasma Science**

**New Orleans, Louisiana, USA  
June 4 – 7, 2000**



**Sponsored by:**

The Plasma Science and Applications Committee  
of the IEEE Nuclear and Plasma Sciences Society

**Co-Sponsors:**

- Mississippi State University  
Department of Electrical and Computer Engineering  
Division of Continuing Education
- Air Force Office of Scientific Research

### Electron Heating in Atmospheric Pressure Air Discharges

Robert H. Stark and Karl H. Schoenbach  
Physical Electronics Research Institute, Old Dominion  
University,  
Norfolk, Virginia 23529

Atmospheric pressure air plasmas have gained interest because of possible use as plasma reactors, light sources, for thin film deposition, surface modification, and as plasma ramparts. For plasma ramparts, which are air plasmas serving as protective shields against incident microwave radiation, the required free electron density must be on the order of  $10^{13} \text{ cm}^{-3}$  at gas temperatures of less than 2000 K. At equilibrium conditions, where the electron energy distribution is determined only by the value of the reduced electric field ( $E/N$ ), the power density required to sustain an atmospheric pressure air plasma of  $10^{13} \text{ cm}^{-3}$  electron density is approximately  $5 \text{ kW/cm}^3$ , a value which makes the generation and sustainment of large plasma volumes extremely expensive. However, since the rate coefficient for electron gain and loss processes, which define the power consumption, are dependent on the electron energy distribution function (EEDF), manipulation of the EED might allow us to reduce the power. Particularly shifting the EEDF towards higher electron energies (electron heating), without heating the gas, will cause an increase in ionization rate and decrease in attachment and recombination rate. Experiments with nanosecond high voltage pulses applied to a dc atmospheric pressure air plasma have been performed to study this effect. A 10 ns high voltage pulse with a rise time of 1 ns, was superimposed to a dc microhollow cathode discharge sustained air glow with a current of 10 mA. The applied pulse generated electric fields of 10-30 kV/cm in the plasma. Electrical measurements of the temporal development of current and voltage and optical measurements of the integral emission intensity during the pulse and in the afterglow of the discharge have shown an increase in electron life time from 200 ns at 10 kV/cm to approximately 1.6  $\mu\text{s}$  at 30 kV/cm. Beyond reduction in power consumption, indicated by the experimental results, pulsed electron heating might also be used to influence the plasma chemistry in high pressure plasma reactors.

[1] Robert H. Stark and Karl H. Schoenbach, "Direct Current High Pressure Glow Discharges," *J. Appl. Phys.*, **85**, 2075 (1999)

[2] Robert H. Stark and Karl H. Schoenbach, "Direct Current Glow Discharges in Atmospheric Air," *Appl. Phys. Lett.*, **74**, 3770 (1999)

#### Acknowledgements

This work was solely funded by the Air Force Office of Scientific Research (AFOSR) in cooperation with the DDR&E Air Plasma Ramparts MURI program.

### Plasma Cathode Sustained Filamentary Glow Discharges in Atmospheric Air

Rolf Block, Abdel-Aleam H. Mohamed, and Karl H. Schoenbach  
Physical Electronics Research Institute, Old Dominion University,  
Applied Research Center, Newport News, VA

Glow-to-arc transitions in filamentary glow discharges in atmospheric air can be largely avoided by use of a plasma cathode, as has been demonstrated in short filamentary discharges in air [1]. In these experiments a dc-driven microhollow cathode discharge (MHCD) was used as a plasma cathode to sustain a stable, direct current discharge between the plasma cathode and a third positively biased electrode. We have, using the same concept, extended the gap distance (distance between plasma cathode and third electrode) from previously 2 mm to the range from 6 mm to 20 mm and have studied the electrical, optical and plasma properties of such long filamentary glow discharges in atmospheric air. The MHCD is ignited between closely spaced molybdenum electrodes, separated by a 130  $\mu\text{m}$  thick alumina layer, with a 130  $\mu\text{m}$  hole through the sample. The filamentary discharge was ignited at small gap distances, in order to keep the ignition voltage at a low level, and then the gap was extended to the desired distance. In a certain range of current the filamentary glow discharge (FGD) current was found to be identical to the microhollow cathode discharge current. In this range control of the FGD by the MHCD is possible. From previous measurements of short gap filamentary discharge the gas temperature was found to be approximately 2,000 K [2], the electron density was estimated as close to  $10^{13} \text{ cm}^{-3}$  [1]. We will report on the results of measurements of these plasma parameters in long filamentary air discharges, and the electrical parameters, which determine the current range of MHCD control of the FGD. Parallel operation of these controlled filamentary glow discharges by using individual or distributed ballast might allow the generation of large volume, high pressure glows in air.

- [1] Robert H. Stark and Karl H. Schoenbach, "Direct Current Glow Discharges in Atmospheric Air," *Appl. Phys. Lett.* **74**, 3770 (1999).
- [2] Robert H. Stark, Uwe Ernst, Mohamed El-Bandrawy, Christophe Laux, and Karl H. Schoenbach, "Direct Current Glow Discharges in Atmospheric Air," *Proc. 30<sup>th</sup> AIAA Plasmadynamics and Lasers Conf.*, Norfolk, VA, July 1999, paper AIAA-99-3666.

This work was solely funded by the Air Force Office of Scientific Research (AFOSR) in cooperation with the DDR&E Air Plasma Ramparts MURI program.

### Parallel Operation of Microhollow Cathode Discharges

Robert H. Stark, Ahmed El-Habachi, and Karl H. Schoenbach  
Physical Electronics Research Institute, Old Dominion  
University, Norfolk, VA 23529

Microhollow cathode discharges (MHCDs) are high pressure gas discharges between a cathode, which contains a circular opening and an arbitrarily shaped anode. The diameter of the cathode hole as well as the electrode gap is approximately 100  $\mu\text{m}$ . Operation on such a small spatial scale enables stable direct current glow discharge operation even at high pressure. Microhollow cathode discharges have been operated at atmospheric pressure in rare gases (e.g. argon, xenon), rare gas halogen mixtures (e.g. argon fluoride, xenon chloride) and in air. Stable dc high pressure glow discharge operation is of interest in lighting, plasma processing, and as plasma cathodes for air plasma ramparts. The required plasma size for these applications exceeds that of a single microhollow cathode discharge and therefore requires their arrangement in arrays. Parallel operation of up to sixteen micro discharges has been reported using distributed ballast<sup>1</sup>. A simpler way to generate arrays is to operate the glow discharges in a range where the voltage current characteristic has a positive slope, e.g. in the abnormal glow region. This can be achieved by limiting the cathode surface to a small value such that even at low currents it is completely covered by the plasma. In order to reduce the cathode area, the cathode surface was covered with a dielectric, such that only the cylindrical surface area of the cathode opening was available as cathode<sup>2</sup>. The current-voltage characteristic for argon microhollow cathode discharges, which without cathode cover, has a normal glow discharge characteristic for currents in excess of 1 mA, changes strongly when the cathode area is restricted in size. For argon at atmospheric pressure, the current-voltage characteristic showed then a positive slope of 10 V/mA for currents ranging from 1.5 mA to 6 mA. Parallel operation of two microhollow cathode discharges, separated by approximately 2 mm, was demonstrated without ballast in this current range. The results indicate the possibility to generate large area plasma sources by using a fourth dielectric layer on top of the usual three layer MHCD structure.

[1] Wenhui Shi, Robert H. Stark, and Karl H. Schoenbach, *IEEE Trans. Plasma Science*, 27, 16 (1999)

[2] Masatoshi Miyake, Hikaru Takakaski, Koich, Yasuoka, and Shozo Ishi, *Conf. Record, IEEE Intern. Conf. Plasma Science, Monterey, CA, 1000*, paper 7P61, p. 326

#### Acknowledgements

This work was solely funded by the Air Force Office of Scientific Research (AFOSR) in cooperation with the DDR&E Air Plasma Ramparts MURI program.

## Measuring Electron Densities in Highly Collisional Plasmas Using a 110 GHz Interferometer

K. L. Kelly<sup>1</sup>, J. E. Scharer<sup>1</sup>, M. Laroussi<sup>2</sup>, R. Block<sup>2</sup>, K. Schoenbach<sup>2</sup>

<sup>1</sup>Department of Electrical and Computer Engineering  
University of Wisconsin, Madison

<sup>2</sup> Old Dominion University, Norfolk, VA

A 110 GHz interferometer is used to measure electron densities in a highly collisional plasma. The plasma is formed and maintained with a helical coil driven at 13.56 MHz. In this regime, the background pressure approaches atmospheric pressure, and the collisionality is of the order  $\nu_{e-n} \approx 10^9 - 10^{13}$ . Probe measurements in this pressure range are inaccurate and unreliable due to complicated effects that electron-neutral collisions have in the sheath. It is necessary to operate an interferometer at a frequency high enough that the dominant characteristic frequency is the operating frequency ( $\omega > \nu_{e-n}$ ) yet low enough that small phase changes can be detected as a wave passes through the plasma. In this experiment, plasma dimensions are of the order 5-10 cm. In addition, the inelastic nature of collisions in this experiment make it necessary to interpret small phase changes with great care. A model has been developed help in that interpretation. Typical operating parameters are pressures of 1-760 Torr, applied magnetic field of 0-1000 Gauss, operating gases of nitrogen, oxygen, argon, and air, and input RF power levels of 100-3000 Watts.

### Acknowledgments

Air Force Office of Scientific research grants (Grant F49620-97-1-0262) Defense Department Research and Engineering Air Plasma Ramparts Multi-University Research Initiative and in part by NSF grant ECS-9632377.

**Electron Density Measurements in Pulsed Atmospheric Pressure Air Plasmas by IR Heterodyne Interferometry**

Frank Leipold, Robert H. Stark, Ahmed El-Habachi, and  
Karl H. Schoenbach  
Physical Electronics Research Institute  
Old Dominion University, Norfolk, VA 23529

Microhollow cathode discharges have been shown to serve as plasma cathodes for atmospheric pressure air discharges [1]. The high pressure discharges are operated dc at currents from 10 mA up to 30 mA and at average electric fields of 1.25 kV/cm. The electron density in the dc discharge was estimated to be in the range of  $10^{12}$  to  $10^{13}$  cm<sup>-3</sup> [1]. In order to determine this value more accurately an interferometric technique has been used. Since sufficient spatial resolution requires the use of light sources with wavelengths on the order and preferable less than the characteristic dimension of the micro plasma (100  $\mu$ m) a CO<sub>2</sub> laser was used. At this wavelength (10.6  $\mu$ m) the index of refraction of atmospheric air plasmas with electron densities of  $10^{13}$  cm<sup>-3</sup> is mainly determined by the heavy particles. In order to obtain information on the electron density, the discharge was operated in a pulsed repetitive mode with pulse duration varying between 100  $\mu$ s and 50 ms. Since the electrons have a much shorter relaxation time than the heavy particles, the fast change of the refractive index of a pulsed discharge during breakdown was considered to represent the electron part in the index of refraction, slower changes the heavy particle part. Conclusions on the dc values of the index of refraction were obtained by reducing the time between repetitive pulses and using the obtained results to extrapolate from pulsed to dc mode. The spatial distribution of the index of refraction was obtained by shifting the discharge volume through the laser beam and by using an inversion method to obtain the radial index profile. For a dc filamentary air discharge with a current of 10 mA, the electron density was found to be  $10^{13}$  cm<sup>-3</sup>. The width of the parabolic electron density profile was 0.6 mm. The diagnostic technique is now being applied to the measurement of the electron density in nanosecond pulsed air discharges at high overvoltage. This mode of operation is used to study electron heating in air plasmas [2]. Results of these studies will be reported.

- [1] Robert H. Stark and Karl H. Schoenbach, Appl. Phys. Lett. 74, 3770 (1999)
- [2] Robert H. Stark and Karl H. Schoenbach, "Electron Heating in Atmospheric Pressure Air Discharges", this conference

**Acknowledgement**

This work was funded by the Air Force Office of Scientific Research in Cooperation with the DDR&E Air Plasma Ramparts MURI Program, and by the National Science Foundation.

17:30

**SL2 5 Microhollow Cathode Discharge Excimer Lamps.\***

K.H. SCHOENBACH, *Physical Electronics Research Institute, Old Dominion University, Norfolk, VA 23529*

character. Reducing the diameter of the cathode hole in a hollow cathode discharge geometry to values on the order of  $100\text{ }\mu\text{m}$  has allowed us to extend the pressure range of stable, direct current hollow cathode gas discharges up to atmospheric pressure. The large concentration of high-energy electrons generated in the cathode fall, in combination with the high neutral gas density, favors three-body processes such as excimer formation. Excimer emission in xenon discharges peaking at  $172\text{ nm}$ , was observed with efficiencies between 6% and 9% at pressures of several hundred Torr. Typical forward voltages are 200 V at dc currents up to 8 mA. Pulsed operation allowed us to extend the current range to 80 mA with corresponding linear increase in optical power. Spatially resolved measurements showed that the source of the excimer radiation at atmospheric pressure and currents of less than 8 mA is confined to the cathode opening. The radiative emittance at 8 mA and atmospheric pressure is approximately  $20\text{ W/cm}^2$ . With reduced pressure and increased current, respectively, the excimer source extends into the area outside the cathode hole. Besides in xenon, excimer emission in argon at a peak wavelength of  $128\text{ nm}$  has been recorded. In addition to operating the discharge in rare gases, we have also explored its use as rare gas-halide excimer source. In a gas mixture containing

1% ArF we were able to generate stable dc discharges in flowing gas at pressures ranging from 100 Torr to atmospheric pressure. The spectra of the high-pressure ArF discharges are dominated by excimer radiation peaking at  $193\text{ nm}$ . The excimer emission of a single ArF discharge at 700 Torr was measured as 150 mW at an efficiency of 3%. Parallel operation of these discharges by means of a resistive anode, which has recently been demonstrated for argon discharges, offers the possibility to use microhollow cathode discharge arrays as dc-excimer lamps, with estimated power densities exceeding  $10\text{ W/cm}^2$ . abstract. note number. be ONLY)

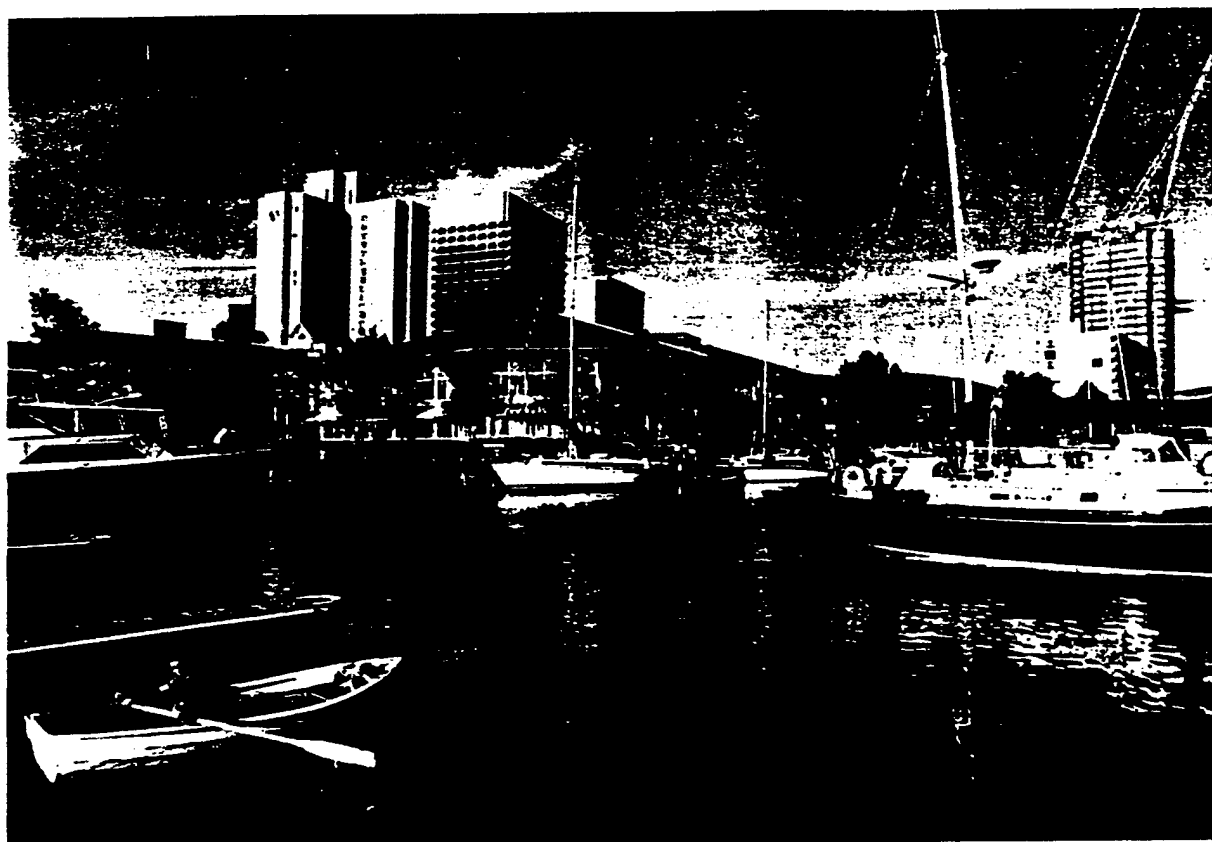
\*Supported by DOE, NSF, and DARPA



# **BULLETIN**

OF THE AMERICAN PHYSICAL SOCIETY

PROGRAM OF THE 52<sup>ND</sup> ANNUAL  
GASEOUS ELECTRONICS CONFERENCE



**Norfolk, Virginia**  
**October 5-8, 1999**

**October 1999**  
**Volume 44, No. 4**

**ETP3 31 Electron Density and Temperature Measurements in an Atmospheric Pressure Air Plasma by Heterodyne Interferometry** FRANK LEIPOLD, ROBERT H. STARK, AHMED EL-HABACHI, KARL H. SCHOENBACH, *Old Dominion University, Norfolk, VA 23529* Measurements of the electron density and gas temperature in a microhollow cathode supported (MCS) glow discharge in 1 atmosphere air have been performed by means of a heterodyne CO<sub>2</sub>-laser Mach-Zehnder interferometer. The index of refraction contains contributions from both electrons and heavy particles, and therefore information on the electron density and the density of the neutral and ionized atoms and molecules, respectively. In order to separate the information on electron density and gas temperature we have measured the temporal development of the index of refraction during the ignition phase of the discharge. Since the generation of electrons occurs on a much faster time scale than heating of the gas, the initial fast decay of the index of refraction was assumed to be due to changes in electron density, the following slower decay to be due to increase in temperature. In first experiments on MCS atmospheric pressure air discharges electron densities of  $10^{13}$  to  $10^{14}$  cm<sup>-3</sup> have been measured. The gas temperature at steady-state was found to be between 1500 K and 2500 K. — This work was funded by the Air Force Office of Scientific Research in Cooperation with the DDR&E Air Plasma Ramparts MURI Program and the National Science Foundation.

### LR2 1 Microhollow Cathode Discharge Excimer Lamps.

KARL H. SCHOENBACH, *Physical Electronics Research Institute, Old Dominion University, Norfolk, VA*

Reducing the diameter of the cathode hole in hollow cathode discharge geometry to values on the order of  $100\text{ }\mu\text{m}$  has allowed us to extend the pressure range of stable, direct current hollow cathode discharges up to atmospheric pressure. The large concentration of high-energy electrons in the nonthermal discharge, in combination with the high neutral gas density favors three-body processes such as rare gas excimer formation. Excimer emission in argon and xenon discharges peaking at  $130\text{ nm}$  and  $172\text{ nm}$ , respectively, was observed with an efficiency for xenon excimer emission between 6% and 9% in a pressure range from 250 Torr and 450 Torr. Typical forward voltages are 200 V at dc currents of up to 8 mA. Pulsed operation allowed us to extend the current range in xenon discharges to 80 mA. At pressures in the hundreds of Torr range the source of the excimer radiation extends over an area of several times the cathode opening. With increasing pressure the source is reduced in size and eventually, at pressures exceeding atmospheric becomes confined to the cathode opening. For a specific pressure the radiative power increases linearly with current at constant radiant emittance. For atmospheric pressure discharges in xenon the radiative emittance is approximately  $20\text{ W/cm}^2$ . In addition to operating the discharge in rare gases, we have also explored its use as rare gas-halide excimer source. In a gas mixture containing 1 % ArF we were able to generate stable dc discharges in flowing gas at pressures ranging from 100 Torr to atmospheric pressure. The spectra of the high-pressure ArF discharges are dominated by excimer radiation peaking at  $193\text{ nm}$ . The excimer emission of an ArF discharge at 700 Torr was measured as 150 mW. With a discharge voltage of 500 V, and a current of 10 mA the efficiency is 3 %. Parallel operation of the micro-discharges by means of a resistive anode offers the possibility to use microhollow cathode discharge arrays as dc-excimer lamps, with estimated power densities exceeding  $10\text{ W/cm}^2$ . -This work is funded by the Department of Energy, Advanced Energy Division, and by the National Science Foundation.

**QF2 3 Atmospheric Pressure Glow Discharges in Air\*** ROBERT H. STARK, KARL H. SCHOENBACH, *Old Dominion University, Norfolk, VA 23529* DC glow discharges at atmospheric pressure, sustained by microhollow cathode discharges could be generated in argon and in air. The differential electric field strength along the discharge axis has been measured by reducing the distance between anode and cathode and by recording the change in voltage at constant current. The electric field was found to be constant for distances greater than 2 mm from the cathode, as expected for the positive column of a glow discharge. It is 130 V/cm for argon and 1.2 kV/cm for air. For less than this distance the electric field decreases to a small value, indicating an electron beam like transport mechanism in this range. Experiments in air with a gap distance up to 1 cm have been performed. The electrical data allow us to determine the electron density by using information on electron mobility. For a current density of  $3.8 \text{ A/cm}^2$ , an electric field of 1.2 kV/cm, and assuming a temperature of 2000 K, the electron density in mid plane of the air glow is  $510^{12} \text{ cm}^{-3}$ . The temperature value was estimated from spectral measurements, and through interferometry. The power density, required to sustain this atmospheric pressure air discharge is  $4.6 \text{ kW/cm}^3$ , which is close to the theoretical value of  $4.0 \text{ kW/cm}^3$ .

\*This work was funded by the Air Force Office of Scientific Research in Cooperation with the DDR&E Air Plasma Ramparts MURI Program.

# ICPPS99

International Conference on Plasma Science

**IEEE CONFERENCE RECORD - ABSTRACTS**

**1999 IEEE INTERNATIONAL CONFERENCE  
ON PLASMA SCIENCE**



***The 26th  
IEEE International  
Conference on  
Plasma Science***

**June 20-24, 1999**

**Monterey California, USA**

**Sponsored by:**

**The Plasma Science &**

**Applications Committee**

**of the**

**IEEE Nuclear & Plasma Sciences Society**

**Co-Sponsors:**

**Sandia National Laboratories**

**Los Alamos National Laboratory**

**Defense Threat Reduction Agency**

## 2B01-2

Invited -

### Test Facility for High Pressure Plasmas

Rolf Block, Mounir Laroussi & Karl H. Schoenbach, Old Dominion University, Norfolk, VA 23529, USA

#### Test Facility for High Pressure Plasmas\*

Rolf Block, Mounir Laroussi, and Karl H. Schoenbach  
Physical Electronics Research Institute/ Appl. Research Center  
Old Dominion University, Norfolk/ Newport News, VA

High pressure nonthermal plasmas are gaining increasing importance because of their wide range of applications, e.g. in air plasma ramparts, gas processing, surface treatment, thin film deposition, and chemical and biological decontamination. In order to compare various methods of plasma generation with respect to efficiency, development of instabilities, homogeneity, lifetime etc., a central test facility for high pressure plasmas is being established.

The facility will allow us to study large volume ( $> 100 \text{ cm}^3$ ), nonthermal (gas temperature:  $< 2000 \text{ K}$ ) plasmas over a large pressure range ( $10^{-6}$  Torr up to more than 1 atmosphere) in a standardized discharge cell. The setup was designed to generate plasmas in air as well as in gas mixtures. The available voltage range extends to 25 kV dc (10 kW power). The electrodes can be water cooled.

Electrical diagnostics include a 400 MHz, 2 GS/s 4-channel oscilloscope for current and voltage measurements and the detection of the onset of instabilities.

For optical diagnostics, a CCD video camera is used to record the appearance of dc discharges. A high-speed light intensified CCD-camera (25 mm MCP with photocathode, gating speed: 200 ps, adjustable in 10 ps steps) allows to study the development of instabilities and can also be utilized in temporally resolved spectroscopic measurements.

Optical emission spectroscopy allows us to determine plasma parameters such as electron density (through Stark broadening measurements) and gas temperature measurements. We have particularly concentrated our efforts on gas temperature diagnostics. The rotational structure of the second positive system of nitrogen contains information on the neutral gas temperature, which is identical with the rotational temperature [1]. Taking the apparatus profile into account, the temperature of the rotational excited molecules is determined by a comparison of simulated and measured data. A spectrograph with an instrument profile of  $\text{FWHM}=0.1 \text{ \AA}$  is available.

Interferometry is well suited for electron density measurements especially in weakly ionized plasmas. A 4 mm microwave interferometer will be used for this diagnostics. Number densities up to  $7 \cdot 10^{13} \text{ cm}^{-3}$  can be measured in this wavelength range. For higher densities we plan to use an IR interferometer with a  $\text{CO}_2$  laser as source.

\* Funded by the Air Force Office of Scientific Research in Cooperation with the DDR&E Air Plasma MURI Program.

[1] Rolf Block, Olaf Toedter and Karl H. Schoenbach, "Temperature Measurement in Microhollow Cathode Discharges in Atmospheric Air", Bull. APS 43, No. 6, NW1 2, p. 1478, 1998.

## 2B03

### Microhollow Cathode Discharges in Atmospheric Air

R.H. Stark, U. Ernst, R. Block, M. El-Bandrawy and  
K.H. Schoenbach, Old Dominion University, Norfolk,  
VA 23529, USA

#### Microhollow Cathode Discharges in Atmospheric Air

R. H. Stark, U. Ernst<sup>1</sup>, R. Block, M. El-Bandrawy,  
and K. H. Schoenbach

Physical Electronics Research Institute, Old Dominion  
University, Norfolk, VA 23529

Microhollow electrode discharges (MHCD) [1] are gas discharges between closely spaced (submillimeter) electrodes containing openings with diameter,  $D$ , on the same order as the electrode gap. In previous experiments the reduction of the size of the cathode opening to  $100\ \mu\text{m}$  has allowed us to generate stable, direct current discharges in air up to atmospheric pressure [2]. The microhollow cathode discharges were operated at currents of up to 20 mA, corresponding to current densities of  $250\ \text{A}/\text{cm}^2$  and at average electric fields of  $16\ \text{kV}/\text{cm}$ . The gas temperature of the MHCD was determined by spectroscopic measurements of the excited vibrational states of the nitrogen molecules. First results indicate that the gas temperature at atmospheric pressure and currents of 20 mA is close to  $2000\ ^\circ\text{K}$ . Parallel operation of MHCDs can be achieved by ballasting each discharge resistively [3]. Without resistive ballast, the discharge itself needs to be resistive, that means the current voltage characteristic of the discharge must have a positive slope. Results of modeling [4] show an increase of the forward voltage with current at high current values. However, overheating of the electrodes prevents dc operation of parallel discharges in atmospheric air in this current range. In order to extend the range of operation into the high current mode, where the discharge becomes resistive, it needs to be pulsed. In pulsed operation, with pulse duration in the range from 1 to 100 microseconds, the current range could be extended to 80 mA. At higher current, glow-to-arc transition was observed. The results show, that pulsed operation at high current might allow to operate discharges in parallel without individual ballast.

[1] K. H. Schoenbach, A. El-Habachi, W. Shi, and M. Ciocca, "High Pressure Hollow Cathode Discharges," *Plasma Sources Science and Technology* 6, 468 (1997).

[2] R. Block, O. Toedter, and K. H. Schoenbach, "Temperature Measurements in Microhollow Cathode Discharges in Atmospheric Air", *Bull. APS* 43, 1478 (1998).

[3] W. Shi, R. H. Stark and K. H. Schoenbach, "Parallel Operation of Microhollow Cathode Discharges", to appear in *IEEE Trans. Plasma Science*.

[4] A. Fiala, L. C. Pitchford, and J. P. Boeuf, *Proc. XXII Conf. Phenomena in Ionized Gases*, Hoboken, NJ, 1995, *Contr. Papers* 4, p.191.

This work was solely funded by the Air Force Office of Scientific Research (AFOSR) in cooperation with the DDR&E Air Plasma Ramparts MURI program.

## 4P02

### Microhollow Cathode Discharges as Plasma Cathodes for Atmospheric Pressure Glow Discharges in Air

Robert H. Stark and Karl H. Schoenbach,  
Old Dominion University, Norfolk, VA 23529, USA

#### Microhollow Cathode Discharges as Plasma Cathodes for Atmospheric Pressure Glow Discharges in Air

Robert H. Stark and Karl H. Schoenbach  
Physical Electronics Research Institute,  
Old Dominion University, Norfolk, VA 23529

One of the main obstacles for dc operation of high-pressure glow discharges is the glow-to-arc transition, an instability that originates in the high field region of the discharge: the cathode fall. Reduction or even elimination of the cathode fall is possible by using a plasma cathode. A microhollow cathode discharge (MHCD) [1] has been used as plasma cathode for a glow discharge in air, sustained between the hollow anode of the MHCD and a third electrode which was positively biased with respect to the MHCD anode [2]. With this method we were able to obtain stable dc operation in air up to atmospheric pressure without reaching the threshold for glow-to-arc transition. Current and voltage characteristics, axial electric field distribution and the visual appearance of this glow discharge and the MHCD were studied in air at atmospheric pressure [3]. In order to obtain the stable air discharge the current in the MHCD needs to exceed a threshold value. Typical threshold currents for a 100  $\mu\text{m}$  diameter hollow cathode are 5-10 mA. Above the threshold, the current in the glow discharge is identical with the MHCD current and can be controlled by varying the MHCD voltage. The glow discharges were operated at currents of up to 22 mA, corresponding to current densities of 3.8 A/cm<sup>2</sup> and at average electric fields of 1.2 kV/cm. Electron densities in the glow were estimated to be on the order of 10<sup>13</sup> cm<sup>-3</sup>. Temperature measurements in one MHCD indicated that the temperature in the glow discharge is below 2000 °K [4]. Parallel operation of these glow discharges by using arrays of MHCDs offers the possibility for large volume high pressure operation [5].

[1] K. H. Schoenbach, A. El-Habachi, W. Shi, and M. Ciocca, *Plasma Sources Sci. Techn.* 6, 468 (1997).

[2] R. H. Stark and K. H. Schoenbach, "Direct Current High Pressure Glow Discharges", to appear in *J. Appl. Phys.*

[3] R. H. Stark and K. H. Schoenbach, "Direct Current Glow Discharges in Atmospheric Air", submitted to *Appl. Phys. Lett.*

[4] R. H. Stark, U. Ernst, R. Block, and K. H. Schoenbach, "Microhollow Cathode Discharges in Atmospheric Air", this conference.

[5] W. Shi, R. H. Stark and K. H. Schoenbach, "Parallel Operation of Microhollow Cathode Discharges", to appear in *IEEE Trans. Plasma Science*.

This work was solely funded by the Air Force Office of Scientific Research (AFOSR) in cooperation with the DDR&E Air Plasma Ramparts MURI program.



## **4P01**

### **Pulsed Operation of Microhollow Cathode Discharges in Atmospheric Air**

Uwe Ernst, Robert H. Stark, Karl. H. Schoenbach, Klaus Frand and Werner Hartmann, University of Erlangen-Nuremberg, Erlangen, Germany

### **Pulsed Operation of Microhollow Cathode Discharges in Atmospheric Air**

Uwe Ernst<sup>1</sup>, Robert H. Stark<sup>2</sup>, Karl H. Schoenbach<sup>2</sup>, Klaus Frank<sup>1</sup> und Werner Hartmann<sup>3</sup>

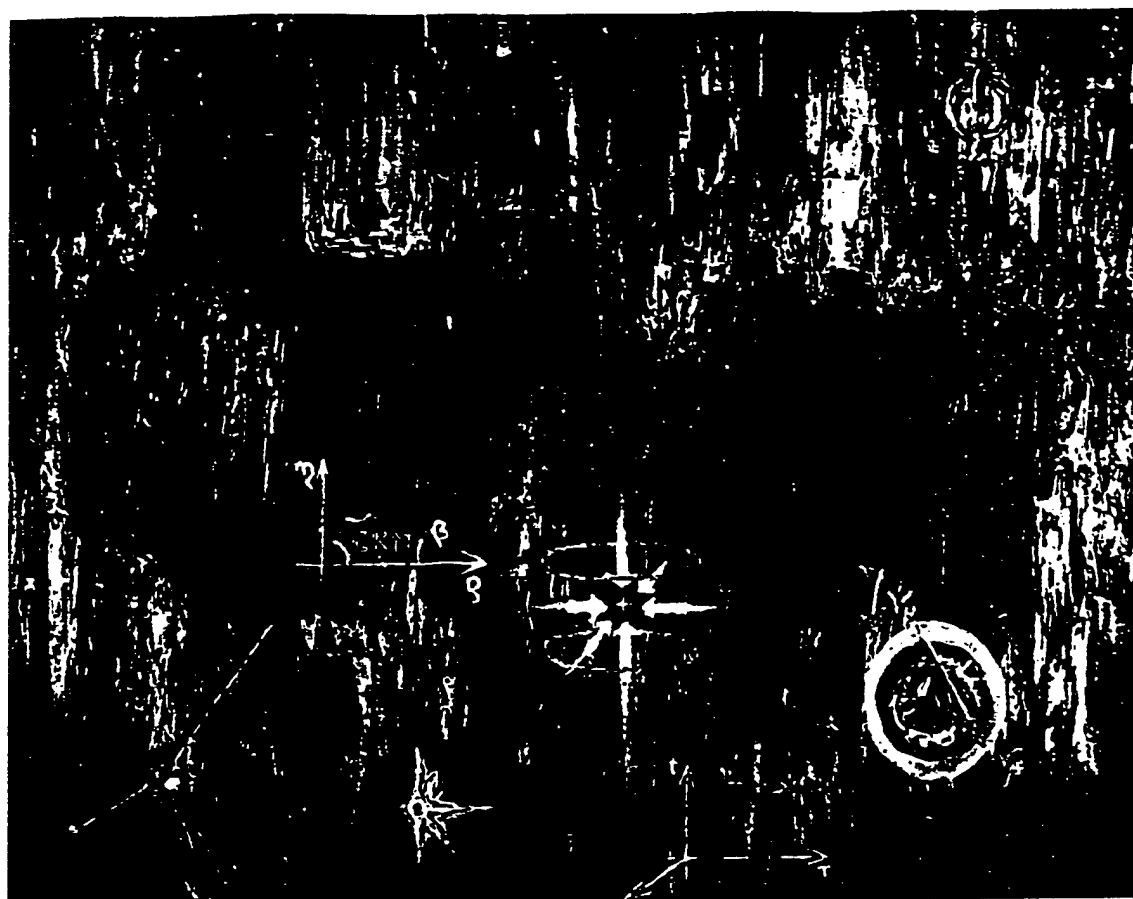
1) Department of Physics, University of Erlangen-Nuremberg, Germany

2) Physical Electronics Research Institute, Old Dominion University, Norfolk, VA 23529, USA

3) Siemens AG Erlangen, Germany

Reducing the diameter of the cathode opening to values on the order of 100 micrometer allowed us to operate stable dc hollow cathode glow discharges in air at atmospheric pressure. Discharge currents of up to 30 mA with forward voltages around 400 V have been realized. In order to generate arrays of microhollow cathode discharges without resistive ballast, the current voltage characteristic of the discharge needs to have a positive slope. Results of modeling show the required increase of the forward voltage with current at high current values. However, overheating of the electrodes prevents dc operation of parallel discharges in atmospheric air in this current range. In order to extend the range of operation into the high current mode, the discharge has been operated pulsed with pulse duration from 1 to 100 microsecond. First experimental results confirm the modeling results. The electrical characteristic and the optical appearance of the discharge plasma in pulsed microhollow cathode discharges and its applications will be discussed.

This work was supported by the National Science Foundation (NSF), the Air Force Office of Scientific Research (AFOSR) and Siemens Germany



# 63. Physikertagung

Deutsche Physikalische Gesellschaft  
Heidelberg, 15.-19. März 1999

gemeinsam mit der  
**Frühjahrstagung 1999**  
der Fachverbände

Atomphysik, Geschichte der Physik, Gravitation und Relativitätstheorie, Kurzzeitphysik, Kybernetik,  
Massenspektrometrie, Molekülphysik, Plasmaphysik, Quatenoptik, Strahlenwirkung und Strahlenschutz,  
Teilchenphysik, Theoretische und Mathematische Grundlagen der Physik, Umweltphysik  
und der Arbeitskreise

Atome Moleküle Quantenoptik und Plasmen, Energie, Physik und Abrüstung  
**Symposien**

Angewandte Optik, Cluster und Fullerene, Laserkühlung und Bose-Einstein-Kondensation,  
Quanteninformationsverarbeitung, Umweltphysik und Spektroskopie,  
Wechselwirkung in starken Laserfeldern

Örtliche Tagungsleitung: Prof. Dr. K. Meier  
Tagungsgeschäftsführer: Dr. H. Hinsch

Tagungsbüro:  
Institut für Hochenergiephysik  
Schröderstrasse 90, D-69120 Heidelberg

Kontakt: Tel: 06221-54-4916, Fax -4917  
e-mail: [dpg99@ihp.uni-heidelberg.de](mailto:dpg99@ihp.uni-heidelberg.de)  
web: [www.ihp.uni-heidelberg.de/dpg99](http://www.ihp.uni-heidelberg.de/dpg99)

### Fachvortrag

**Direct Current Atmospheric Pressure Glow Discharges —**  
•ROBERT H. STARK and KARL H. SCHOENBACH — Physical Electronics Research Institute, Old Dominion University, Norfolk, VA 23529, USA

A novel plasma cathode for the sustainment of large volume, high pressure dc glow discharges has been developed. A microhollow cathode discharge (MHCD) with 100 micrometer diameter cathode and anode holes was used to provide electrons for a large volume glow discharge, sustained between the hollow anode of the MHCD and a third electrode. Current and voltage characteristics, and the visual appearance of the glow discharge and MHCD were studied in argon and air. We are able to get stable dc operation in argon and air up to 1 atm. The glow discharge is ignited when the current in the plasma cathode (MHCD), which is on the order of mA, reaches a threshold value. This threshold current increases with reduced applied voltage across the main gap. Above this transition the current in the glow discharge is identical to the MHCD current and can be controlled by varying the MHCD voltage. Then the electrical characteristic of this system of coupled discharges resembles that of a vacuum-triode. The electron density in the plasma column is on the order of  $10^{11}$  to  $10^{13}$  cm<sup>-3</sup>. Parallel operation of microhollow cathode discharges have indicated that large area high pressure stable glow discharges can be obtained by using arrays of MHCDs as electron sources.

This work was funded by the Air Force Office of Scientific Research (AFOSR) in cooperation with the DDR&E Air Plasma Ramparts MURI Program, and the National Science Foundation (NSF).

**Pulsed Operation of Microhollow Cathode Discharges in Atmospheric Air** — •UWE ERNST<sup>1</sup>, ROBERT H. STARK<sup>2</sup>, KARL H. SCHOENBACH<sup>2</sup>, KLAUS FRANK<sup>1</sup>, and WERNER HARTMANN<sup>3</sup> —  
<sup>1</sup>Department of Physics, University of Erlangen-Nuremberg, Germany  
— <sup>2</sup>Physical Electronics Research Institute, Old Dominion University, Norfolk, VA 23529, USA — <sup>3</sup>Siemens AG Erlangen, Germany

Reducing the diameter of the cathode opening to values on the order of 100 micrometer allowed us to operate stable dc hollow cathode glow discharges in air at atmospheric pressure. Discharge currents of up to 30 mA with forward voltages around 400 V have been realized. In

order to generate arrays of microhollow cathode discharges without resistive ballast, the current voltage characteristic of the discharge needs to have a positive slope. Results of modeling show the required increase of the forward voltage with current at high current values. However, overheating of the electrodes prevents dc operation of parallel discharges in atmospheric air in this current range. In order to extend the range of operation into the high current mode, the discharge has been operated pulsed with pulse duration from 1 to 100 microsecond. First experimental results confirm the modeling results. The electrical characteristic and the optical appearance of the discharge plasma in pulsed microhollow cathode discharges and its applications will be discussed. This work was supported by the National Science Foundation (NSF), the Air Force Office of Scientific Research (AFOSR) and Siemens Germany.

P 24.20 Di 16:30 PY

**Parallel Operation of Microhollow Cathode Discharges —**  
•ROBERT H. STARK, WENHUI SHI, and KARL H. SCHOENBACH —  
Physical Electronics Research Institute, Old Dominion University, Norfolk, VA 23529, USA

The dc current-voltage characteristics of microhollow cathode discharges has, in certain ranges of the discharge current, a positive slope. In these current ranges it should be possible to operate multiple discharges in parallel without individual ballast. Such arrays could be used as flat panel excimer lamps or large area plasma cathodes. In order to

verify this hypothesis we have studied the parallel operation of two microhollow cathode discharges of 100 micrometer hole diameter in argon at pressures from 100 torr to 800 torr. Stable dc operation of the two discharges, without individual ballast, was obtained if the voltage-current characteristics of the individual discharges had a positive slope greater than 10 V/mA over a voltage range of more than 5 % of the sustaining voltage. In order to obtain parallel operation over the entire current range of the microhollow cathode discharges, which includes regions of negative differential conductivity, we have replaced the metal anode by a semi-insulating semiconductor, which serves as distributed resistive ballast. With this method, we were able to ignite and sustain an array of 16 dc microhollow cathode discharges over a wide range of pressure and discharge current.

This work was funded by the Department of Energy, Advanced Energy Division, and by the Air Force Office of Scientific Research (AFOSR) in cooperation with the DDR&E Air Plasma Ramparts MURI Program.

# BULLETIN

OF THE AMERICAN PHYSICAL SOCIETY



**Program of the 51st Annual Gaseous Electronics Conference  
and the 4th International Conference on Reactive Plasmas**

**October 19-22, 1998**

**Maui, Hawaii**

**October 1998**

**Volume 43, No. 5**

**JTP6 8 Parallel Operation of Microhollow Cathode Discharges** ROBERT H. STARK, WENHUI SHI, KARL H. SCHOENBACH, *Physical Electronics Research Institute, Old Dominion University, Norfolk, VA 23529* The dc current-voltage characteristics of microhollow cathode discharges has, in certain ranges of the discharge current, a positive slope [1]. In these current ranges it should be possible to operate multiple discharges in parallel without individual ballast, and be used as flat panel excimer lamps [2] or large area plasma cathodes. In order to verify this hypothesis we have studied the parallel operation of two microhollow cathode discharges of 100 micrometer hole diameter in argon at pressures from 100 Torr to 800 Torr. Stable dc operation of the two discharges, without individual ballast, was obtained if the voltage-current characteristics of the individual discharges had a positive slope greater than 10 V/mA over a voltage range of more than 5 to obtain parallel operation over the entire current range of the microhollow cathode discharges, which includes regions of negative differential conductivity, we have replaced the metal anode by a semi-insulating semiconductor, which serves as distributed resistive ballast. With this method, we were able to ignite and sustain an array of dc microhollow cathode discharges over a wide range of pressure and discharge current. [1] K.H. Schoenbach et al. Appl. Phys. Lett. 68, 13 (1996). [2] A.El-Habachi and K.H.Schoenbach, APL 72, 1 (1998). This work was funded by the Department of Energy, Advanced Energy Division, and by the Air Force Office of Scientific Research (AFOSR) in cooperation with the DDR&E Air Plasma Ramparts MURI Program.

13:15

**NW1 1 Plasma Cathodes as Electron Sources for Large Volume, High-Pressure Glow Discharges** ROBERT H. STARK, KARL H. SCHOENBACH, *Physical Electronics Research Institute, Old Dominion University, Norfolk, VA 23529* A method to suppress the glow-to-arc transition in high pressure glow discharges is the use of a plasma cathode consisting of microhollow cathode discharges (MHCD) [1]. In our experiment a microhollow cathode discharge with a 100 micrometer diameter cathode hole and identical anode hole was used to provide electrons for a large volume main discharge, sustained between the hollow anode of the MHCD and a third electrode. Current and voltage characteristics, and the visual appearance of the main discharge and MHCD were studied in argon and air by using the micro plasma cathode as electron source. We are able to get stable dc operation in argon up to 1 atm and in air up to 600 torr. The main discharge is ignited when the current in the plasma cathode (MHCD), which is on the order of mA, reaches a threshold value. This threshold current increases with reduced applied voltage across the main gap. Above this transition the current in the main discharge is on the same order as the MHCD current and can be controlled by the MHCD current. Experiments with two MHCDs in parallel have indicated that large area high pressure stable glow discharges can be generated by using arrays of MHCDs as electron sources. [1] K. H. Schoenbach et al, Plasma Sources Sci. Techn. 6, 468 (1997). This

work was solely funded by the Air Force Office of Scientific Research (AFOSR) in cooperation with the DDR&E Air Plasma Ramparts MURI program.



13:30

NW1 2 Temperature Measurement in Microhollow Cathode Discharges in Atmospheric Air ROLF BLOCK, OLAF TOEDTER, KARL H. SCHOENBACH, *Physical Electronics Research Institute, Old Dominion University, Norfolk, VA, USA* By reducing the diameter of the cathode opening in hollow cathode discharge geometry to values on the order of one hundred micrometers we were able to operate the discharges in a direct current mode at atmospheric pressure in air. The possibility to operate microhollow cathode discharges (MHCD) in parallel [1] in atmospheric air opens a wide range of applications. At atmospheric pressures, the electric power of a single discharge was measured as 8W. The power density in the microhollow exceeds  $1\text{MW}/\text{cm}^3$ . This leads to strong thermal loading of the electrodes. In order to study the thermal properties of the discharge we have used a method based on emission spectroscopy. The rotational structure of the emitted lines corresponding to the second positive system of nitrogen contains information on the neutral gas temperature. Taking the apparatus profile into account the temperature of the rotational excited molecules can be estimated by a comparison of simulated and measured data. Measurements on MHCD up to atmospheric pressure show an increase in the neutral gas temperature to values exceeding 1000K. In addition to the gas temperature the electrode temperatures were measured and the thermodynamic behavior of the electrode configuration was calculated. [1] W. Shi, K.H. Schoenbach Parallel Operation of Microhollow Cathode Discharges, ICOPS98, Raleigh, NC, USA, 1998 This work was funded by the Air Force Office of Scientific Research (AFOSR) in cooperation with the DDR&E Air Plasma Ramparts MURI program, and by the Department of Energy, Advanced Energy Division.

**25th Anniversary**

**IEEE CONFERENCE RECORD — ABSTRACTS**

**1998 IEEE International  
Conference on Plasma Science**



North Raleigh Hilton  
Raleigh, North Carolina  
June 1-4, 1998

Sponsored by  
Plasma Science and Applications Committee  
of the  
IEEE Nuclear and Plasma Sciences Society

### Plasma Cathodes for Large Volume, High-Pressure Glow Discharges

Robert H. Stark and Karl H. Schoenbach  
Physical Electronics Research Institute,  
Old Dominion University, Norfolk, VA 23529

Research in high pressure glow discharges is motivated by applications such as instantly activated reflectors and absorber for electromagnetic radiation, plasma processing, gas lasers, and the remediation of gaseous pollution. One of the main obstacles for dc operation of high-pressure glow discharges is the glow-to-arc transition; an instability that originates in the high field region of the discharge: the cathode fall. A way to suppress this instability is the use of a plasma cathode consisting of microhollow cathode discharges (MHCD) [1]. In our experiment a microhollow cathode discharge with a 100  $\mu\text{m}$  diameter cathode hole and identical anode hole was used to provide electrons for a large volume main discharge, sustained between the hollow anode of the MHCD and a third electrode. The distance of this electrode from the MHCD anode was varied between 2.5 mm to 9.5 mm, a value large compared to the 200  $\mu\text{m}$  anode-cathode gap of the MHCD. Current and voltage characteristics, and the visual appearance of the main discharge and MHCD were studied in argon and air at pressures up to several hundred Torr. Using the micro plasma cathode as electron source to support the main discharge we are able to get a stable dc operation in argon up to pressures of more than 400 Torr without reaching the threshold for glow-to-arc transition. The results in air were similar to those in argon, however, the transition from a stable discharge into a filamentary occurred at lower pressure (<60 Torr). The main discharge is ignited when the current in the plasma cathode (MHCD), which is on the order of mA, reaches a threshold value. This threshold current increases with reduced applied voltage across the main gap. Above this transition the current in the main discharge is on the same order as the MHCD current. The experimental results indicate the presence of an "electron-beam" in the hollow cathode discharge phase, that is emitted through the anode hole [2]. The demonstrated controllability of a relatively large volume glow discharge by means of one MHCD indicates the possibility to generate large volume high pressure plasmas through parallel operation of MHCD supported glow discharges.

[1] K. H. Schoenbach et al, Plasma Sources Sci. Techn. 6, 468 (1997).

[2] R. Stark et al, this conference.

This work was solely funded by the Air Force Office of Scientific Research (AFOSR) in cooperation with the DDR&E Air Plasma Ramparts MURI program.

# Microhollow Cathode Discharges as Electron Sources

Robert H. Stark and Karl H. Schoenbach

Physical Electronics Research Institute, Old Dominion University,  
Norfolk, VA 23529

Microhollow electrode discharges (MHCD) [1] are gas discharges between closely spaced (submillimeter) electrodes containing openings with diameter,  $D$ , on the same order as the electrode gap. Reducing the size of the cathode opening to 100  $\mu\text{m}$  has allowed us to generate stable, direct current discharges in argon and xenon up to atmospheric pressure, in air up to 400 Torr [2]. Results of previous experiments with a hollow electrode configuration in air at several Torr indicated the presence of an "electron-beam" emitted through the anode hole [3]. Experiments in a similar geometry but at much higher pressure, in air and in argon [4], point again to the fact that the energy distribution of the electrons emitted through the anode hole is anisotropic, with a strong component in forward direction. The dependence of the directed emission of electrons through the hollow anode from the hollow cathode discharge parameters, was studied in argon and air for pressures up to several hundred Torr, using a third, biased electrode as electric probe. A model for the observed directed electron emission, and its effect on the sustainment of a large volume discharge between hollow anode and the third electrode [4] will be presented.

[1] K. H. Schoenbach et al, Plasma Sources Sci. Technol. 6, 468 (1997)

[2] A. Khedr et al, this conference

[3] K. H. Schoenbach et al, Proc. Gas Discharges and Their Applications, Greifswald, Germany, 1997, p. 280.

[4] Robert H. Stark et al, this conference

This work was solely funded by the Air Force Office of Scientific Research (AFOSR) in cooperation with the DDR&E Air Plasma Ramparts MURI program.

Measurement of Electron Densities in Weakly Ionized  
Atmospheric Pressure Air

Karl H. Schoenbach, *Old Dominion University, Norfolk, VA*,  
Erich E. Kunhardt, *Stevens Institute of Technology, Hoboken, NJ*,  
Christophe O. Laux, and Charles H. Kruger, *Stanford University  
Stanford, CA*

Research on weakly ionized atmospheric air is motivated by applications such as reflectors and absorbers of electromagnetic radiation (plasma ramparts), large volume material processing, gaseous pollution remediation, and field enhanced combustion. The

electron densities for these applications range between  $10^{11}$  and  $10^{15} \text{ cm}^{-3}$ . Particularly, applications as plasma ramparts require electron densities on the order of  $10^{13} \text{ cm}^{-3}$ . Measurements of electron densities with sufficient spatial and temporal resolution to explore the development of instabilities, such as glow-to-arc transitions, are essential for the characterization of these air plasmas. Two diagnostic techniques have been identified as best suited for this application: interferometric techniques, and techniques based on emission spectroscopy. Microwave interferometry is well suited for plasmas where the electron density integrated over the path length is less than  $10^{15} \text{ cm}^{-2}$ . For higher values of the density times path length integral far infrared lasers are required. Emission spectroscopy measurements of the Stark-broadened Balmer  $\beta$  line of hydrogen represent a very effective technique for the determination of electron densities in excess of  $5 \times 10^{13} \text{ cm}^{-3}$  with high spatial resolution. This technique is however more difficult to apply at electron number densities below  $5 \times 10^{13} \text{ cm}^{-3}$  as instrumental and Doppler broadenings become comparable to Stark broadening. Other diagnostic techniques such as Thomson scattering and electric probe measurements are well established for low pressure plasmas. Their potential for the measurement of electron densities in weakly ionized atmospheric pressure air has yet to be explored. We will, in this paper, discuss the potential and the limitations of the various electron density diagnostic techniques for the characterization of weakly ionized atmospheric air.

This work was funded by the Air Force Office of Scientific Research (AFOSR) in cooperation with the DDR&E Air Plasma Ramparts MURI program.

## Parallel Operation of Microhollow Cathode Discharges

Wenhui Shi and Karl H. Schoenbach  
Physical Electronics Research Laboratory  
Old Dominion University, Norfolk, VA 23529

The dc current-voltage characteristics of microhollow cathode discharges has, in certain ranges of the discharge current, a positive slope [1]. In these current ranges it should be possible to operate multiple discharges in parallel without individual ballast, and be used as flat panel excimer lamps [2] or large area plasma cathodes. In order to verify this hypothesis we have studied the parallel operation of two microhollow cathode discharges of 100  $\mu\text{m}$  hole diameter in argon at pressures from 100 Torr to 800 Torr. Stable dc operation of the two discharges, without individual ballast, was obtained if the voltage-current characteristics of the individual discharges had a positive slope greater than 10 V/mA over a voltage range of more than 5 % of the sustaining voltage. Small variations in the discharge geometry generated during fabrication of cathode holes or caused by thermal effects during discharge operation are detrimental to

parallel operation. Varying the distance between the discharges from twice the hole diameter to approximately five times did not affect the parallel operation. The total current was always slightly larger than the sum of the currents measured for the individual discharges, indicating coupling between the two discharges.

In order to obtain parallel operation even for microhollow cathode geometries with large variations, we have studied the effect of distributed resistive ballast on the operation of such discharges. A distributed resistive ballast was simulated by using 22 k $\Omega$  ballast resistors for the individual discharges and a variable resistor between the discharges in a geometry with segmented anode. In order to initiate the discharges the coupling resistor needed to be on the order of 100 k $\Omega$ . After ignition it could be reduced to the same value as the ballast resistors without affecting the parallel operation. These results indicate that a resistive film on a segmented anode would stabilize the discharges and allow the formation of large arrays in a flat panel arrangement. They also indicate that parallel operation of microhollow cathode discharge is possible without ballast if the variation in discharge geometries is reduced to the order of percent.

[1] K.H.Schoenbach et al. Appl. Phys. Lett. 68, 13 (1996).

[2] A.El-Habachi and K.H.Schoenbach, APL. 72, 1 (1998).

This work was funded by the Department of Energy, Advanced Energy Division, and by the Air Force Office of Scientific Research (AFOSR) in cooperation with the DDR&E Air Plasma Ramparts MURI Program.